IDENTIFICATION AND FUNCTIONAL CHARACTERIZATION OF POWDERY MILDEW EFFECTORS

Inaugural-Dissertation

zur

Erlangung des Doktorgrades

der Mathematisch-Naturwissenschaftlichen Fakultät

der Universität zu Köln

vorgelegt von

Sarah Maria Schmidt

aus Marburg an der Lahn

Köln, September 2009

Die vorliegende Arbeit wurde am Max-Planck-Institut für Züchtungsforschung in Köln in der Abteilung für Molekulare Phytopathologie (Direktor: Prof. Dr. P. Schulze-Lefert) angefertigt.

Berichterstatter:	Prof. Dr. Paul Schulze-Lefert
	Prof. Dr. Martin Hülskamp
	Ass.-Prof. Dr. Frank Takken
Prüfungsvorsitzender:	Prof. Dr. Ulf-Ingo Flügge
Tag der Disputation:	30. November 2009

Publications

Schmidt, S.M., and Panstruga, R. (2007). Cytoskeleton functions in plant-microbe interactions. Physiol. Mol. Plant Pathol. 71, 135-148.

Table of Contents

Abbreviations

-	fused to (in the context of gene/protein fusion constructs)
%	percent
°C	degrees Celsius
µ	micro
µm	micromolar
A6	*Bgh* isolate A6
AC	avirulence candidate
ARF	adenosine diphosphate ribosylation factor
Arg	arginine
Asp	asparagine
Arabidopsis	*Arabidopsis thaliana*
Asp	aspartate
Avr	avirulence
Bg	*Blumeria graminis*
Bgh	*Blumeria graminis* forma specialis *hordei*
Bgt	*Blumeria graminis* forma specialis *tritici*
BiFC	Bimolecular Fluorescence Complementation
C	carboxy-terminal
CC	coiled-coil
cDNA	complementary DNA
CEBiP	Chitin Elicitor-Binding Protein
CERK1	Chitin Elicitor Receptor Kinase 1
Cf	*Cladosporium fulvum*
CFEM	8-cysteine, fungal, extracellular membrane
CFP	cyan fluorescent protein
CLSM	confocal laser scanning microscopy
COGEME	Consortium for the function Genomics of Microbial Eukaryotes
Col-0	*Arabidopsis thaliana* ecotype Columbia-0
con	contig
cv.	cultivar
Da	dalton
DAMPs	danger-associated molecular patterns
DH14	*Bgh* isolate DH14
EC	effector candidate
Ecp	Extracelluar *Cladosporium* protein
EST	expressed sequence tag
ER	Endoplasmatic Reticulum
ETI	effector-triggered immunity
FRET	Fluorescence Resonance Energy Transfer
FLIM	Fluorscence Lifetime Imaging
f.sp.	forma specialis
ff. sp.	formae speciales
dpi	days post infection
Ep	*Erysiphe pisi*
Go	*Golovinoyces orontii*
GAP	GTPase-activating factor

GEF	GTP-exchange factor
GFP	Green fluorescent protein
GAL	galactose
GLU	glucose
Gly	glycine
GUS	ß-glucuronidase
GWY	Gateway®
H	histidine
h	hour
His	histidine
hpi	hours post infection
HR	hypersensitive response
Hv	*Hordeum vulgare*
i.e.	*id est*
K1	*Bgh* isolate K1
kDa	kilo Dalton
L	leucine
LRR	leucine-rich repeat
m	milli
M	molar (mol/l)
MAMP	microbe-associated molecular patterns
MLA	Mildew resistance locus A
MLO	Mildew resistance locus O
N	N-terminal
NACHT	NAIP (neuronal apoptosis inhibitory protein), CIITA (MHC class II transcription activator), HET-E (incompatibility locus protein from *Podospora anserina*) and TP1 (telomerase-associated protein)]
NCBI	National Center for Biotechnology Information
NOD	nucleotide binding and oligomerization domain
NFκB	nuclear factor κB
n	nano
nm	nanometer
ORF	open reading frame
P01	near-isogenic barley line in ‘Pallas’ background containing MLA1
P03	near-isogenic barley line in ‘Pallas’ background containing MLA6
PAGE	polyacrylamide gel electrophoresis
PAMP	pathogen-associated molecular patterns
PCD	programmed cell death
PCR	polymerase chain reaction
PR	pathogenesis related
PRR	pattern recognition receptor
PTI	PAMP-triggered immunity
pv.	pathovar
q	quantitative
R	arginine
R	resistance
RLK	Receptor-like kinase
RNase	ribonuclease
ROS	reactive oxygen species
RPP	Recognition of *Peronospora parasitica*
RT-PCR	reverse transcription PCR

SD	synthetic dropout
SDS	sodium dodecylsulfate
SMS	S-adenosylmethionine-synthetase
SP	signal peptide
Ser	serine
SNP	single nucleotide polymorphism
T	tryptophane
TIR	Toll/interleukin 1 receptor
T-DNA	tansferred DNA
TLR	Toll-like receptor
TM	transmembrane
TPMT	thiopurine methyl-transferase
U	uracile
UBC	ubiquitin conjugating enzyme
Uf	*Uromyces fabae*
X-gal	bromo-chloro-indolyl-galactopyranoside
YFP	yellow-fluoresent protein

Summary

The ascomycete *Blumeria graminis* f.sp. *hordei* (*Bgh*) is the causal agent of the powdery mildew disease of the monocot barley (*Hordeum vulgare*). Suppression of host defense responses and accommodation of the intracellular feeding structure (haustorium) are indispensable for this obligate biotrophic phytopathogen. To manipulate its host plant, *Bgh* presumably employs small, secreted effector proteins. We bioinformatically identified effector candidates from the barley powdery mildew fungus by screening publicly available EST databases for cDNAs encoding small, secreted proteins of unknown function. A subset of these effector candidates (ECs) enhanced *Bgh* haustorium formation upon transient expression in barley cells. EC proteins are encoded by single-copy genes, are sequence conserved among different *Bgh* isolates and exhibit distinct expression patterns during fungal pathogenesis. Plant interacting proteins for two of the effector candidates were identified by a yeast two-hybrid screen in a barley cDNA library. EC4 interacts with a barley thiopurine methyltransferase (*Hv*TPMT) whereas EC6 interacts with a barley ubiquitin conjugating enzyme (*Hv*UBC-E2). Both interactions were confirmed *in planta* by bimolecular fluorescence complementation, suggesting that EC4 might target the host vesicle trafficking pathway while EC6 might be involved in controlling the synthesis of a yet unknown volatile compatibility compound.

We also identified a multigene family encoding putative secreted RNase-like effectors in the *Bgh* genome. The RNase-like proteins are highly polymorphic and fulfill the proposed criteria for *Bgh* effectors that are recognized by barley MLA resistance proteins (avirulence canidates (ACs)). We isolated a range of AC cDNAs from two *Bgh* isolates and tested a subset of them for their avirulence function. The results of these experiments do not support an avirulence function for the AC proteins so far.

Zusammmenfassung

Der Schlauchpilz (Ascomycet) *Blumeria graminis* f.sp. *hordei* (*Bgh*) verursacht die Pflanzenkrankheit Mehltau auf der monokotyledonen Pflanze Gerste (*Hordeum vulgare*). Als obligat biotrophischer Pathogen muss der Mehltau-Erreger sein intrazelluläres Organ zur Nährstoffausnahme (Haustorium) in die Wirtszelle einbringen und die Abwehrreaktionen der Wirtspflanze unterdrücken. Um die Wirtspflanze zu manipulieren nutzt *Bgh* vermutlich kleine, sekretierte Effektorproteine. Wir haben bioinformatisch Effektorkandidaten des Gerste-Mehltau Erregers identifiziert, indem wir verfügbare *Bgh* EST Datenbanken nach kleinen, sekretierten Proteinen mit unbekannter Funktion durchsucht haben. Einige dieser Effektorkandidaten (EC) erhöhen die Ausbildung von *Bgh* Haustorien wenn sie transient in Gerstezellen exprimiert werden. EC-Proteine werden von single-copy Genen kodiert, sind in ihren Sequenzen in verschiedenen *Bgh*-Isolaten konserviert und werden während der pilzlichen Pathogenese unterschiedlich exprimiert. Für zwei der EC Proteine wurden interagierende Pflanzenproteine mit einem Yeast-Two-Hybrid Screen einer Gerste cDNA-library identifiziert. EC4 interagiert mit einer Gerste-Thiopurin-Methyltransferase (*HvT*PMT), während EC6 mit einem Gerste Ubiquitin-konjugierendem-Enzym (*Hv*UBC-E2) interagiert. Beide Interaktionen wurden in der Pflanze mit bimolekularer Fluoreszenz-Komplementation bestätigt und weisen darauf hin, dass EC4 in den Vesikelverkehr des Wirts eingreift. EC6, hingegen, könnte in die Kontrolle der Synthese eines noch unbekannten flüchtigen Kompatibilitätsfaktors involviert sein.

Desweiteren haben wir eine Multigen-Familie im *Bgh*-Genom identifiziert, die für potenzielle RNase-ähnliche Effektoren kodiert. AC Proteine sind polymorph und erfüllen die Kriterien, die für *Bgh* Effektoren vorgeschlagen wurden, die von Gerste MLA Resistenzproteinen erkannt werden (Avirulenzkandidaten (ACs)). Wir haben viele AC cDNAs aus zwei *Bgh* Isolaten kloniert und auf ihre Avirulenzfunktion getestet. Bisher unterstützen die Ergebnisse dieser Experimente keine Avirulenzfunktion der AC Proteine.

.

1 Introduction

1.1 Plants defend themselves with an evolutionary ancient innate immune system

Plants as well as vertebrates employ a complex immune system to cope with the myriads of microbes they encounter constantly. Plants rely solely on an innate immune system to recognize and respond to microbial attacks (Ausubel, 2005). In contrast, vertebrates engage both an innate immune system for the initial phase of pathogen defense and an adaptive immune system for the late phase of infection and the immunological memory (Akira et al., 2006). Both plant and vertebrate innate immune systems consist of two layers and both employ pattern-recognition receptors (PRRs) to distinguish between "self" and "non-self" (Ausubel, 2005). The first layer recognizes conserved "microbial-associated molecular patterns" (MAMPs) that are not present in the host, whereas the second layer recognizes molecules resulting from microbial activity inside the host. Certain defense components and defense outputs (e.g. production of reactive oxygen species (ROS)) of the innate immune system among plants and vertebrates are very similar. Nevertheless, the two innate immune systems were likely shaped by convergent evolution (Ausubel, 2005; Lotze et al., 2007).

1.1.1 First layer- recognition of conserved microbial patterns

In plants, the response triggered by MAMP recognition has been referred to as "basal resistance" or "PAMP-triggered immunity" (Boller and Felix, 2009). The term "PAMP" (pathogen-associated molecular pattern) preceded implementation of the term "MAMP" (Mackey and McFall, 2006; He et al., 2007). The term "PAMP" is inaccurate, because the majority of PAMPs/MAMPs are exogenous molecules of both pathogenic and non-pathogenic microbes (Sato et al., 2009). Vertebrates recognize MAMPs via plasma-membrane resident Toll-like receptors (TLRs). TLRs mediate MAMP recognition by external leucine-rich repeat (LRR) motifs, whereas an intracellular Toll/Interleukin-1 receptor (TIR) domain initiates a defense signaling cascade (Akira et al., 2006). Analogously, plants recognize extracellular MAMPs via the LRR domains of membrane-resident receptors. However, the signaling is mediated by an intracellular kinase domain. MAMP recognition in plants usually does not result in cell death (Boller and Felix, 2009).

Fungal cell walls comprise various MAMPs, including ß-glucans and mannans that are recognized by many different TLRs in mammals. These TLRs signal into partly converging pathways. The outcome of the fungal MAMP recognition depends on the amount of signal convergence, thus conferring specificity to the host-fungus interaction (van de Veerdonk et al., 2008). In plants, less receptors are known for fungal MAMPs. Recently, two proteins recognizing chitin, a major component of the fungal cell wall, were identified in rice and Arabidopsis respectively. The rice transmembrane protein CEBiP (Chitin Elicitor Binding Protein) binds extracellular chitin, but is thought to require a co-receptor for signaling, because it lacks a significant intracellular domain (Kaku et al., 2006). A potential co-receptor, Chitin Elicitor Receptor Kinase (CERK1) was identified by two independent groups in *Arabidopsis thaliana*. CERK1 is involved in chitin perception and signaling via its intracellular serine/threonine kinase activity (Miya et al., 2007a; Wan et al., 2008). Though binding of CERK1 to chitin was not yet demonstrated, it is thought that CEBiP and CERK1 recognize chitin through LysM motifs in their extracellular domain and that homologs of CERK1 exist in rice and, vice versa, Arabidopsis contains a homolog of CEBiP (Kaku et al., 2006; Miya et al., 2007; Wan et al., 2008). In summary, these findings indicate that different MAMPs and their respective receptors have been identified so far in mammalian and plant perception of fungal pathogens.

1.1.2 Second layer- recognition of microbial activity

Differences in pathogen perception in vertebrates and plants become more manifest in contemplation of the second layer of innate immunity. Vertebrates perceive intracellular pathogens through presence of intracellular MAMPs or DAMPS (danger-associated molecular patterns). DAMPs include degradation products of peptidoglycan, a constituent of the cell wall of gram-negative bacteria (Ishii et al., 2008). Intracellular NACHT-LRR or NOD (nucleotide-binding (NB) and oligomerization domain)-LRR receptors recognize both intracellular MAMPs and DAMPs. Extra- and intracellular recognition of MAMPs and DAMPs collectively funnel into signaling cascades, which eventually activate nuclear factor κB (NF- κB), a key transcription factor in directing expression of antimicrobial and pro-inflammatory genes (Akira et al., 2006).

In plants, the second layer of immunity has been called "*R*-gene mediated resistance", because the receptors are encoded by plant resistance (*R*) genes and are known to confer isolate-specific resistance to pathogens (Boller and Felix, 2009). Resistance genes encode refined receptors for the perception of pathogen activity inside the host. Structurally, these

plant receptors resemble intracellular vertebrate receptors in consisting of a central NB and a C-terminal LRR domain (Takken and Tameling, 2009). However, in contrast to vertebrate intracellular receptor, plant receptors mostly, perhaps exclusively, recognize proteins. These proteins can either be of pathogen origin (effectors) or host proteins that have been modified by the activity of a pathogen effector (Rairdan and Moffett, 2007). Recognition of a pathogen activity in plants typically results in a so-called “hypersensitive response” (HR) and is often associated with cell death, thereby restricting pathogen growth (Nimchuk et al., 2003). Additionally, plants are also able to sense DAMPs (formerly called “endogenous elicitors”) including cutin monomers and cell wall fragments, but knowledge about plant DAMP receptors is scarce (Boller and Felix, 2009). Plant NB-LRR receptors not only bind more molecules; they are also greatly expanded in number compared to vertebrate NACHT/NOD-LRRs (Rairdan and Moffett, 2007).

1.1.3 Limitations

The first and the second layer of plant innate immunity have been coined PAMP-triggered immunity (PTI) and effector triggered immunity (ETI) in a momentous review (Jones and Dangl, 2006). Based on results obtained from bacterial-plant interactions, the authors proposed a catchy zigzag-model of co-evolution in the plant pathogen interaction. This model implies a clear separation of the two layers of the immune system. However, several plant immune receptors cannot clearly be assigned to one or the other layer. Examples include the tomato transmembrane *Cf*-resistance proteins and the rice transmembrane receptor-like kinase resistance protein Xa21, which both resemble PAMP receptors on the basis of their domain organization and subcellular localization, but recognize isolate-specific effector proteins (De Wit et al., 1997; Song et al., 1997). Another example is the membrane-resident, seven transmembrane protein MLO (Jorgensen, 1992b). Absence of this protein in barley confers broad-spectrum resistance to all tested isolates of *Blumeria graminis* f. sp. *hordei* (*Bgh*), the causal agent of powdery mildew disease on barley (Jorgensen, 1992b). Consequently, in a recent review, the overcharging principle of both layers of the plant immune system was determined as the perception of danger signals (Boller and He, 2009). In vertebrates, this concept has long been accepted. Both layers of the vertebrate innate immune system are thought to function next to each other. The perception of MAMPs and DAMPs is required to distinguish between beneficial and pathogenic microbes, as the presence of extracellular microbes does not necessarily result from a pathogen insult, whereas the presence of intracellular microbes is closely associated

with tissue damage (Sato et al., 2009). In other words, the amplitude of defense responses and thus often the outcome of the host-microbe interaction depends on the amount of damage incurred by the host (Casadevall and Pirofski, 2003).

1.2 Prokaryotic and eukaryotic pathogens have adapted to cause disease in plants

Microbial pathogens cause disease in plants by evading or subverting the plant immune system. In plants, both prokaryotic and eukaryotic pathogens colonize diverse niches within their host and utilize different modes of nutrient acquisition. Most bacterial (prokaryotic) pathogens do not enter plant cells. Eukaryotic filamentous pathogens, on the other hand, have evolved multiple strategies for plant invasion. Necrotophic fungi like *Fusarium oxysporum* or *Rhynchosporium secalis* quickly kill their host and feed saprophytically on dead plant tissue. Biotrophic fungi like *Ustilago maydis* and *Cladosporium fulvum* cause limited injury to the host and feed on living host cells. Hemibiotrophic fungi like *Magnaporthe grisea* have an initial biotrophic phase that is followed by a necrotrophic stage (Panstruga, 2003). The most sophisticated pathogens, the obligate biotrophs, establish intimate relationships with their hosts by inserting specialized feeding structures, so-called haustoria, into the host cell. Strictly speaking, haustoria are not intracellular, because they remain separated from the host cytoplasm by a modified host membrane, the extrahaustorial membrane, thus generating an extrahaustorial matrix (EHM) in the space between the haustorial and the extrahaustorial membrane as a communication platform between the pathogen and the plant (Mendgen and Hahn, 2002). Haustorium formation induces manifold structural, cellular and biochemical changes in the invaded cells (Gjetting et al., 2007; Schmidt and Panstruga, 2007; Fabro et al., 2008), suggesting active remodeling mediated by the pathogen.

Obligate biotrophs cannot be cultivated in absence of the host plant and comprise a group of phylogenetically unrelated organisms comprising oomycetes, basidiomycetes (e.g. rust fungi) and ascomycetes (e.g. powdery mildew fungi) (Panstruga, 2003; O'Connell and Panstruga, 2006). Among the oomycetes both obligate biotrophs like *Hyaloperonospora arabidopsidis*, causing downy mildew on Arabidopsis, and hemibiotrophs like *Phytophthora* ssp. form haustoria. Oomycetes are filamentous pathogens that morphologically resemble fungi; yet they are members of the chromista and more closely related to brown algae than fungi (Hein et al., 2009). The fungal phyla ascomycetes and basidiomycetes diverged around the same time as plants colonized land 460 million years

ago (Berbee, 2001). Convergent evolution of haustoria among this diverse group suggests a selective advantage for these pathogens, e.g. in gaining intracellular nutrients or suppressing host defense responses and cell death (Perfect and Green, 2001).

The intimate association between a plant host and a pathogen growing exclusively on plants sometimes favors specialization to a single host species as manifested by some members of the ascomycete clade Erysiphales (powdery mildews), which comprises some of the world's most frequently encountered plant pathogenic fungi (Glawe, 2008). Within the Erysiphales the tribe Blumeria includes only the genus *Blumeria*. The single species of this genus *Blumeria graminis* occurs only on Poaceae (Glawe, 2008). Among the morphological species of *B. graminis,* highly specialized formae speciales (ff. spp.) developed gradually through co-evolution with a single host species, e.g. *Bgh* for barley. Phylogenetic analyses revealed nine distinct groups among *B. graminis* formae speciales (Inuma et al., 2007). Even though they share common loci for pathogenicity, a forma specialis adapted to one host species is not adapted to cause disease on another host species (nonhost) (Tosa, 1989). Additionally, following a gene-for-gene relationship, single isolates of a given forma specialis, e.g. *Bgh*, are avirulent on host plants carrying cognate resistance genes (isolate-specific resistance) (Jorgensen, 1992a).

1.3 Co-evolution of plant resistance and pathogen effector proteins

Perhaps due to the unusual host specialization several gene-for-gene interactions have been studied with respect to obligate biotrophic pathogens. (Flor, 1955; Rairdan and Moffett, 2007). Especially in crop plants like barley, flax, rice, tomato and potato gene-for-gene interactions gained a great deal of attention, because they allow breeding for resistant crops. The major class of plant resistance proteins contains a central nucleotide-binding (NB) domain and a C-terminal LRR domain. Subclasses are distinguished by the C-terminal extension, which is either a TIR domain or a coiled-coil (CC) domain (Takken and Tameling, 2009). Pathogen avirulence genes are isolate-specific and encode structurally diverse effector proteins. Resistance protein-mediated defense signaling usually results in an HR and terminates pathogen growth. Effector recognition can be either direct or indirect.

1.3.1 Direct effector recognition

Direct binding of the plant resistance protein to its cognate effector protein (receptor-ligand model) has been experimentally verified in only a few cases. As an example, physical

interaction between the rice (*Oryza sativa*) resistance protein Pi-ta and its cognate rice blast (*Magnaporthe grisea*) effector protein AvrPita was demonstrated in yeast-two-hybrid and *in vitro* binding assays (Jia et al., 2000). *Pi-ta* encodes a cytoplasmic NB-LRR protein and *AvrPita* encodes a putative metalloprotease. Remarkably, single amino acid substitutions in either the fungal effector protease motif or the plant R protein LRR domain abolished interaction between the two proteins, indicating that Pi-ta binds Avr-Pita via its LRR domain (Jia et al., 2000).

The receptor-ligand model implies that plants must carry numerous *R* genes to cope with the effectors of myriads of microbes. This constraint is compounded by the diversity and marginal similarity among effector proteins (Grant et al., 2006; Gohre and Robatzek, 2008; Hogenhout et al., 2009). Given that the *A. thaliana* Col-0 genome encodes only 149 NB-LRR proteins (Meyers et al., 2003), direct recognition is most likely not the common mode of recognition.

1.3.2 Indirect effector recognition

Indirect effector recognition, described by the “guard model”, envisages resistance proteins physically interacting with host targets of effector proteins. In this model, effector-induced alterations of the guarded host protein activate the resistance protein thus initiating defense responses (Dangl and Jones, 2001). Host target proteins may include defense components and host proteins involved in nourishing the pathogen (Dangl and Jones, 2001).

The conceptual framework of the guard model encompasses complex interactions involving host proteins targeted and guarded by multiple effector and resistance proteins. One of the best studied interactions involves Arabidopsis RIN4 (RPM1 Interacting Protein 4), which is guarded by the two CC-NB-LRR proteins RPM1 (Resistance to *P. syringae* pv. Maculicola 1) and RPS2 (Resistance to *P. syringae* 2) (Axtell et al., 2001; Mackey et al., 2002). RIN4 is targeted by three sequence-unrelated *P. syringae* effectors - AvrRpm1, AvrB and AvrRpt2. AvrRpt2 is a cysteine protease and cleaves RIN4, thereby activating RPS2 (Axtell and Staskawicz, 2003; Mackey et al., 2003). Intriguingly, AvrRpt2 is delivered into the host cell as a pre-protein that requires activation by a host cyclophilin (Coaker et al., 2005). Likely, RIN4 is not the physiological main target of AvrRpt2, because it still enhances bacterial growth in a *rin4* mutant plant and because AvrRPT2 cleavage sites exist in ca. 125 Arabidopsis proteins (Belkhadir et al., 2004; Chisholm et al., 2005; Kim et al., 2005b). RIN4 has been suggested as a convergence point between ETI

and PTI due to its interaction with the NDR1 (Non-Race specific Disease Resistance 1) protein and the observation that RIN4 appeared to be required to retain RPS2 and RPM1 in an inactive state (Axtell and Staskawicz, 2003; Mackey et al., 2003; Day et al., 2006). Recently, another important function of RIN4 was put forward in regulating stomatal aperture to allow pathogen entry through interaction with the plasma membrane ATPases AHA1 and AHA2 (Liu et al., 2009). In a similar fashion, two rapeseed resistance proteins, Rlm4 and Rlm7, guard the same virulence target of the *Leptosphaeria maculans* effector AvrLm4-7 (Parlange et al., 2009) indicating an important role in pathogenicity for this virulence target. However, no functions have been assigned to either the involved effector or the plant target. Despite its comprehensive framework, the guard model only allows recognition of effectors with host targets. It is ineffective against effectors with defensive targets, e.g. effectors masking MAMPs (Stergiopoulos and de Wit, 2009).

1.3.3 Resistance genes against haustoria-forming, obligate biotrophic pathogens

Effectors of obligate biotrophic oomycetes and fungi are recognized by intracellular TIR-NB-LRR or CC-NB-LRR resistance proteins. Recognition is thought to occur via the LRR domain, while the NB domain is believed to mediate downstream defense signaling (DeYoung and Innes, 2006; Takken and Tameling, 2009). Surprisingly, effector recognition of obligate biotrophic fungi (rusts and powdery mildews) appears to be mainly direct.

Resistance against the oomycete *H. arabidopsidis* is, among others, mediated by the RPP13 (Recognition of *Peronospora parasitica* 13) intracellular CC-NB-LRR protein. Highly diverse alleles encoded by a single locus determine recognition of *H. arabidopsidis* isolates encoding the ATR13 effector protein (Bittner-Eddy et al., 1999). By combining functional studies with phylogenetic analysis, Hall and colleagues determined that ATR13 recognition is mediated by alleles in just one *RPP13* clade (Hall et al., 2009). The authors concluded that *RPP13* alleles in other clades detect further effector proteins. Additionally, they demonstrated, that a least one resistance gene, unlinked to *RPP13*, also detects *ATR13* (Hall et al., 2009).

Flax (*Linum usitatissimum*) encodes 31 specificities at five loci, designated *K, L, M, N* and *P*, for resistance against the basidiomycete *Melampsora lini*, causal agent of flax rust (Ellis et al., 2007). All five loci encode TIR-NB-LRR proteins, predicted to be intracellular. Alternative alleles of a single gene at the L locus revealed that the highest level of

sequence diversity occurs in the LRR encoding domains (Ellis et al., 2000). Direct binding of the flax rust effector AvrL567 to the flax resistance proteins L5 and L6 was demonstrated in a yeast two-hybrid assay (Dodds et al., 2006).

Resistance to *Bgh* in barley is governed by at least 85 dominant or semi-dominant mildew (*ML*) resistance genes including around 30 allelic genes at the *Mildew resistance locus A* (*MLA*). *MLA* genes encode CC-NB-LRR proteins, sharing > 90% sequence identity and conferring cell-autonomous resistance to different *Bgh* isolates by different, yet overlapping LRRs and by the C-terminal non-LRR region (Jorgensen, 1994; Halterman et al., 2001; Zhou et al., 2001; Shen et al., 2003; Halterman and Wise, 2004; Shen et al., 2007). The majority of the MLA10 protein localized to the cytoplasm and approximately 5% to the nucleus. Perturbation of the nucleo-cytoplasmic partitioning decreased MLA10-mediated disease resistance (Shen et al., 2007). Furthermore, a recent study revealed 34 sites of positive selection in the MLA proteins. The positively selected sites are mainly located in the solvent-exposed loops of the LRR domain (Seeholzer, 2009, submitted). Due to this domain-restricted pattern of positive selection, direct binding of *Bgh* AVR_A effectors to MLA receptors was predicted (Seeholzer, 2009, submitted).

1.3.4 Avirulence genes of haustoria-forming, obligate biotrophic pathogens

Much less is known about the structure and function of the cognate effector proteins from obligate biotrophs. Six cytoplasmic effectors from oomycete pathogens were discovered through their avirulence function including Avr3a, AVR-blb1 and Avr4 from *Phytophthora infestans*; Avr1b-1 from *Phytophthora sojae* as well as ATR1 and ATR13 from *H. parasitia* (Allen et al., 2004; Armstrong et al., 2005; Rehmany et al., 2005; Vleeshouwers et al., 2008; Van Poppel et al., 2009). Known oomycete intracellular effectors are modular proteins with an N-terminal signal peptide for secretion, followed by a translocation motif and a C-terminal domain associated with both virulence and avirulence activity (Kamoun, 2006; Win et al., 2007). While *P. infestans* virulent and avirulent *Avr3a* alleles encode proteins that only differ at two amino acid positions, *H. arabidopsidis* ATR13 exhibits extreme levels of amino acid diversity (Allen et al., 2004; Armstrong et al., 2005). Sequencing of *ATR13* in 16 *H. arabidopsidis* isolates not only revealed that polymorphisms occur across the entire protein, but also identified distinct sites for RPP13 recognition specificity and conserved sites involved in pathogenicity (Allen et al., 2008).

In flax rust, genetic analysis determined approximately 30 *Avr* genes (Lawrence et al., 1981b; Lawrence et al., 1981a). Recently, four flax rust effectors, AvrP4, AvrM, AvrP123 and AvrL567, were identified among haustorially expressed secreted proteins (HESPs) as having avirulence activity in the contex of their cognate flax resistance proteins (Catanzariti et al., 2006). Of twelve *AvrL567* sequence variants - from six flax rust isolates - only seven variants induced HR in flax encoding the cognate resistance genes and interacted with the respective resistance proteins in yeast (Dodds et al., 2006). In addition, evidence for diversifying selection acting on the *AvrL567* genes suggested that these genes have been involved in a gene-specific arms race with the corresponding flax *R* genes (Dodds et al., 2004; Dodds et al., 2006). The positively selected sites were surface-exposed and structural modeling indicates similar physical properties of avirulence and virulence variants (Wang et al., 2007). Taken together, selection seems to have acted on *AvrL567* to modify binding affinity to flax R proteins, yet to retain a presumed virulence function.

In barley powdery mildew (*Bgh)* isolates more than 25 independent *AVR* genes have been described (Brown and Jessop, 1995; Jensen et al., 1995). By positional cloning Ridout and colleagues isolated the first (barley) powdery mildew effectors, AVR_{A10} and AVR_{K1} (Ridout et al., 2006). Presence of AVR_{A10} was shown to stimulate the nuclear association between MLA10 and the plant-specific transcription factor WRKY2. This association is thought to result in PTI repression (Shen et al., 2007). Surprisingly, the expression of AVR_{A10} in host epidermal cells of the *MLA10* genotype did not result in HR-like cell death (Shen et al., 2007). The presumptive *Bgh* effector proteins are peculiar in being the only effectors from haustoria-forming pathogens and in fact the majority of effectors proteins from filamentous pathogens that do not have a predicted signal peptide for secretion. Besides this discrepancy, the *Bgh* effector genes as well as the other characterized *Avr* loci of obligate biotrophs encode small proteins with no sequence similarity to known proteins.

1.4 Effectors – executive pathogenicity agents

Effectors were initially identified by their ability to elicit a host resistance response. Meanwhile, these structurally and functionally diverse proteins are accepted as crucial components for pathogen virulence. By targeting diverse cellular functions in the host, effectors create a favorable environment for growth and proliferation of the pathogen. Common effector functions involve suppression or evasion of the host immune system and might also involve nutrient acquisition from the host. Indirect evidence for host defense suppression during the barley-*Bgh* interaction is provided by observations that barley cells

containing *Bgh* haustoria were more susceptible to otherwise avirulent or non-adapted powdery mildew isolates (Kunoh et al., 1990; Lyngkjaer et al., 2001).

Effectors have been described by plant pathologist in other terms, including elicitor, avirulence protein, virulence protein and toxin. Each of these terms only denotes a single function to the pathogen protein, which has been observed experimentally. The neutral term “effector” comprises all the possible functions of a pathogen molecule and is better suited to capture the ambivalent nature of effectors resulting from their virulence activity, which may betray them to the host and restrict growth by eliciting an HR (Kamoun, 2007). Effector targeting of host proteins implies that effectors are translocated from the pathogen into host cells. Pinpointing a translocation signal in bacteria and oomycete pathogens has greatly advanced the identification of effectors in these pathogens.

1.4.1 Effector translocation into the host

Bacterial effectors from Gram-negative bacteria are delivered into plant host cells via a needle-like type III secretion system that is encoded by the *HR and pathogenicity* (*hrp*) and *hrp conserved* (*hrc*) genes (Collmer et al., 2004; Galan and Wolf-Watz, 2006). Numerous type III effectors were identified based on the presence of a signal peptide (SP), conserved HrpL-dependent sequences in the promoter and the combination with translocation assays involving nonpathogenic strains (Lindeberg et al., 2006). Similarly, cytoplasmic oomycete effectors can be identified by the presence of a signal peptide and the RXLR translocation motif that is present in all characterized oomycete effectors (Kamoun, 2006, 2007). Position and sequence of the RXLR motif are similar to and interchangeable with the host targeting signal (PEXEL motif) required for translocation of proteins from the malaria parasite (*Plasmodium* spp.) into host red blood cells (Bhattacharjee et al., 2006). Fusion of the bacterial *ß-glucuronidase* (*GUS*) gene to the SP-RXLR domain resulted in GUS activity only in plant cells inclosing haustoria, pointing to haustoria as the source for effector delivery (Whisson et al., 2007).

Haustoria have also been suggested as a source for effectors in plant-fungal interactions, because transcripts encoding flax rust effectors were enriched in and isolated from haustoria-specific cDNA libraries (Catanzariti et al., 2006). Furthermore, the bean rust effector *Uf*-RTP1 was detected inside the EHM and the host cytoplasm by immunofluorescence and electron microscopy thus providing direct evidence for effector translocation into the host cells (Kemen et al., 2005). So far, no fungal translocation motif

is known. However, uptake of the intracellularly acting protein toxin Ptr ToxA from *Pyrenophora tritici-repentis* (*Ptr*) in sensitive wheat cultivars appears to depend on a solvent exposed Arg-Gly-Asp (RGD)-containing loop that interacts with the plasma membrane (Manning et al., 2008). The crystal structure of ToxA supports the model of toxin binding to an integrin-like receptor to gain entry into the host cell (Sarma et al., 2005). Pathogen presence is not required for the translocation of proteins from oomycete and fungal pathogens, indicating a host-encoded translocation mechanism (Catanzariti et al., 2006; Dou et al., 2008a; Birch et al., 2009).

1.4.2 Virulence function of bacterial effectors

Studies on virulence function of effectors are most advanced in Gram-negative bacteria, owing to the genetic amenability and ease of quantitative infection assays available for these pathogens. Individual type III effectors interfere with host gene expression, cellular processes, signaling pathways, RNA metabolism and protein degradation (Block et al., 2008).

The *P. syringae* effector HopAA1-1 was identified in a large scale screen for type III effectors inhibiting yeast growth and it induces cell death in both yeast and plants by interfering with mitochondrial respiration (Munkvold et al., 2008). RNA metabolism was targeted by *P. syringae* effector HopU1, a mono-ADP-ribosyltransferase (ADP-RT) presumably by disrupting the function of the glycine-rich RNA-binding protein (GR-RBP) GRP7. GR-RBPs are thought to stabilize or process specific pathogen-responsive mRNAs. HopU1 disruption of GRP7 could thus reduce the amount of immunity-related mRNA in favor of the pathogen (Fu et al., 2007). Another *P. syringae* effector, HopM1, interfered with cell-wall associated defense responses by targeting the host protein AtMIN7 to proteasomal degradation (DebRoy et al., 2004; Nomura et al., 2006). AtMIN7 is a GTPase-exchange factor (GEF) of the adenosine diphosphate ribosylation factor (ARF) subfamily. ARF-GEFs are important for vesicle trafficking by activation of Ras-like small GTPases (Mouratou et al., 2005). HopM1 is thought to act as an adaptor for the ubiquitination machinery that marks proteins for proteasomal degradation (Nomura et al., 2006). Direct targeting of the host ubiquitination machinery was shown for the *Shigella flexneri* effector OspG, a protein kinase binding ubiquitin conjugating enzymes (UBCs), thus interfering with NFκB activation (Kim et al., 2005a).

Both mammalian and plant pathogenic bacteria mimic components of eukaryotic protein machineries (e.g. ubiquitin and small GTPases) to interfere with host processes (Abramovitch et al., 2003; Angot et al., 2006; Janjusevic et al., 2006; Angot et al., 2007; Block et al., 2008; Galán, 2009). For this reason the primary amino acid sequences of type III effectors often do not provide information about the function. Functional redundancy further impedes the elucidation of a biological task, because deletion of single type III effectors rarely affects the noticeable virulence of a given strain (Grant et al., 2006). Consequently, both the biochemical activity and the host target that serves as the effector substrate are only known for few type III effectors.

1.4.3 Virulence function of oomycete effectors

Among eukaryotic pathogens, the identification of oomycete effectors is most advanced. Sequenced genomes of several oomycete species enabled the genome-wide identification of potential effector repertories, resulting in the distinction of intracellular and extracellular effectors (Kamoun, 2006). The virulence function of many extracellular effectors involves protection against hydrolytic host enzymes, among them several plant pathogenesis-related (PR) proteins such as chitinases, proteases and glucanases (van Loon et al., 2006). Protection against host hydrolases is thought to have evolved as an active counter-defense mechanism (Rooney, 2005; van der Hoorn and Kamoun, 2008). The *Phytophthora infestans* effectors EPIC2B, EPI1 and EPI10 exert this function to inhibit the apoplastic protease PIP1 (*Phytophthora*-inhibited protease 1) (Tian et al., 2007). Additionally, *Phytophthora* spp. secrete glucanase inhibitors that inhibit the host apoplastic enzyme endo-β-1,3 glucanase (Rose et al., 2002; Damasceno et al., 2008).

Little is known about the intracellular activity of oomycete effectors. The avirulent form of the *P. infestans* RXLR effector Avr3a suppressed INF-mediated cell death in *Nicotiana benthamiana* (Bos et al., 2006). Similarly, *P. sojae* Avr1b suppressed PCD triggered by the mouse BAX protein in yeast and *in planta* (Dou et al., 2008a). Suppression of PCD depends on conserved motifs in the C-terminal domains of Avr1b, which were identified by computational analysis (Dou et al., 2008b; Jiang et al., 2008). ATR1 and ATR13 from *H. arabidopsidis* have been implicated in PTI suppression (Sohn et al., 2007). Suppression of PCD is unquestionable an important prerequisite for biotrophic pathogens depending on living host cells. Nevertheless, only the physiological effector targets and the intrinsic effector activity will ultimately help to unravel how oomycetes interfere with host signaling and how they establish disease.

1.4.4 Virulence function of fungal effectors

Several extracellular fungal effectors were biochemically purified from plant intercellular fluids. One of these effectors, *C. fulvum* Avr2, inhibits apoplastic tomato cysteine proteases like Rcr3 (required for *Cladosporium* resistance 3). Intriguingly, Avr2 also targets the same protease PIP1 as the oomycete effectors EPIC2B, EPI1 and EPI10 (Rooney, 2005; Tian et al., 2007; Shabab et al., 2008), indicating that PIP1 is a common host target for different pathogens. Two further *C. fulvum* effector proteins, Avr4 and Ecp6, contain chitin-binding motifs (Van Den Burg et al., 2006; Bolton et al., 2008). Whereas the biochemical activity of the lysine-motif (LysM-) containing Ecp6 proteins remains to be discovered, the invertebrate chitin binding domain-containing protein Avr4 was found to protect the fungal cell wall from hydrolysis by plant chitinases (Van Den Burg et al., 2003; Van Den Burg et al., 2006).

Besides protection against hydrolytic enzymes at least one more interesting function is described for fungal effectors. Recently, the *Fusarium oxysporum* f. sp. *lycopersici* (Fol) effector Avr1 was found to suppress *R*-gene mediated resistance (Houterman et al., 2008). Secretion of this effector by the xylem-invading *Fol* fungus triggers resistance in the tomato plants carrying the matching *I-1* resistance gene, but suppresses resistance in tomato plants carrying one of two other *R* genes, *I-2* or *I-3*. Even though Avr1 was isolated from xylem sap of *Fol*- infected tomato plants, it remains to be shown where it exerts its function (Houterman et al., 2008).

Furthermore, the *U. maydis* effector Protein Essential during Penetration1 (Pep1) was identified by a genome-wide screen for secreted proteins without matches in data base entries (Doehlemann et al., 2009). Pep1 accumulates at sites of cell-cell passage in the apoplast and appears to be involved in the suppression of plant defense responses. Complementation of a Δpep1 mutant strain with an orthologous sequence of the barley smut fungus *Ustilago hordei* led to the conclusion that Pep1 has a conserved, yet unknown, function essential for establishing compatibility between host and plant (Doehlemann et al., 2009).

PEP1 is an exceptional effector, because Δpep1 mutants arrest during penetration of the epidermal cell and elicit a strong plant defense response, indicating that its loss imposes a severe fitness penalty on the fungus (Doehlemann et al., 2009). Contrastingly, many fungal effectors are not required for virulence (Stergiopoulos and de Wit, 2009). Partly this might

be due to overlapping functions of effectors as illustrated by the *C. fulvum* effectors Ecp6 and Avr4, which protect the fungus against plant chitinases, yet deploy completely different protective mechanisms. Additionally, insensitive infection assays might result in ignorance towards subtle changes.

1.5 Aim of thesis

To shed light on the pathogenicity mechanisms of obligate biotrophic pathogens, we attempted to identify effector proteins from the barley powdery mildew fungus *Bgh* by screening publicly available EST databases for *Bgh* ESTs encoding small, secreted, novel proteins. Effector candidates enhancing *Bgh* haustorium formation in a transient expression assay were further examined by yeast-based functional assays, localization studies and expression analyses. A yeast two-hybrid approach led to the identification of host targets for two *Bgh* effector candidates.

Genome sequencing of *Bgh* and two further powdery mildew species (*Golovinomyces orontii* and *Erysiphe pisi*) was underway during the course of my thesis. Towards the end of my thesis, raw sequence data became available and allowed the identification of a *Bgh*-specific gene family. Intriguingly, this gene family fulfilled the recently predicted criteria for cognate effectors of the allelic series of barley *MLA* resistance genes. These *Bgh* gene family members encode predicted secreted ribonucleases, thus indicating a presumptive virulence activity inside the host cell. Characterization of the gene family by phylogenetic and functional analyses complemented the study of *Bgh* effectors and their host targets.

2 Materials and Methods

2.1 Plant and Fungal Material

The following barley (*Hordeum vulgare*) lines were used for this study: 'Ingrid' (*MLO*), 'Golden Promise' (*MLO*), 'I10' (near-isogenic line in 'Ingrid' background containing *MLA12*), 'P01' (near-isogenic line in 'Pallas' background containing *MLA1*), 'P03' (near-isogenic line in 'Pallas' background containing *MLA6* and *MLA14*). All barley seedlings were grown at 20° C and 16 h light/8 h darkness in a protected environment.

The barley powdery mildew *Bgh* (*Blumeria graminis* f. sp. *hordei*) isolates K1 (*AvrMLA1, virMLA6, virMLA12, virMLG*) and A6 (*virMLA1, AvrMLA6, AvrMLA12, AvrMlLG*) were propagated on barley lines 'I10' and 'P01', respectively, for mutual exclusion. Plants or detached leaves were kept at 20° C, 60% relative humidity, and 16 h light/8 h darkness after inoculation with *Bgh* conidiospores.

The wheat powdery mildew *Bgt* (*Blumeria graminis* f. sp. *tritici)* isolate JIW2 was propagated on the susceptible wheat (*Triticum aestivum*) cultivar Cerco cultivated at22 °C 16 h light/8 h darkness, 60 % relative humidity (Elliott et al., 2002) .

The Arabidopsis (*Arabidopsis thaliana*) powdery mildew *Golovinomyces orontii* was propagated on Arabidopsis Col-0 plants cultivated at 20° C and 16 h light/ 8 h darkness, 80% humidity in a protected environment. Inoculated *A. thaliana* plants were kept at 22° C, 70% humidity, 500 $\mu Em^{2}/s$ and 12h light/12 h darkness in a protected environment.

2.2 EC and AC cDNA Isolation and Sequence Analysis

Total RNA was isolated from *Bgh* -infected barley leaves (cv. Golden Promise) with the RNA-Easy kit (Quiagen) according to the manufacturer's instructions. Two micrograms of RNA were used for cDNA synthesis with the SuperScriptTM II RNase Reverse Transcriptase kit (INVITROGEN) according to the manufacturer's instructions. Sequencing reactions were performed using the Big Dye-terminator chemistry (Sanger et al., 1977) and analyzed with Applied Biosystems (Weiterstadt, Germany) Abi Prism 377 and 3700 sequencers. BLAST searches were made at the Consortium for the Functional Genomics of Mircobial Eukaryotes (http://cogeme.ex.ac.uk/; (Soanes et al., 2002; Soanes and Talbot, 2006) and the National Center for Biotechnology Information

(http://www.ncbi.nlm.nih.gov/BLAST; (Altschul et al., 1990; Altschul et al., 1997). Putative signal peptides were predicted by SignalP 3.0 (http://www.cbs.dtu.dk/services/SignalP/; (Nielsen et al., 1997; Dyrløv Bendtsen et al., 2004). Local BLAST searches against the draft genome sequence of *Blumeria graminis* f.sp. *hordei*, *Erysiphe pisi* and Golovinomyces *orontii* were performed with the BioEdit software (http://www.mbio.ncsu.edu/BioEdit/bioedit.html). Searches for protein motifs were performed by InterProScan (http://www.ebi.ac.uk/Tools/InterProScan/; (Quevillon et al., 2005). Three dimensional structure predictions were obtained with the Protein Homology/analogY Recognition Engine (http://www.sbg.bio.ic.ac.uk/phyre/; (Kelley and Sternberg, 2009). Pairwise and multiple sequence were aligned with ClustalW (http://www.ebi.ac.uk/Tools/clustalw2/index.html; (Larkin et al., 2007) and manually edited with the BioEdit software.

2.3 Plasmid constructs

Gateway® cloning technology (INVITROGEN, www.invitrogen.com) was used to create the destination vectors used in this study (Supplementary Table 1). Briefly, PCR products containing inserts flanked by attB sites were recombined into the vector pDONR201 (INVITROGEN) by a BP reaction to create entry clones with attL sites. Inserts of the entry clones were recombined into the destination vector by a LR reaction to create the expression constructs. The pUCSPYNE, pUCSPYCE, pESPYNE and pESPYCE vectors harboring N- and C-terminal segments of enhanced YFP were adapted to be Gateway® compatible and were previously described (Walter et al., 2004; Waadt and Kudla, 2008) The pSST-GWY vector harboring the truncated yeast invertase was adapted to be Gateway® compatible (Cristina Micali).

2.4 Transient gene expression in single barley epidermal cells

Ballistic transformation of detached barley leaves was carried out as described previously (Schweizer et al., 1999; Shirasu et al., 1999). Briefly, gold particles of 1 µm diameter were coated with reporter plasmids plus effector plasmids, followed by biolistic delivery into seven days old barley leaves using a particle gun equipped with a Hepta adapter (Bio-Rad Biolistic PDS-1000/He).

To determine the haustorium index after transient effector gene expression, bombarded leaves were inoculated with a high density of powdery mildew conidiospores at four hours after bombardment. Two days after inoculation, bombarded leaves were infiltrated with

GUS staining solution (Schweizer et al., 1999). Epiphytic fungal structures were marked by Coomassie Brilliant Blue. Leaf epidermal cells attacked by the appressorial germ tube of powdery mildew sporelings were evaluated by light microscopy for the presence or absence of haustoria. The haustorium index was calculated as the percentage of transformed cells exhibiting one or multiple haustoria in relation to the total number of transformed cells attacked by powdery mildew sporelings.

2.5 RNA isolation and quantitative RT-PCR

Total RNA was isolated from *Bgh* K1 infected barley leaves (cv. Golden Promise) at different time points after inoculation (0, 3, 6, 12, 24, 48 hpi) as described above. Quantitative RT-PCR was performed using the cDNA and gene specific primers (Supplementary Table 1). Each cDNA was amplified by real-time PCR using SYBR Green and the IQTM5 PCR system (BIO-RAD). *Bgh β-tubulin* expression was used to normalize the expression value in each sample, and relative expression values were determined against the average value of time point 0 hpi with the comparative Ct method ($2^{-\Delta\Delta Ct}$). Three to four technical replicates per sample were included. Experiments were repeated twice with independent biological material.

2.6 Transformation of *Arabidopsis thaliana*

Full-length and truncated version, lacking the N-terminal signal peptide, of GoEC2 were cloned into the binary destination vectors pPAM-PAT-GWY and pAM-PAT-GWY-3x HA and ecotype Col-0 was transformed with the resulting constructs using the floral-dip method as described (Clough and Bent, 1998).

2.7 Transformation of yeast

Preparation of chemocompetent yeast cells and transformation by the high-efficiency lithium acetate method was performed as described (Gietz and Woods, 2002).

2.8 Yeast signal sequence trap

The N-termini of EC1-EC7 and AVR_{A10} were cloned into the entry vector pDONR201 and recombined into the destination vector pSST-GWY. Constructs were transformed into yeast strain YTK12 and transformed cells were grown for four days at 30°C on synthetic dropout (SD) medium containing glucose lacking trytophane (SD-GLU/-T) to select for the presence of the plasmid. Transformed yeast cells were grown overnight in SD-GLU –T.

Equal amounts of yeast cells were transferred to SD medium containing sucrose and yeast growth was monitored for 10 hours. The SST vector harboring the full-length invertase and the SST vector harboring the truncated invertase, lacking both its START methionine codon and its signal peptide, were used as a positive and negative control, respectively (Jacobs et al., 1997).

2.9 Yeast BAX Assay

To determine whether EC-encoding plasmids rescued yeast from BAX-induced lethality, truncated *EC1, 2, 5* and *6* genes lacking the N-terminal sequence encoding the signal peptide were cloned under the control of a galactose-inducible promoter in the destination vector pYES2. The constructs were co-transformed with a construct harboring mouse BAX into yeast strain WCGN. Mouse Bcl-xL cloned into pYES2 was used as a positive control for PCD suppression in these experiments. Cells were grown for four days at 30°C on SD medium with glucose lacking uracile and leucine (SD-GLU/–UL) to select for the presence of both plasmids. Co-transformed cells were plotted as serial dilutions on SD medium containing galactose lacking uracile and leucine (SD-GAL/-UL) to induce expression of the proteins from the galactose-inducible promoter. Cells were incubated for four days and photographed. Experiments were performed twice.

2.10 Yeast Growth Inhibition Assay

Yeast transformants containing the pYES2-EC fusion constructs (see above) were plotted as serial dilutions on SD medium containing galactose and lacking uracile to induce expression of the proteins from the galactose-inducible promoter. Plates were incubated for two days at 30° C and photographs were taken. Experiments were performed twice.

2.11 Fluorescent Microscopy

For subcellular localization studies, barley leaves were biolistically co-transformed with various EC-YFP (yellow fluorescent protein) or BiFC fusion constructs and an ER-marker fused to either CFP (cyan fluorescent protein) or mCherry (Nelson et al., 2007). Confocal microscopy of the transformed leaves was carried out using the Zeiss LSM510 META confocal microscope (ZEISS, www.zeiss.com). A 40x plan-apochromat water immersive lens (ZEISS) with a numerical aperture of 1.2 was used. CFP and YFP were excited with the 458 or 514 nm laser line of an Argon-ion laser, respectively. Fluorescence and excitation light were separated by a dual dichroic mirror, which reflected both the 458 and

514 nm laser lines. A second dichroic NFT515 filter was used to split the emission light into the CFP and YFP detection channels. The CFP fluorescence was selected by a 480-520 nm bandpass filter and YFP fluorescence was recorded by the META detector array with the wavelength range set to 526-569 nm. mCherry and YFP were excited with the 543 or 514 nm laser line of an Argon-laser, respectively. Again, a dual dichroic mirror reflected both the 543 and the 514 nm laser line. The second dichroic FNT543 filter was used to split the emission light into the mCherry and YFP detection channels. YFP fluorescence was recorded as described above and mCherry fluorescence was selected by a 565-615 nm bandpass filter. For all fluorophores, excitation and detection of emission light using the filter combinations described above was performed in independent tracks to limit spectral bleed through.

To determine the number of GFP expressing barley cells, bombarded leaves were examined at two and four days after bombardment using a microscope with an excitation filter of 450-490 nm. The emission light was filtered through a 515-565 nm bandpass filter before observation (Leica, GFP plus).

2.12 FRET analysis

FRET APB (acceptor photobleaching) experiments were performed essentially as described (Karpova et al., 2003). Barley leaf epidermal cells were ballistically co-transformed with plasmid constructs encoding either EC4–YFP and *Hv*UBC-E2-CFP or EC6-YFP and *Hv*TPMT-CFP. To assess the occurrence of FRET in cells co-expressing both fluorescent proteins the YFP fluorophores were bleached by iteratively scanning a selected ROI (region of interest) 40–50 pulses with the 514 nm argon laser line set to 100% intensity. Before and after APB, CFP and YFP intensity images were recorded to follow and evaluate changes in donor and acceptor fluorescence. In case FRET occurred between the donor and acceptor molecules, an increase in CFP fluorescence intensity in the bleached area will be visible. From the increase in CFP fluorescence the FRET efficiency can be calculated, which can be used to compare independent FRET measurements. The FRET efficiency (*E*F) was calculated using the following formula $EF = (I5 - I4) \times 100 / I5$, where $I5$ is the CFP fluorescence intensity after YFP photobleaching and $I4$ is the intensity just before photobleaching in the selected ROI (Karpova et al., 2003).

2.13 Yeast two-hybrid screen

Bait constructs were generated by cloning EC1, EC2, EC3, EC4, EC5 and EC6 RT-PCR products lacking the N-terminal signal peptide into the Gateway compatible expression vector pLexA. The plasmids were transformed into *Saccharomyces cerevisiae* strain EGY48 (MATa, *ura3, his3, trp1, LexAop (x6)-LEU2*, containing p8op-*lacZ*) to assess LexA-EC-mediated protein expression, transcriptional activity and leucine requirement as described (Shen et al., 2007). A prey cDNA library from RNA of *Bgh*-infected barley leaves, amplified with a poly T primer (Courtesy of Pietro Piffanelli) was transformed into strain YM4271 (MAT α, *ura3- 52, his3- 200, lys2-801, ade2-101, ade5, his3, trp1, trp1-901, leu2-3, 112, tyr1-501, gal4Δ, gal80Δ,ade5::hisG*). Cells were plated on SD medium lacking tryptophane (SD –T) and grown at 30°C for 2-3 days to select for primary transformants. Colonies were scraped from plates and suspended in chilled YPAD medium and stored as 1 ml aliquots with glycerol at 25% final concentration in -80°C. Interaction mating was essentially performed as described (Kolonin et al., 2000). Briefly, overnight bait cultures were raised in SD medium containing 4% glucose lacking uracile and histidine (SD-UH). The frozen prey library aliquots were re-generated in 20 times volume of pre-warmed YPAD for 1 h at 30°C. 2 x 10^8 cells of each bait culture were mixed with 2 x 10^8 cells of the library and subjected to mating on YPAD plates overnight at 30°C. Expression of the prey library fusion was induced in GAL/-UHT medium for 6 h at 30°C. Cultures were plated on GAL/-UHLT plates to select for barley cDNA clones interacting with either EC4 or EC6. Colonies were picked and stamped onto GAL/-UHT + X-gal plates to assess the strength of the interactions. Yeast strains were also selected on media containing glucose for negative controls: GLC/-UHT X-Gal and GLC/-UHTL. Colony PCR using dark blue colonies, indicative of strong interactions, was performed to amplify cDNAs using pB42AD primer set S39/S40 flanking the cDNA insertion site (Supplementary Table1). Amplified inserts were sequenced and analyzed by BLAST. Individual pB42AD plasmids were isolated and retransformed into yeast strain YM4271 to confirm the interaction. We also isolated full-length coding sequences for *HvARF-GAP*, *HvUBC-E2* and *HvTPMT* by RT-PCR from barley leaves based on EST sequence information obtained from EST clones of the epidermis-specific HO barley cDNA library (Zierold et al., 2005) and retransformed these into YM4271 to confirm interactions as described above.

2.14 Yeast Crude Protein Extracts

Yeast cells transformed with LexA-EC fusion constructs were grown overnight in SD medium lacking histidine and uracile and yeast cultures grown to similar OD_{600} units were pelleted by centrifugation. Crude extracts were made from these pellets by freezing in liquid nitrogen and subsequent boiling for five minutes for at least three rounds. Equal volumes of crude extracts dissolved in loading buffer were separated by SDS-PAGE and analyzed by immunoblotting. Proteins were visualized by chemiluminescence using anti-LexA (Santa Cruz Biotechnology) primary antibody and horseradish peroxidase (HRP)-labeled secondary antibody and ECL reagent (GE Biosciences).

2.15 Phylogenetic Analyses

The AC protein sequences were aligned with the ClustalW program using default parameters. A phylogenetic tree was constructed using the neighbor-joining method (Saitou and Nei, 1987) of the Molecular Evolutionary Genetics Analysis (MEGA) software version 4.1 (http://www.megasoftware.net/index.html; (Kumar et al., 2008) with the following parameters: pairwise deletion of gaps, Poisson correction, both transitions and transversions substitutions included and 1000 bootstrap replicates. Fungal and plant RNAses were identified in the protein databases hosted by NCBI. These proteins were analyzed using InterProScan to detect the RNase domain. Those protein parts of the RNases and the AC proteins corresponding to the RNase domain were included in a ClustalW alignment that was used for construction of the phylogenetic tree with the MEGA 4.1 software employing the same method and parameters as listed above.

3 Results

3.1 Identification and functional characterization of effector candidates

3.1.1 Candidate effectors were identified bioinformatically

The majority of previously described fungal effector proteins are characterized by their small size, their N-terminal signal peptide for secretion and their unknown biochemical activity (Dodds et al., 2004; Kemen et al., 2005; Catanzariti et al., 2006; Van Den Burg et al., 2006). Applying these criteria, we screened the publicly available COGEME database (Soanes and Talbot, 2006) that contains 6944 *Bgh* ESTs comprising 3241 unisequences for sequences that had no homology to known genes or proteins. This criterion holds true for 72% of the *Bgh* unisequences in the COGEME database (Soanes et al., 2002). Unisequences represent a set of unique gene sequences, each consisting of either a single EST or a sequence contig composed of a group of overlapping ESTs. A subset (224) of the unisequences predicted to be "unknown" was selected as "candidate effector cDNAs" based on the presence of a potential full-length open reading frame (ORF) including a putative start codon, a stop codon and a polyA tail. The conceptual protein sequences of these "candidate effector" unisequences were analyzed for the presence of a predicted signal peptide using the SignalP 3.0 algorithm (Bendtsen et al., 2004). In 28% (62 unisequences) the presence of a signal peptide was predicted for the "candidate effector" unisequences.

To verify their COGEME annotation as "unknown proteins", each of these 62 unisequences was subjected to analysis against homologous sequences in the GenBank non-redundant (nr) database using the BLASTX and tBLASTX algorithm with a cut-off for significant homology of EXPECT value $<1e^{-5}$ (Altschul et al., 1990). For the majority of these pre-selected *Bgh* unisequences the best BLAST matches were to fungal proteins annotated as "hypothetical", "predicted" or "putative", i.e. proteins of unknown function that were predicted from automated whole-genome sequencing and annotation projects. Some BLASTX matches were to proteins of known function. Out of these, only those unisequences were chosen for further analysis in which the similarity was related to structural features of the conceptual protein sequence, e.g. glycine-rich proteins, or in which the annotated function was potentially related to pathogenesis, e.g. proteases. Additional protein domains were identified by analysis with InterProScan (Quevillon et al.,

2005) and included protease-motifs, proline-rich domains, cysteine-rich domains and cerato-platanin motifs. As a result of these bioinformatic analyses, 46 *Bgh* unisequences were selected as “candidate effectors”.

The 46 “candidate effector” cDNAs were amplified from RNA of *Bgh*-infected barley leaves. Given that many ESTs are single-pass sequences (reads from one DNA strand only) that frequently contain nucleotide polymorphisms between sequences of one contig as well as frame shifts (Soanes et al., 2002) we re-sequenced all isolated “effector candidate” cDNAs and subjected them again to SignalP analysis. In many cases, the isolated cDNAs were much smaller than the predicted ORF, suggesting potential mis-assemblies in the unigenes. In other cases, re-sequencing revealed sequencing errors in the ESTs that led to loss of the signal peptide prediction. In the end, 14 *Bgh* unisequences were chosen for further analysis and transient expression in barley (**Table 1**).

These 14 *Bgh* unisequences encode small proteins (ranging from 49 to 254 amino acids) with a predicted cleavable secretion signal peptide of 17-24 amino acids. One of these 14 unisequences, BgCon0039, has similarity to glycine-rich proteins (**Table 1**). BgCon0062 and BgCon0254 contain CFEM (8-cysteine, fungal, extracellular membrane) domains. These 60 amino acids long, cysteine-rich domains were initially identified in *M. grisea* and were found to be common in - but not restricted to - extracellular fungal membrane proteins (Kulkarni et al., 2003). For BgCon0034 a transmembrane domain is predicted at the C-terminus in addition to the N-terminal signal peptide. However, this domain did not direct a fluorophore-tagged version of the protein to a membrane and therefore appears to be a hydrophobic region (see below, **Figure 6**). BgCon1245 contains a cerato-platanin motif (**Table 1**). Cerato-platanin is a phytotoxic protein secreted by the ascomycete *Ceratocystis fimbriata*, which is similar to fungal hydrophobins (Carresi et al., 2006; Pazzagli et al., 2006).

Table 1. *Bgh* "candidate effectors" identified in the COGEME database

COGEME contig[A]	EC[B]	BLASTX (nr)	*E*-value[C]	Organism	SignalP score[D]	Protein signature[E]	Size (aa)	MW[F] (kD)
BgCon0039	EC1	Hypothetical protein	9 e-09	*Branchiostoma floridae*	0,977	SP[1]	155	16
BgCon0034	EC6	-	n.a.	n.a.	0,999	SP[1], TM[2]	114	11
BgCon0062	EC2	Predicted protein	4 e-06	*Botryotinia fuckeliana*	1,000	SP[1], CFEM[3]	133	14
BgCon0194	EC3	Serine protease 2	2 e-70	*Pyrenopeziza brassicae*	0,635	Peptidase S8 and S53, subtilisin, kexin, sedolisin	240	26
BgCon0232		Hypothetical protein	1 e-53	*Sclerotinia sclerotiorum*	0,856	SP[1], YgfY-like	254	29
BgCon0254	EC4	Predicted protein	6 e-19	*Botryotinia fuckeliana*	0,998	SP[1], CFEM[4]	235	24
BgCon0314		-	n.a.	n.a.	0.982	SP[1]	177	19
BgCon0329		-	n.a.	n.a.	0,988	SP[1]	49	5
BgCon0549		-	n.a.	n.a.	0,991	SP[1]	164	16
BgCon0895		-	n.a.	n.a.	0,967	SP[1]	75	8
BgCon1160	EC5	-	n.a.	n.a.	1,000	SP[1]	139	16
BgCon1245	EC7	Hypothetical protein	4 e-39	*Sclerotinia sclerotiorum*	0,989	SP[1], cerato-platanin	136	14
BgCon1691		-	n.a.	n.a.	0,562	SP[1]	38	4
Bg13901727		-	n.a.	n.a.	0,672	SP[1]	110	12

[A] http://cogeme.ex.ac.uk/index.html (Soanes & Talbot, 2006)
[B] effector candidates that were functionally characterized in this study
[C] E-value cutoff 10^{-5}
[D] Translated sequences were analyzed with the SignalP Hidden Markov Model (HMM) and the SignalP Neural Network (not shown) algorithms.
[E] Protein signature was assigned using InterProScan, a tool for functional analysis of protein sequences using the InterPro database of protein families, domains and functional sites in which identifiable features found in known proteins can be applied to unknown protein sequences. http://www.ebi.ac.uk/InterProScan/index.htm
[F] molecular weight;
[1] signal peptide; [2] transmembrane domain; [3] eight cysteine-containing domain present in fungal extracellular membrane proteins.
n.a. not applicable

BgCon0194 contains a subtilisin-protease motif. During the course of this study, *Bgh* genome data became available and BLAST searches with the BgCon0194 protein sequence against the draft genome sequence resulted in identification of a genomic DNA contig encoding a full-length subtilisin-like serine protease (DH14_7906). Alignment of the BgCon0194 amino acid sequence with the deduced protein sequence of DH14_7906 revealed that we had isolated a partial cDNA sequence. DH14_7906 encodes a secreted protease of 523 amino acids and thus cannot be considered a small protein. For this reason, we analyzed BgCon0194 (designated EC3, see below, **Table 1**, **Supplementary Figure 1**) in most of the assays, but we excluded it as a putative effector once the *Bgh* genome data became available.

3.1.2 ECs enhance *Bgh* haustorium formation

The “candidate effectors” were tested for their capacity to enhance virulence of the *Bgh* fungus. To date, no reliable transformation protocol is available for *Bgh*. Targeted gene knock-out of the “candidate effector” genes was thus precluded. Instead, we transiently expressed the “candidate effector” genes under the control of the constitutive maize ubiquitin-promoter in single barley epidermal cells via bombardment with DNA-coated gold particles. Subsequently, we inoculated the transformed cells with *Bgh* conidiospores. Examination of individual, transformed cells is suitable because powdery mildew fungi colonize single epidermal cells and during early fungal pathogenesis plant defense remains cell-autonomous (Shirasu et al., 1999).

We transiently expressed constructs encoding the “effector candidates”, both as full-length variants and truncated variants lacking the signal peptide, together with a *β-glucuronidase* (*GUS*) reporter gene construct in barley leaves. Following inoculation with *Bgh* conidiospores, GUS activity was visualized at 48 hours post inoculation (hpi) by incubation in X-gal solution, resulting in greenish-blue staining of transformed cells. Epicuticular fungal structures were visualized by staining with Coomassie Brilliant Blue. Fungal haustorial indices were scored as the ratio of successfully invaded cells marked by an intracellular haustorium (susceptible cells) and non-penetrated cells (resistant cells) marked by an attacking, extracellular appressorium (**Figure 1, Panel A**). Baseline susceptibility of the epidermal cells in a compatible interaction is reflected by the *Bgh* haustorium index of 68% after expression of the GUS reporter construct alone. Expression of a plasmid encoding MLO, a compatibility factor for powdery mildew fungi

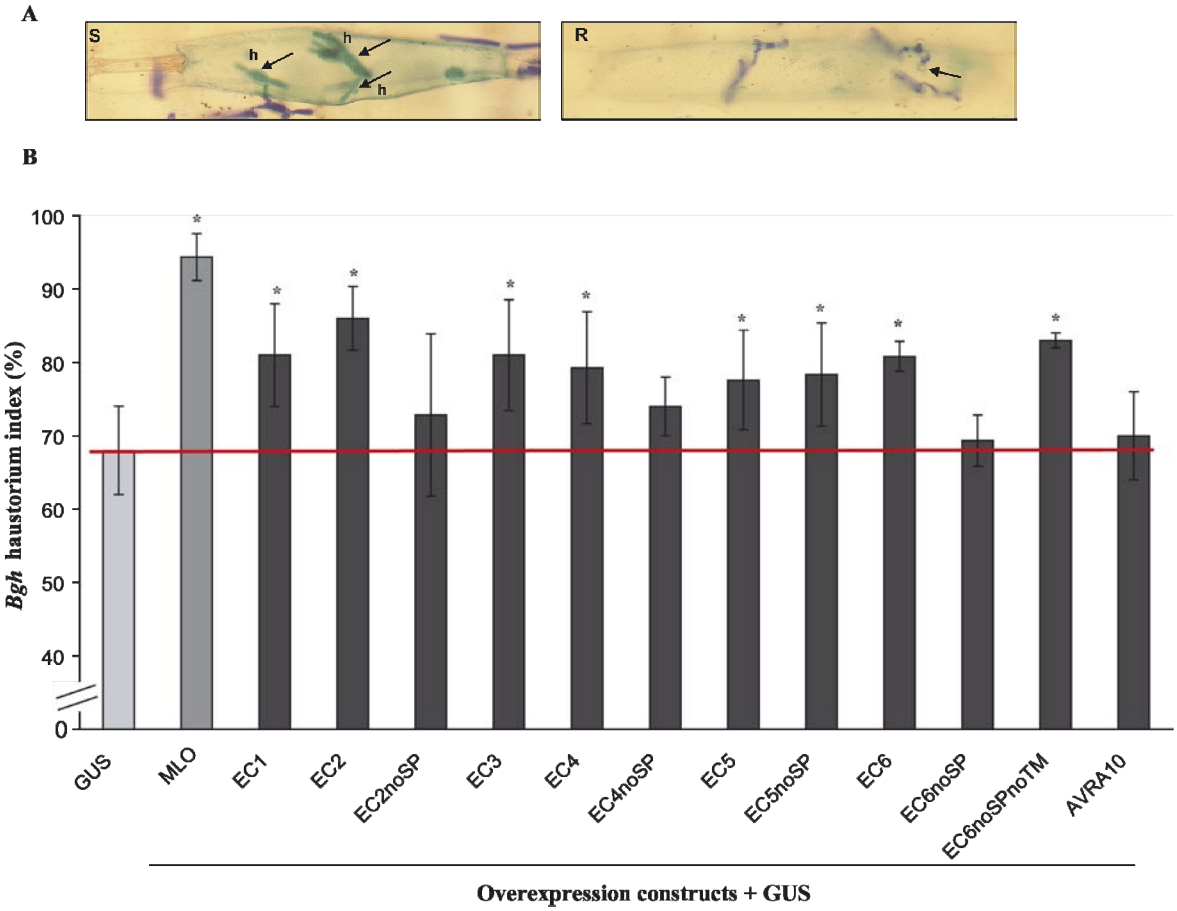

Figure 1. EC proteins enhance *Bgh* haustorium formation. Single epidermal cells of seven days old barley leaves (cv. Golden Promise) were ballistically transformed with either a ß-Glucuronidase (GUS) reporter construct alone or together with an overexpression construct of the ECs. Subsequently leaves were inoculated with *Bgh* conidiospores and at 48 hpi stained for GUS activity, which renders transformed cells greenish-blue. Epiphytic fungal structures were stained with Coomassie Brilliant Blue. **(A)** Successful penetration (S) results in formation of an intracellular haustorium (h, indicated by arrow). Non-penetrated resistant cells (R) are marked by the presence of a papilla (arrow) that coincides with penetration arrest. **(B)** The ratio of transformed cells enabling haustorium formation divided by the total number of attacked transformed cells results in the haustorium index and is a measure for the impact of the tested gene on the infection success. Data shown represent means ± SD from at least three experiments. For each experiment and tested gene construct at least 100 transformed cells were evaluated. Barley MLO was used as a positive control. Asterisks indicate $p \leq 0{,}01$ (Student's t-test) compared to the negative control (GUS alone). Abbreviations: noSP: constructs lacking the predicted N-terminal secretion peptide, noSPnoTM: construct lacking both the predicted N-terminal secretion peptide and the predicted C-terminal transmembrane domain, of the respective EC protein.

(Jorgensen, 1992b; Eichmann and Huckelhoven, 2008), leads to super-susceptibility of barley and increased the haustorium index to 94% (**Figure 1, panel B**).

Only ten "candidate effectors" could be tested in the transient expression assay, because 4 of the 14 selected cDNAs were not compatible with the Gateway-based cloning system we employed. Six of the ten tested candidates led to statistically significantly (Student's t-test, $p < 0.01$) enhanced haustorium indices of 79 to 86 % when expressed as full-length proteins (**Figure 1, panel B**).

We designated these proteins "Effector Candidates" (EC): EC1 to EC6 (**Table 1**). *EC1* expression enhanced the *Bgh* haustorium index to 81%, *EC2* expression to 86%, *EC3* expression to 81%, *EC4* expression to 79%, *EC5* expression to 78% and *EC6* expression to 81%. By contrast, transient expression of the cloned *Bgh* effector AVR_{A10} (Ridout et al., 2006) did not enhance the fungal haustorium index under our experimental conditions (**Figure 1, panel B**). Expression of constructs harboring versions of EC2, EC4 and EC6 without the signal peptide (noSP) was less effective in enhancing the haustorium index than expression of the respective full-length constructs (EC2noSP: 73%; EC4noSP: 74%; EC6noSP: 69%). On the other hand, removal of the signal peptide did not alter the increased haustorium index after expression of *EC5* (EC5noSP: 78%). Thus, an EC signal peptide was in some, but not all cases required for EC proteins to enhance the *Bgh* haustorium index.

For *EC6* we also expressed a construct harboring a truncated EC6 protein, lacking both the signal peptide and the presumptive transmembrane domain (noSPnoTM) to determine whether the predicted transmembrane domain was important for the ability of EC6 to enhance the haustorium index. Expression of the truncated *EC6* variant was as sufficient in enhancing the *Bgh* haustorium index (EC6noSPnoTM 83%) as expression of the full-length EC6 protein (**Figure 1, panel B**). Thus, the predicted transmembrane domain appears to be dispensable for EC6 function and its absence even compensated the reduced haustorium index of the EC6 variant lacking the signal peptide.

In summary, expression of the EC proteins in barley epidermal cells enabled increased haustorium formation of the *Bgh* fungus. The enhanced *Bgh* haustorium index after transient expression of the "*candidate effectors*" could be either due to distortion of the barley cells or to a positive role of the expressed *Bgh* proteins in promoting haustorium formation. Given that global perturbation of cellular functions usually results in a state of

enhanced defence, we concluded that EC proteins likely contribute to virulence of the fungus.

3.1.3 EC proteins have a signal peptide that is functional in yeast

Some EC proteins (EC2, EC4 and EC5) appeared to require the signal peptide for the promotion of haustorium formation (**Figure 1**), while EC5 did not require the signal peptide to enhance the fungal haustorium index. This discrepancy could be due to a non-functional signal peptide in some of the effector candidates. To verify that the predicted signal peptides were fully functional we employed the yeast signal sequence trap, which has been frequently used to identify secreted proteins, e.g. from cDNA libraries from the bean rust *Uromyces fabae* and the corn pathogen *Colletotrichum graminicola* (Jacobs et al., 1997; Krijger et al., 2008; Link and Voegle, 2008). This assay relies on the fact that *Saccharomyces cerevisiae* requires a secreted invertase for growth on medium containing sucrose as the sole carbon source. Yeast strain YTK12 has a genomic deletion at the *SUC2* locus (Klein et al., 1996) and therefore this strain cannot secrete invertase.

The N-termini containing the predicted signal peptides of EC1 to EC5, EC7 and AVR_{A10} were cloned into the yeast SST shuttle vector upstream of the *Saccharomyces cerevisae* invertase gene lacking its own start codon and signal peptide. Growth of yeast strains transformed with these constructs was monitored for 10 hours in liquid medium containing sucrose as the sole carbon source.

Yeast strains transformed with the N-termini of EC1, EC2, EC4, EC5 and EC7 (high SignalP score, **Table 1**) grew exponentially like yeast strains transformed with the full length invertase (positive control, **Figure 2**). Analogous to transformation of YTK12 with the empty SST vector, transformation of constructs harbouring the N-termini of EC3 and AVR_{A10} (EC3: low SignalP score, AVR_{A10}: no signal peptide predicted) did not enable the yeast strains to grow in sucrose-containing medium (**Figure 2**). Consequently, the signal peptides of EC1, EC2, EC4, EC5 and EC7 were able to direct secretion of the invertase protein and are therefore functional in yeast. It remains a formal possibility that the EC signal peptides are functional in yeast, but non-functional in plant cells. However, considering that the EC signal peptides were also able to direct EC proteins to the ER upon transient expression in barley cells (see below), we concluded that the differential requirement of ECs for a signal peptide to enhance the *Bgh* haustorium indices in the transient barley expression assay was not due to non-functional signal peptides.

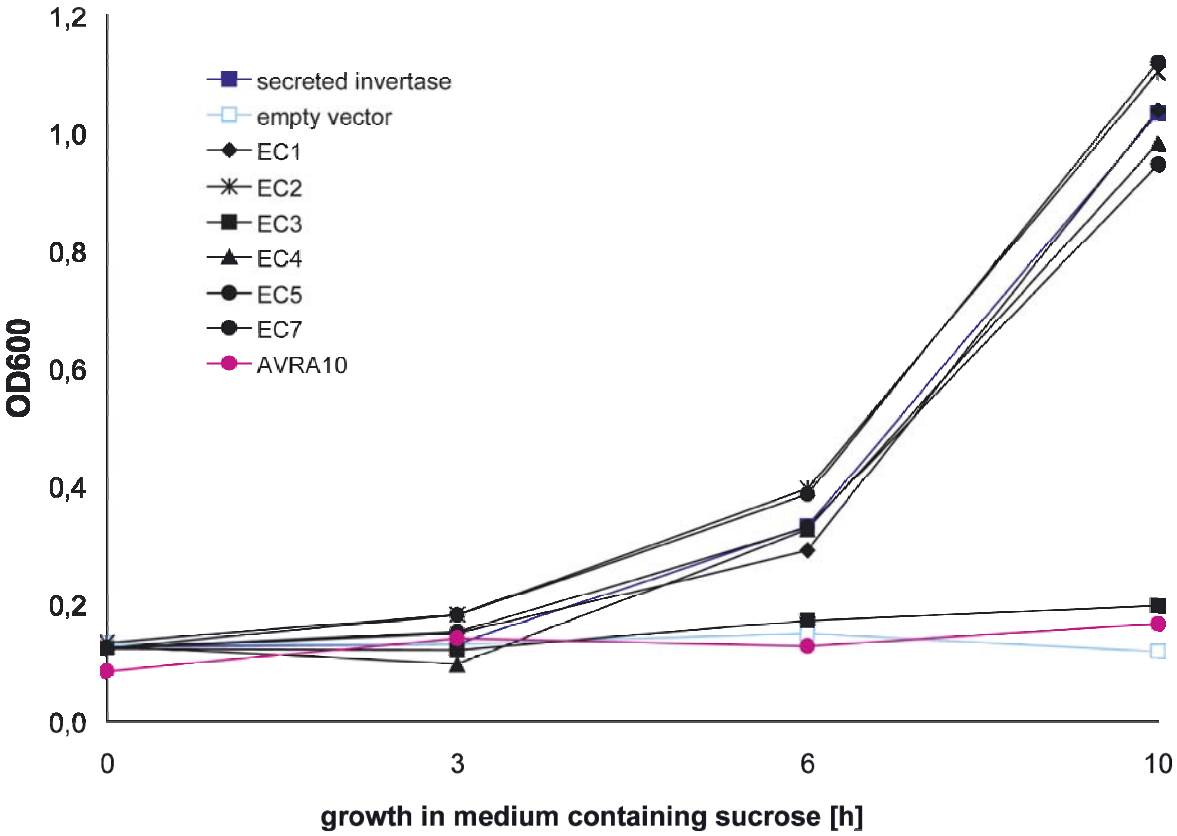

Figure 2. EC proteins contain a signal peptide that is functional in yeast. Yeast strain YTK12 carries the *SUC2*$^-$ mutation in the gene encoding the secreted invertase and can therefore not grow in medium containing sucrose as the sole carbon source. However, growth in medium containing sucrose is restored when a secreted invertase is supplied *in trans* (dark blue line). The N-termini of the EC genes (encoding the predicted secretion peptide) and AVR_{A10} were cloned in frame with the invertase-encoding gene of the SST vector and transformed into a yeast strain carrying the *SUC2*$^-$ mutation (EC1 1-65 aa; EC2 1-82 aa; EC3 1-88 aa; EC4 1-96 aa; EC5 1-100 aa; EC7 1-72 aa; AVR_{A10} 1-129 aa). Growth of the transformed yeast cells in medium containing sucrose was spectrophotometrically monitored for 10 hours (indicated by OD600). Data shown represent mean values of three technical replicates. The experiment was repeated twice yielding similar results.

3.1.4 EC proteins do not alter nonhost resistance to *Bgt*

Next, we addressed the question whether EC proteins possess a more general virulence function, i.e. a function that is not restricted to the compatible interaction between *Bgh* and barley. To investigate EC protein function in a nonhost interaction we expressed the EC proteins in barley using particle bombardment as described above. Subsequently we

inoculated the bombarded leaves with conidiospores of the non-adapted fungus *Blumeria graminis* f. sp. *tritici* (*Bgt*), the causal agent of powdery mildew disease in wheat. *Bgt* spores germinate on the nonhost plant barley, but most sporelings fail to enter the respective epidermal cells. Only in a few instances *Bgt* is able to form haustoria inside barley cells as reflected by the low haustorium index of 5% after expression of the GUS reporter construct alone (**Supplementary figure 2**). Consistent with previous reports (Elliott et al., 2002; Freymark et al., 2007), expression of *MLO* partially breached *Bgt*-barley nonhost resistance and increased the *Bgt* haustorium index to 19% (**Supplementary figure 2**). *EC1*, *EC2* and *EC4* expression did slightly increase *Bgt* haustorium indices to 6% (EC1 and EC2) and 7% (EC4), whereas *EC6* expression did not enhance the haustorium index compared to *GUS* expression alone (5%) (**Supplementary figure 2**). Initially it seemed as if EC5 did partially breach nonhost resistance by increasing the *Bgt* haustorium index to 10% (**Supplementary figure 2**). However, due to low transformation efficiencies and sparse germination of the *Bgt* spores, the variability of the results obtained from independent experiments was too large to allow reliable conclusions. The same holds true for the expression of ECs without their signal peptides. Therefore, this assay did not allow us to draw any conclusion about a potential virulence function of the EC proteins that contributes to breaching nonhost resistance.

3.1.5 EC proteins are encoded by single copy genes and are in part conserved among powdery mildew species

To assess whether the *EC* genes are members of multigene families and whether they are specific to *Bgh*, we performed BLAST searches in draft genome sequences of three powdery mildew species. The *Bgh* genome has been sequenced by the BluGen consortium using traditional Sanger sequencing (http://www.blugen.org) and will be annotated soon. Kindly, we were allowed to use the draft sequences for this study. In addition, the genomes of the powdery mildew fungi *Golovinomyces orontii* (*Go*), virulent on the dicot reference species *Arabidopsis thaliana*, and *Erysiphe pisi* (*Ep*), virulent on pea, have been pyrosequenced by our lab and the sequence reads (ca. 7x coverage each) were assembled into a preliminary genome sequence. BLAST searches using the draft *Bgh* genome sequences indicated that the *EC* genes are not members of gene families. For each *EC*, except for *EC6*, a single homologous genomic DNA sequence contig was identified in the *Bgh* genome, indicating that they are single-copy genes. For *EC6* no genomic contig was identified in the draft *Bgh* genome. *EC2*, *EC3* and *EC4* had

homologous gene sequences in the genomes of *Ep* and *Go*. Lack of homologous sequences in the genomes of the barley, pea and Arabidopsis powdery mildew species could be due to the fact that the current coverage of the respective genomes is incomplete. Alternatively, EC1 and EC5 could be indeed *Bgh*-specific proteins.

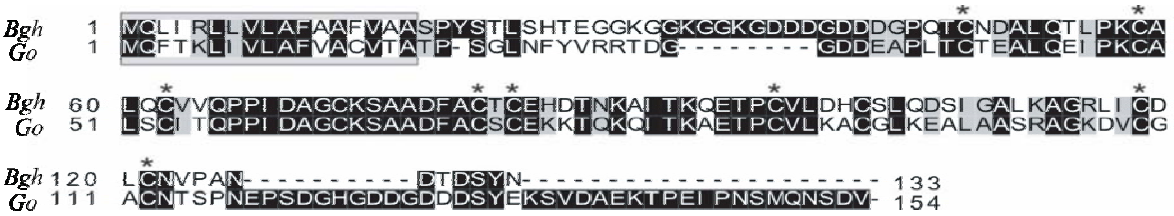

Figure 3. *EC2* has a homolog in the *Go* genome. Pairwise alignment of the deduced protein sequences of EC2 and the *Go* contig 11790 (*Go*EC2). The *EC2* homologous DNA contig was identified by BLAST searches against the draft genome sequence of the Arabidopsis powdery mildew pathogen. The predicted signal peptide is boxed in grey. Cysteine residues forming the CFEM domain are conserved in both species (marked with *). Identical amino acids are shaded black, conserved amino acids are shaded grey and non-conserved amino acids are not shaded. Abbreviations: *Bgh*: *Blumeria graminis* f. sp. *hordei* EC2; *Go*: *Golovinoymes orontii* contig11790.

Pairwise alignment of the deduced amino acid sequences of *EC2* and the homologous sequence contig in the *Go* genome (contig11790) indicates that the positions of the predicted signal peptide as well as the CFEM domain are conserved (**Figure 3**). To examine the function of the putative effector encoded by this contig during *G. orontii* infection of Arabidopsis, we isolated the homologous cDNA sequence, designated *Go*EC2, by RT-PCR from RNA of *Go*-infected Arabidopsis plants and cloned it into the binary expression vectors pAM-PAT and pAM-PAT-GWY-3xHA. Subsequently *A. thaliana* Col-0 plants were transformed with various pAM-PAT constructs harboring either full-length *Go*EC2 or truncated *Go*EC2 versions lacking the N-terminal secretion signal. Currently, we are evaluating the pathogen phenotype of the respective transgenic Arabidopsis plants.

3.1.6 EC proteins are highly sequence conserved among six *Bgh* isolates

Next, we investigated whether the EC proteins are present in different *Bgh* isolates and whether they are subjected to diversifying selection. To identify polymorphic sites in the *EC* gene products we performed RT-PCR on six different *Bgh* strains (K1, A6, CC52, CC146, CC148, DH14) and sequenced the respective PCR amplicons. Remarkably few

amino acid polymorphisms were found in the deduced EC protein sequences. EC2, EC4 and EC6 are completely conserved among the six isolates, while a single polymorphic amino acid was identified at the C-terminus of EC1 (**Figure 4**). EC5 is the most variable protein with two amino acid polymorphisms throughout the protein sequence; one polymorphism was detected at the C-terminus and one within the N-terminal signal peptide. In conclusion, EC1, EC2, EC4, EC5 and EC6 are not only present, but also highly sequence conserved among different *Bgh* isolates.

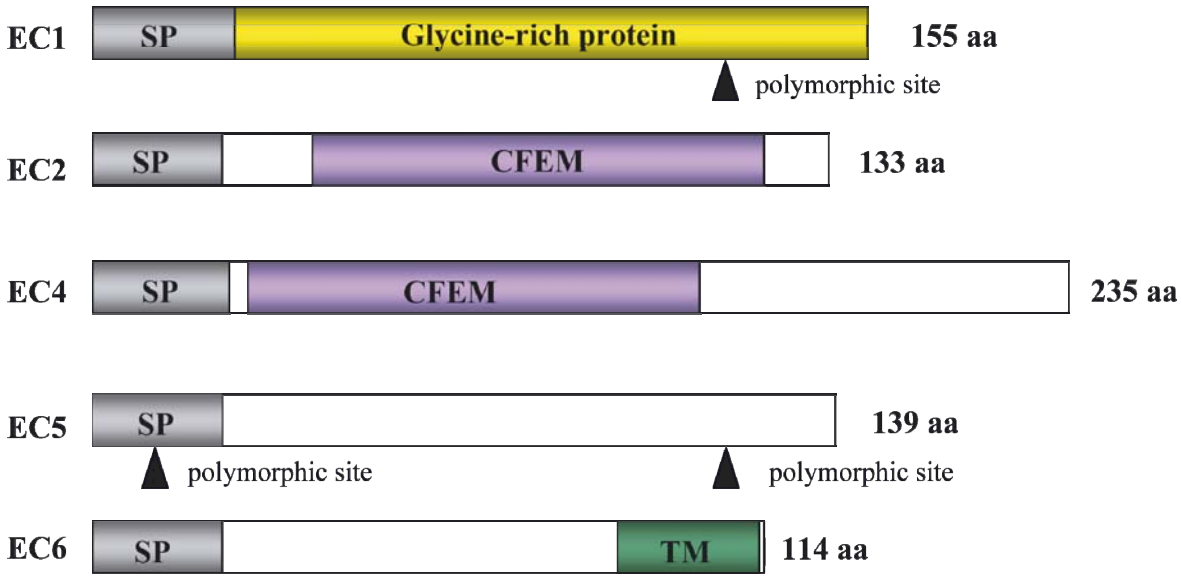

Figure 4. EC proteins are structurally diverse, but they are not polymorphic amongst different *Bgh* isolates. The scheme depicts the predicted EC protein signatures. Amino acid polymorphisms were identified by sequencing the EC cDNAs of six different *Bgh* isolates and are indicated by black arrowheads. Abbreviations: SP: signal peptide; CFEM: cysteine-rich fungal extracellular membrane protein; TM: transmembrane domain.

3.1.7 *EC* genes are differentially expressed during the infection process

We next investigated the expression pattern of the *EC* genes during *Bgh* infection. Expression of an *EC* gene early during the infection process might denote its involvement in host defense suppression and counter-defense mechanisms, while expression late during infection might rather indicate effector functions in interference with the host metabolism to gain nutrients from the plant host. We employed quantitative reverse transcription-PCR (qRT-PCR) using total RNA that was isolated from *Bgh*-infected barley leaves at six different time points post inoculation. These time points coincide with the landing of the conidiospores on the leave surface (0 hours post inoculation; hpi),

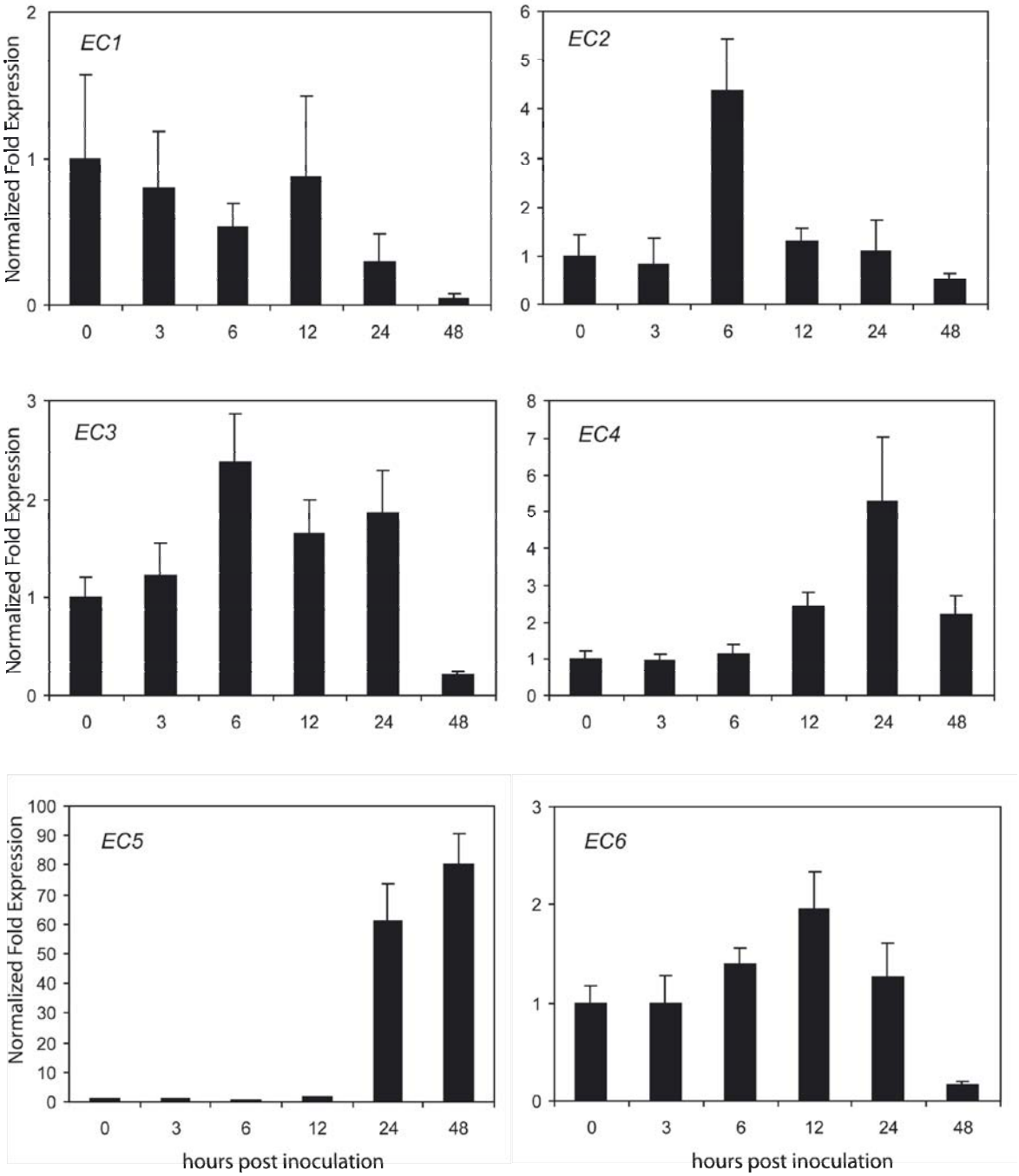

Figure 5. *EC* genes are differentially expressed during *Bgh* infection. The expression levels of *EC1- EC6* were monitored during the compatible interaction of *Bgh* isolate K1 with *H. vulgare* (cv. Golden Promise) at 0, 3, 6, 12, 24 and 48 hours post inoculation (hpi). Total RNA was isolated from barley leaves at the indicated time points. Quantitative RT-PCR was performed for the *EC* genes as indicated on each panel. *Bgh ß-tubulin* expression was used to normalize the expression value in each sample, and expression values were determined against the average expression value at time point 0 hpi. The standard deviation was calculated from three to four technical replicates each. Experiments were repeated twice with

independent biological material, yielding similar results, except for *EC4* (**Supplementary Figure 3**) and *EC6* (only one experiment).

appressorium emergence (3 hpi), appressorium maturation (6 hpi), host papilla formation (12 hpi), haustorium formation (24 hpi) and secondary hyphae spreading on the leaf surface (48 hpi) (**Figure 5**). Transcript abundance of the *EC* genes was compared with the average value at time point 0 hpi, arbitrarily set to 1 (**Figure 5**). Transcript abundance in each sample was normalized against the constitutively expressed *ß-tubulin* gene to correct for the increase in fungal biomass during infection (Zhang et al., 2004; Grell et al., 2005).

Transcript levels of *EC1* decreased during the infection process until the levels were marginally low at 48 hpi (**Figure 5**). Similarly, abundance of *EC2*, *EC3* and *EC6* transcripts drastically decreased at this late infection time point (48 hpi), however *EC3* and *EC6* transcript levels transiently increased two-fold during the penetration process (6 hpi and 12 hpi, respectively) compared with time point 0 hpi (**Figure 5**). Transcript abundance of *EC2* was strikingly high at the time point of appressorium emergence (four-fold compared with time point 0 hpi) (**Figure 5**). By contrast, *EC4* and *EC5* transcript levels increased at the later stages of infection. *EC4* transcript accumulation was four-fold increased at 24 hpi compared with time point 0 hpi, while changes in *EC5* transcription levels were more drastic. When haustoria were fully developed (24 hpi) *EC5* transcription levels were dramatically higher (60-fold compared with time point 0 hpi) and increased further when secondary hyphae developed at 48 hpi (80-fold compared with time point 0 hpi) (**Figure 5**).

In summary, *EC1*, *EC3* and *EC6* expression profiles suggest that the respective proteins play a general role during penetration until haustoria are fully developed at 24 hpi. After this, their transcript abundance decreases. On the other hand, *EC2* and *EC4* transcript accumulation coincides with the development of appressoria and haustoria, respectively, suggesting that EC2 might be involved in the penetration process and EC4 might be involved in the development or maintenance of the haustorium. The drastic decrease in *EC5* transcript levels at 24 and 48 hpi suggests that *EC5* is expressed in and/or secreted from haustoria. EC5 could function in sustaining plant defense suppression or in gaining nutrients for the fungus from the plant cell.

3.1.8 EC proteins localize to the plant cytoplasm

Next, we explored the spatial distribution of EC proteins inside the plant cell. We reasoned that the subcellular localization of the EC proteins could provide an indication of their function. To investigate the cellular localization of the EC proteins, we transiently expressed yellow fluorescent protein (YFP)-tagged EC-fusion proteins in single barley epidermal cells using the constitutive maize ubiquitin-promoter. Subcellular localization was examined by confocal laser scanning microscopy (CLSM). YFP-EC1, -EC2, -EC4, -EC5 and -EC6 all co-localized with an ER (Endoplasmatic Reticulum)-marker-mCherry fusion protein that was co-expressed with the respective YFP-EC fusion protein. Occasionally, we observed distinct punctuate foci for the YFP-EC fusion proteins. These foci were reminiscent of Golgi stacks, but they did not co-localize with a Golgi-marker-mCherry fusion protein (data not shown) and might be artifacts of the over-expression. The YFP-EC fusion proteins were excluded from the nucleus and like the ER-marker-mCherry fusion protein formed a ring-like structure around the nucleus, which is a typical feature of ER localization (Nelson et al., 2007).

Even though it is unknown how fungal effectors are translocated inside the host cells it is likely that the effector signal peptide is cleaved off before the effector enters the plant cell. Taking this assumption into account we also investigated localization of YFP-EC fusion proteins lacking the N-terminal signal peptide (noSP). Expression of the YFP-EC fusion proteins without the signal peptide always resulted in cytoplasmic localization marked by a loss of co-localization with the co-expressed ER-marker-mCherry fusion protein (**Figure 6**). Additionally, YFP-ECs were present in distinct “blobs” in the net-like cytoplasmic structure. In barley epidermal cells, the ER visualized with the ER-mCherry marker is visible as a net-like structure when the focal plane of the microscope is positioned to the top of the cell (**Figure 6**). Due to the turgor of the large central vacuoles in these cells, both the ER and the cytoplasm are pressed against the cell wall. The cytoplasm, visualized by cytoplasmically localized YFP (**Figure 6**), occupies the space between the other organelles (causing the “blobs”) and often follows the net-like structure of the ER. In addition to the localization of YFP-ECnoSP fusion proteins in the cytoplasm we also observed the fusion proteins inside the plant nucleus. The YFP-EC protein fusions encode polypeptides of 38 - 43 kDa. Their size is below the size exclusion limit of 40-60 kDa for the nuclear pore complex (Talcott and Moore, 1999) thus allowing passive flow into the nucleus. In conclusion, the mature forms of EC1, EC2, EC4, EC5 and EC6

localize to the plant cytoplasm and possibly fulfill their function in this cellular compartment.

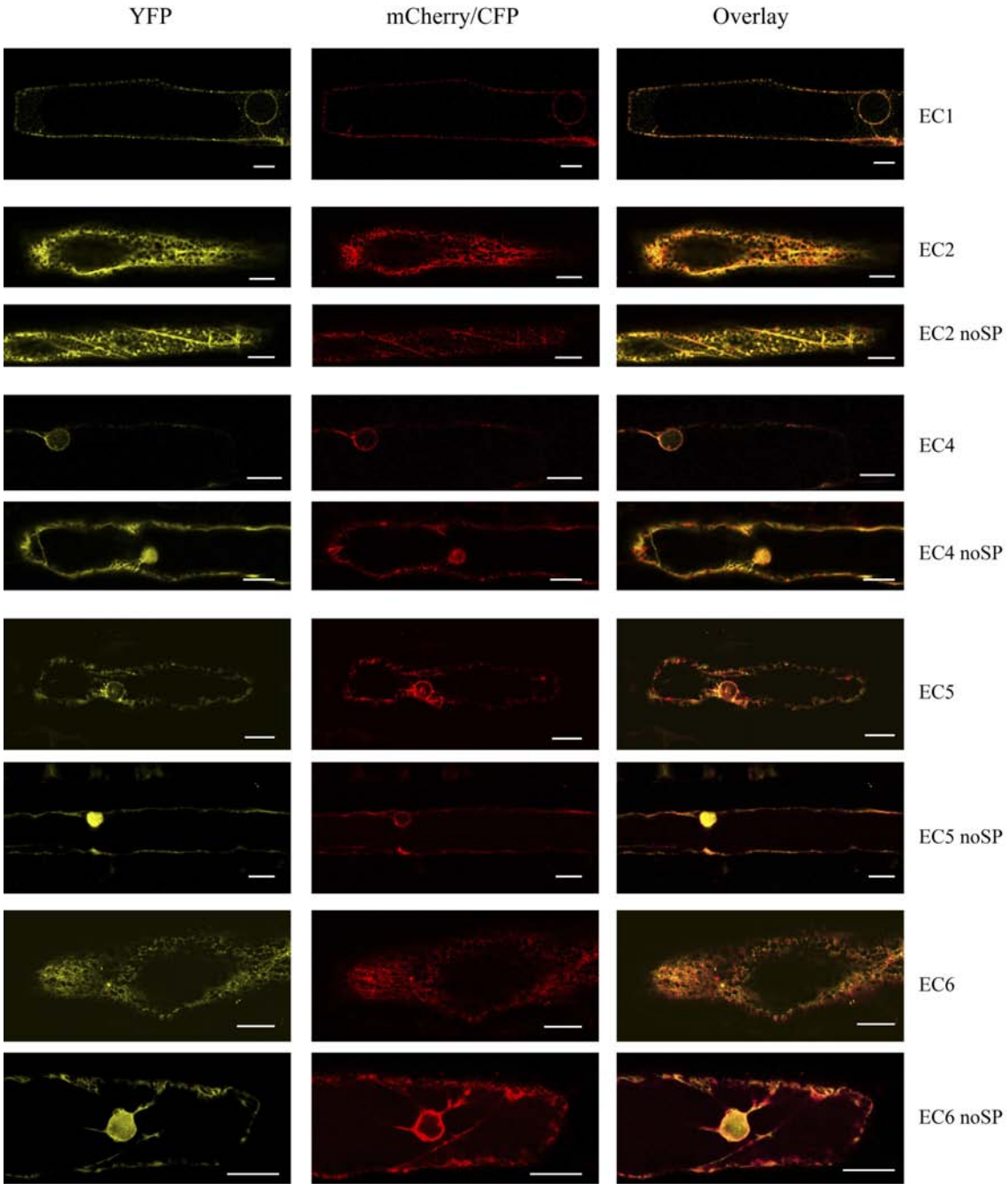

Figure 6. EC proteins localize to the cytoplasm of the host cell. Constructs encoding translational fusions between the EC proteins and YFP were transiently co-expressed with an ER-marker, fused to either mCherry or CFP, in single barley epidermal cells. EC proteins were C-terminally fused to YFP either as full-length proteins or as truncated versions lacking the N-terminal signal peptide (noSP). Two days after the bombardment fluorescence was examined by confocal laser microscopy. Pictures are false-coloured. Size bars indicate 20 µm.

3.1.9 EC proteins do not suppress BAX-induced cell death

To gain information about the potential role of the cytoplasmic EC proteins, we employed yeast-based assays to probe for known effector activities. A well-documented effector function is the suppression of programmed cell death (PCD) (Armstrong et al., 2005; Bos et al., 2006; Dou et al., 2008b). PCD is one of the defence responses that plants engage to prevent the spread of an infecting pathogen. Given that this response is particularly effective against obligate biotrophs like the powdery mildew fungi that rely on the living plant cell for growth and proliferation, we tested whether EC1, EC2, EC5 or EC6 could suppress BAX-induced cell death. BAX is a proapoptotic protein that induces PCD in mammals, plants and yeast (Zha et al., 1996; Liston et al., 2003; Ogawa et al., 2005). A yeast strain expressing BAX under a galactose-inducible promoter was transformed with plasmids harbouring the respective EC cDNAs lacking the N-terminal signal peptide to prevent secretion of the respective protein. Transfer of the yeast from glucose-containing to galactose-containing medium results in expression of BAX, thereby leading to cell death of the yeast. Co-transformation with a suppressor of this type of PCD will rescue the yeast. Growth of a yeast strain transformed with a plasmid encoding the known BAX inhibitor BclXL (Liston et al., 2003) was restored on glucose-containing medium. However, none of the strains transformed with any of the EC constructs were able to restore yeast growth on the galactose-containing selection medium, indicating that none of the tested EC proteins could suppress BAX-induced cell death (data not shown).

3.1.10 EC proteins do not cause growth inhibition in yeast

A converse effector function to suppression of programmed cell death might be the induction of growth inhibition or cytotoxic effects caused by interference with universal eukaryotic processes. Recently, 7 out of 27 tested *P. syringae* effectors were found to inhibit growth or cause cell death (cytotoxic effects) when expressed in yeast (Munkvold et al., 2008). To assess potential growth inhibiton effects of the EC proteins, we transformed yeast strains with plasmids encoding the EC proteins under the control of a galactose-inducible promoter (pYES2).

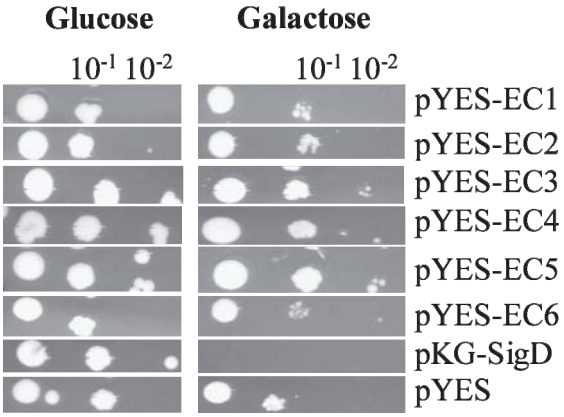

Figure 7. EC proteins do not inhibit growth in yeast. Yeast strain WCGN was transformed with the expression vector pYES2 harboring the effector candidates under control of a galactose-inducible promoter. Serial dilutions of the transformants were plated on medium containing glucose for two days and subsequently spotted on medium containing galactose as serial dilutions. The experiment was repeated twice yielding similar results.

Again, constructs harboring the candidates were generated without the signal peptide to prevent secretion of the respective proteins. As a positive control we used the *Salmonella typhimurium* effector SigD, which has been reported to inhibit yeast growth by inducing loss of actin polymerization (Aleman et al., 2005). As expected, SigD expression completely inhibited yeast growth on galactose-containing medium. By contrast, none of the tested EC proteins (EC1-EC7) inhibited yeast growth (**Figure 7**). These data indicate that none of the tested EC proteins causes deleterious effects in yeast.

3.1.11 EC4 interacts with a *Hv*UBC-E2 and a *Hv*ARF-GAP; EC6 interacts with a *Hv*TPMT in yeast

Since screening for known effector functions in a targeted manner did not shed light on the mode of action of the EC proteins and the mechanisms that enable them to enhance the *Bgh* haustorium index, we screened for plant interacting targets of the EC proteins by performing a yeast-two-hybrid screen. LexA-EC protein fusions served as baits and a cDNA library from *Bgh*-infected barley leaves as the prey. We employed the mating interaction method in which the bait plasmids and the prey library DNA were separately transformed into two yeast strains of different mating types. Prior to the mating, the bait strains were tested for expression of the respective LexA-EC fusion proteins as well as for auto-activation of the reporter genes *LEU2* and *LacZ*. All LexA-EC fusion proteins were expressed in yeast (**Figure 8, Panel A**) except for EC1, which could not be cloned as a

fusion to LexA. EC2 and EC5 auto-activated the reporters and were excluded from the analysis (data not shown).

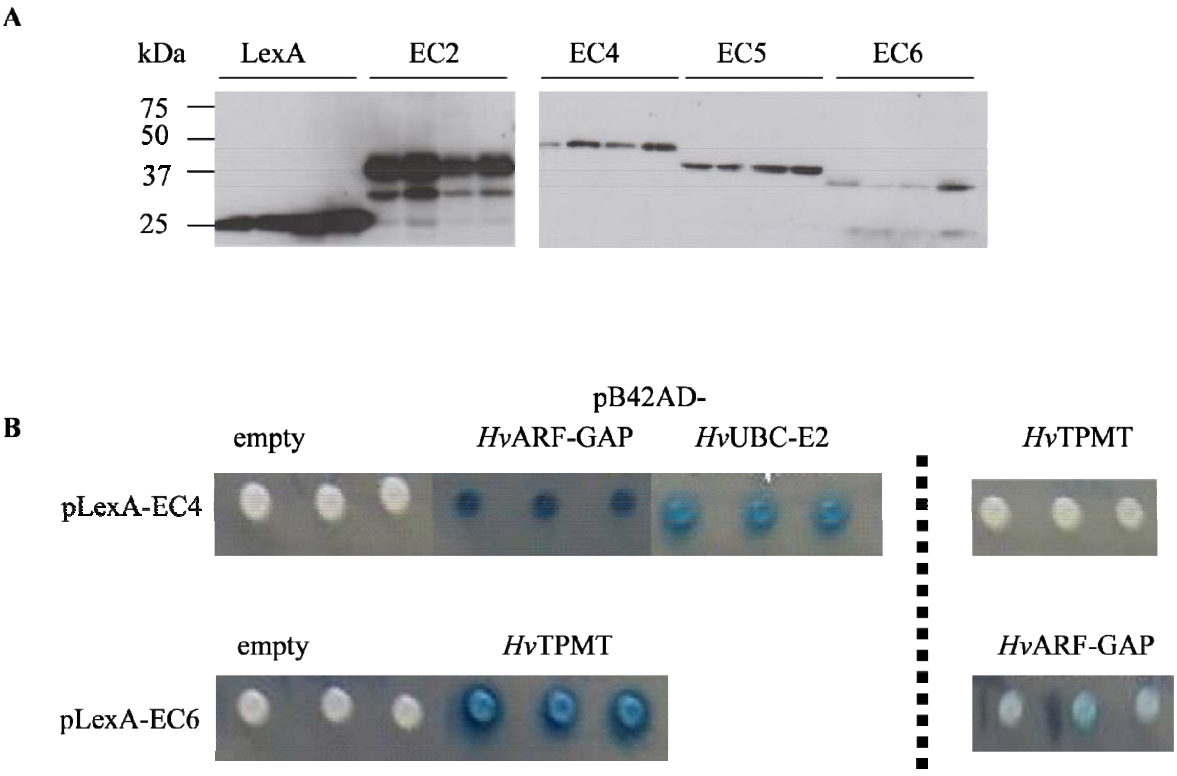

Figure 8. EC4 and EC6 interact with different barley proteins in yeast. (A) EC bait proteins fused to the LexA binding domain were expressed in yeast strain EGY48. Fusion proteins were detected by immunoblotting with a LexA antibody in crude yeast protein extracts from four independent transformants per construct. Molecular marker masses are indicated on the left. **(B)** EC6 interacts with *Hv*TPMT; EC4 interacts with *Hv*ARF-GAP and *Hv*UBC-E2. Full-length *Hv*TPMT, *Hv*ARF-GAP and *Hv*UBC-E2 were fused to the B42 activation domain in the pB42AD-GWY prey vector. Yeast strains co-expressing EC6 or EC4 and *Hv*TPMT, *Hv*ARF-GAP or *Hv*UBC-E2 were grown on an inductive carbon source (galactose and raffinose) and assayed for activation of the *ß-galactosidase* reporter gene. ß-galactosidase activity was observed by a blue staining on X-Gal containing medium.

Table 2. EC interacting proteins from barley

Bait	Number of prey clones [a]	EC interactor [b]	Protein domains [c]	Predicted coding sequence[d]	Max. cDNA length isolated[e]	Specificity of interaction[f]
EC4	2	*Hordeum vulgare* cDNA clone (AK249655)	-	252	129	n.t.
	12	*Zea mays* ubiquilin-1 (EU960149)	ubiquitin-conjugating enzyme, E2; ubiquitin-associated/translation factor EF1B (UBA)	195	68	+
	1	*Zea mays* protein phosphatase (EU959782)	proteins serine/threonine phospatase 2C	n.d.	102	-
	1	*Zea mays* hemoglobin 2 (NM001112349)	globin/ plant globin	n.d.	121	-
	6	*Zea mays* ARF-GAP like zinc finger-containing protein ZIGA3 (EU964854)	-	464	227	+
	1	*Leymus chinensis* chloroplast oxygen-evolving enhancer protein (EF583851)	photosystem II manganese-stabilizing protein	n.d.	149	n.t.
EC6	8	*Hordeum vulgare* putative AdoMet synthase3 (AM039895)	S-adenosylmethionine-synthetase	349	208	-
	27	*Oryza sativa* m-RNA (NM001058402)	thiopurine S-methyltransferase	247	151	+
	1	*Oryza sativa* m-RNA (NM001058192)	protein phosphatase 2C-related	n.d.	139	-

[a] cDNA clones of the same protein but of variable lengths were isolated independently as EC-interactors.
[b] Matching sequence with the highest E-value identified with tBLASTx.
[c] Protein domains predicted with InterProScan.
[d] Predicted length of the coding sequence (in amino acids) based on sequence information from ESTs of the epidermis-specific barley HO cDNA library (Zierold et al., 2005)
[e] length is listed in amino acids
[f] Specificty of the interaction was tested by retransforming bait and prey clones into yeast and assaying the reporter gene activity. + indicates specific interaction with the respective EC protein, – indicates interaction with more than one EC protein.
n.d.: no data; n.t.: not tested

With the LexA-EC4 and LexA-EC6 constructs we screened 10^8 yeast transformants and identified 21 partial cDNAs representing six different proteins for EC4 and 36 partial cDNAs representing three different proteins for EC6 (**Table 2**). Proteins were annotated by similarity searches using tBLASTx and InterProScan analysis. Four EC4 interactors shared homology with (1) a *H. vulgare* cDNA clone, (2) a chloroplast protein, (3) a plant globin and (4) a protein phosphatase. Also, one EC6 interactor shared homology with a protein phosphatase. These interacting proteins were represented by only one or two cDNA clones and therefore not further characterized in this study. The other cDNAs were identified multiple times. They encode an ubiquitin-conjugating enzyme (UBC-E2; 12 cDNA clones) and an ADP-ribosylation factor (ARF)–GTPase-activating protein (GAP) (ARF-GAP; six cDNA clones) as barley interacting proteins of EC4. UBC-E2 proteins transfer a ubiquitin moiety from a ubiquitin activating enzyme (E1) to the ubiquitin ligase (E3), which than attaches the ubiquitin moiety to a target protein. ARF proteins are GTP-binding protein that regulate intracellular vesicle trafficking. ARF-GAPs inactive ARF by inducing hydrolysis of the ARF-bound GTP and are also thought to function as subunits of vesicle coat proteins (Nie and Randazzo, 2006).

EC6 barley interacting cDNAs encode an S-adenosylmethionine-synthetase (SMS; eight cDNA clones) and a thiopurine-methyl-transferase (TPMT; 27 cDNA clones). SMS synthesizes S-adenosyl-L-methionine (SAM). Methyltransferases depend on SAM as a cofactor for activity, because it serves as the methyl donor in the transfer of the methyl group to the target molecule (Wang et al., 2005). As SMS interaction with EC6 was not specific (**Table 2**), we reasoned that SMS likely is not the primary target of EC4. EC4 might have interacted with SMS either due to structural similarities of the TPMT and the SMS proteins or because SMS was associated with TPMT during a methylation process. *TPMT* genes are conserved among species from bacteria to mammals, but their cellular functions remain largely elusive (Scheuermann et al., 2003). A bacterial TPMT homolog converts selenium-and tellurium-containing compounds to less toxic, volatile methylated derivatives (Ranjard et al., 2004; Favre-Bonté et al., 2006).

Full-length sequences of the interacting proteins were identified based on sequence information obtained from EST clones of the epidermis-specific barley HO cDNA library (Zierold et al., 2005). The coding sequences were amplified by RT-PCR from RNA of *Bgh*-infected barley leaves, cloned into the prey vector and transformed into the prey yeast strain. Subsequent mating with the bait strains containing plasmids encoding either EC4 or

EC6 resulted in a strong interaction in yeast visualized by intense blue staining on GAL-UHTL+X-gal selection medium for the interaction of EC6 with the *Hv*TPMT and the interaction between EC4 and both *Hv*ARF-GAP and *Hv*UBC-E2 (**Figure 8, Panel B**). The strength of the interaction, indicated by dark blue staining of the yeast colonies, was comparable to the strength of the interaction between EC4/EC6 and the partial cDNA clones of their respective host interactors. Within the tested controls, these interactions are specific, because no interaction was detected between EC4 and *Hv*TPMT and between EC6 and *Hv*ARF-GAP (**Figure 8, Panel B**) or *Hv*UBC-E2 (data not shown). This demonstrates that in yeast EC4 physically interacts with a *Hv*UBC-E2 and a *Hv*ARF-GAP while EC6 physically interacts with a *Hv*TPMT.

3.1.12 EC4 interacts with a *Hv*UBC-E2; EC6 interacts with a *Hv*TPMT *in planta*

We next employed the bimolecular fluorescence complementation (BiFC) assay to monitor the EC4/*Hv*ARF-GAP, EC4/*Hv*UBC-E2 and EC6/*Hv*TPMT interactions *in planta.* For the BiFC assay (Walter et al., 2004), non-fluorescent N-terminal and C-terminal segments of YFP (YFP^N and YFP^C) were fused to the N- and C-termini of the full-length test proteins (i.e., EC4, EC6, full-length *Hv*ARF-GAP, *Hv*UBC-E2 and *Hv*TPMT). For the barley proteins, we created additional fusion constructs between the C-terminal parts of the interacting cDNAs in the yeast-two-hybrid screen, and the N-and C-terminal parts of YFP. Interactions between the respective fusion proteins were tested in barley epidermal cells using transient gene expression via particle bombardment. In total, eight different combinations were possible for EC4/*Hv*UBC-E2 and EC6/*Hv*TPMT (**Supplementary Table 3**). Out of theses possible combinations, three were tested for EC4/HvUBC-E2 and two combinations resulted in YFP fluorescence. Additionally, two combinations of constructs harboring EC4 and the C-terminal part of *Hv*UBC-E2 fused to YFP segments were tested and no YFP fluorescence was observed (**Supplementary Table 3**). Out of eight possible combinations for EC6/*Hv*TPMT, seven were tested and expression of three combinations resulted in YFP fluorescence. Two possible combinations with constructs harboring EC6 and the C-terminal part of *Hv*TPMT were tested in the BiFC assay and one of these combinations resulted in YFP fluorescence (**Supplementary Table 3**). Only four combinations were tested in the BiFC assay for the EC4/*Hv*ARF-GAP interaction, because we could not obtain *Hv*ARF-GAP fusion constructs with a C-terminal tag. The four tested combinations as well as two combinations with fusion constructs harboring EC4 and the C-

terminal part of *Hv*ARF-GAP did not result in YFP fluorescence (**Supplementary Table 3**).

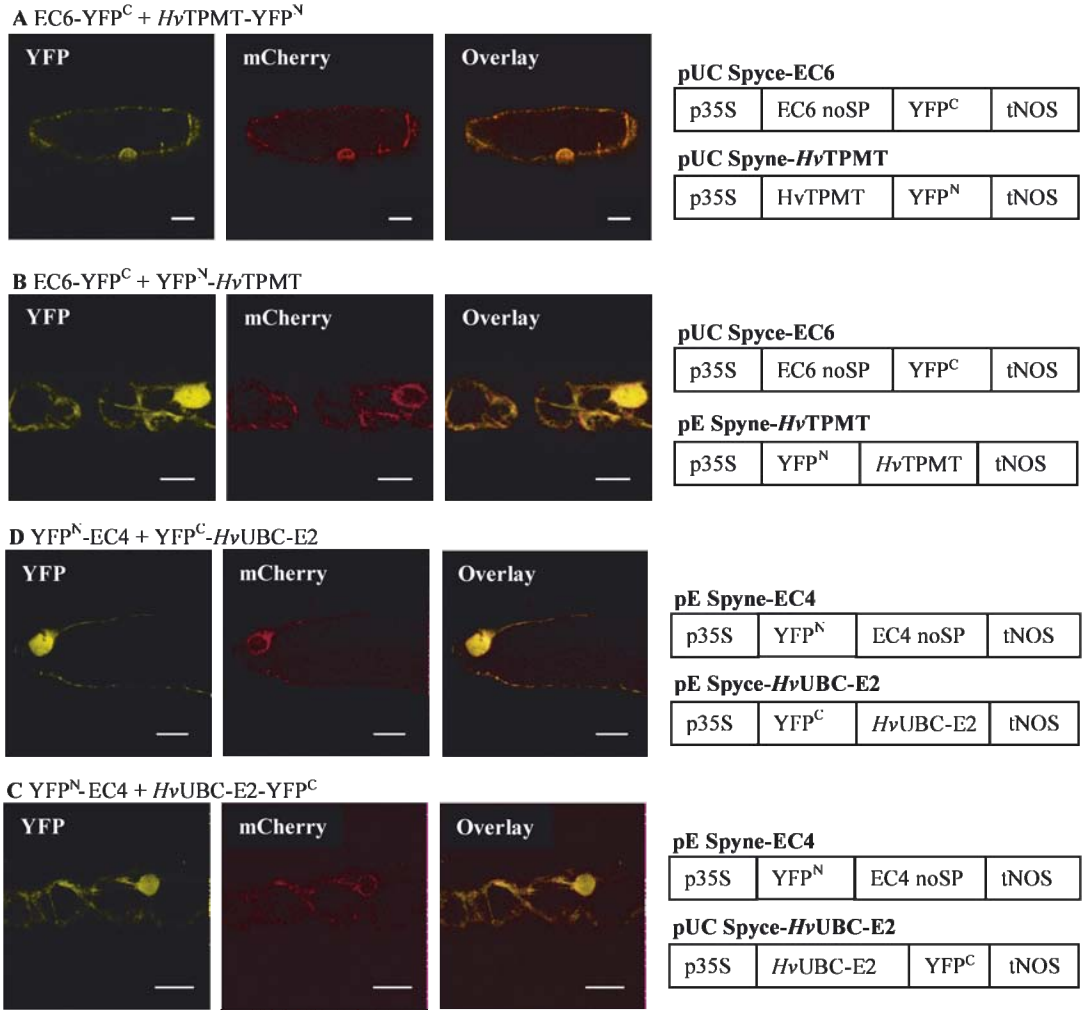

Figure 9. EC6 and EC4 interact with barley proteins *in planta*. Bimolecular fluorescence complementation (BiFC) of the interaction between EC proteins and their respective barley targets was examined by confocal laser scanning microscopy after bombardment of the respective gene constructs into single barley epidermal cells. To identify transformed cells prior to YFP analysis a control plasmid encoding an ER-marker fused to mCherry was always co-bombarded. Yellow fluorescence indicates interaction of EC6 and *Hv*TPMT (A and B) and EC4 and *Hv*UBC-E2 (C and D). On the right, schematic representations of the BiFC plasmids are depicted. The coding regions of the *EC4*, *EC6*, *HvTPMT* and *HvUBC-E2* genes were fused with the N-terminal (YFP^N; 1-155 aa) and C-terminal (YFP^C; 156-239 aa) segments of YFP, respectively. Abbreviations: p35S, cauliflower mosaic virus 35S promoter; tNOS, terminator of the *nopaline synthase* (*NOS*) gene; noSP, coding region lacking the N-terminal secretion peptide. Size bars indicate 20 µm.

Fluorescence was observed upon co-expression of EC6-YFP^C/*Hv*TPMT-YFPN and YFPN-EC4/*Hv*UBC-E3-YFPC protein pairs in the cytoplasm and in the nucleus (**Figure 9**). Co-expression of different variants of tagged *Hv*ARF-GAP and EC4 variants did not result in visible YFP fluorescence, indicating that these proteins do not interact in this assay (data not shown). Taken together, the BiFC data demonstrate that EC4 interacts with *Hv*UBC-E2 and EC6 interacts with *Hv*TPMT *in planta*.

3.1.13 FRET analysis

The irreversibility of the re-established YFP complex formation is at the same time an advantage as well as a drawback of the BiFC approach. It traps weak or transient associations, but can also stabilize unspecific interactions (Bhat et al., 2006). To eliminate false-positive BiFC results caused by high expression levels of the interacting proteins, we applied Fluorescence Resonance Energy Transfer (FRET) techniques that are largely independent of fluorophore concentrations (Sekar and Periasamy, 2003). FRET results from non-radiative energy transfer from an excited state donor fluorophore to a nearby acceptor. It occurs when two proteins fused to e.g. YFP and CFP, respectively, are in a distance corresponding to protein-protein interactions (5-10 nm) (Sekar and Periasamy, 2003). First, we applied Acceptor Photo Bleaching (APB) to record FRET. In this method, the YFP-tagged protein (the FRET “acceptor”) is photobleached at a cellular site of interest and the intensity of the CFP-tagged protein (the FRET “donor”) is measured at the same site. In principle, FRET is detected when the CFP intensity increases after the photobleaching of YFP (Karpova et al., 2003). We generated fusion constructs of *EC4, EC6,* and *HvTPMT* with genes encoding YFP and CFP (cyan fluorescent protein) and transiently expressed them in barley epidermal cells. Mean FRET efficiencies of 10-19% were obtained for energy transfer between EC4-YFP and *Hv*UBC-E2-CFP. However, movement of fluorescent protein, due to cytoplasmic streaming, interfered with both the bleaching and the fluorescence recovery of the bleached region (**Figure 10**). This possibly resulted in false-positive or untrustworthy recording of FRET.

Another method to determine FRET is fluorescence lifetime imaging (FLIM) of the CFP-donor molecule. Interaction between CFP and YFP molecules leads to a reduction in lifetime of the CFP donor molecule. Live-cell FRET measurements based on donor fluorescence only are more reliable using FLIM, because lifetimes are largely independent of probe concentration and light path length (Verveer et al., 2006). FLIM experiments are

currently undertaken to substantiate the BiFC data on *in planta* interaction of EC4/*Hv*UBC-E2 and EC6/*Hv*TPMT.

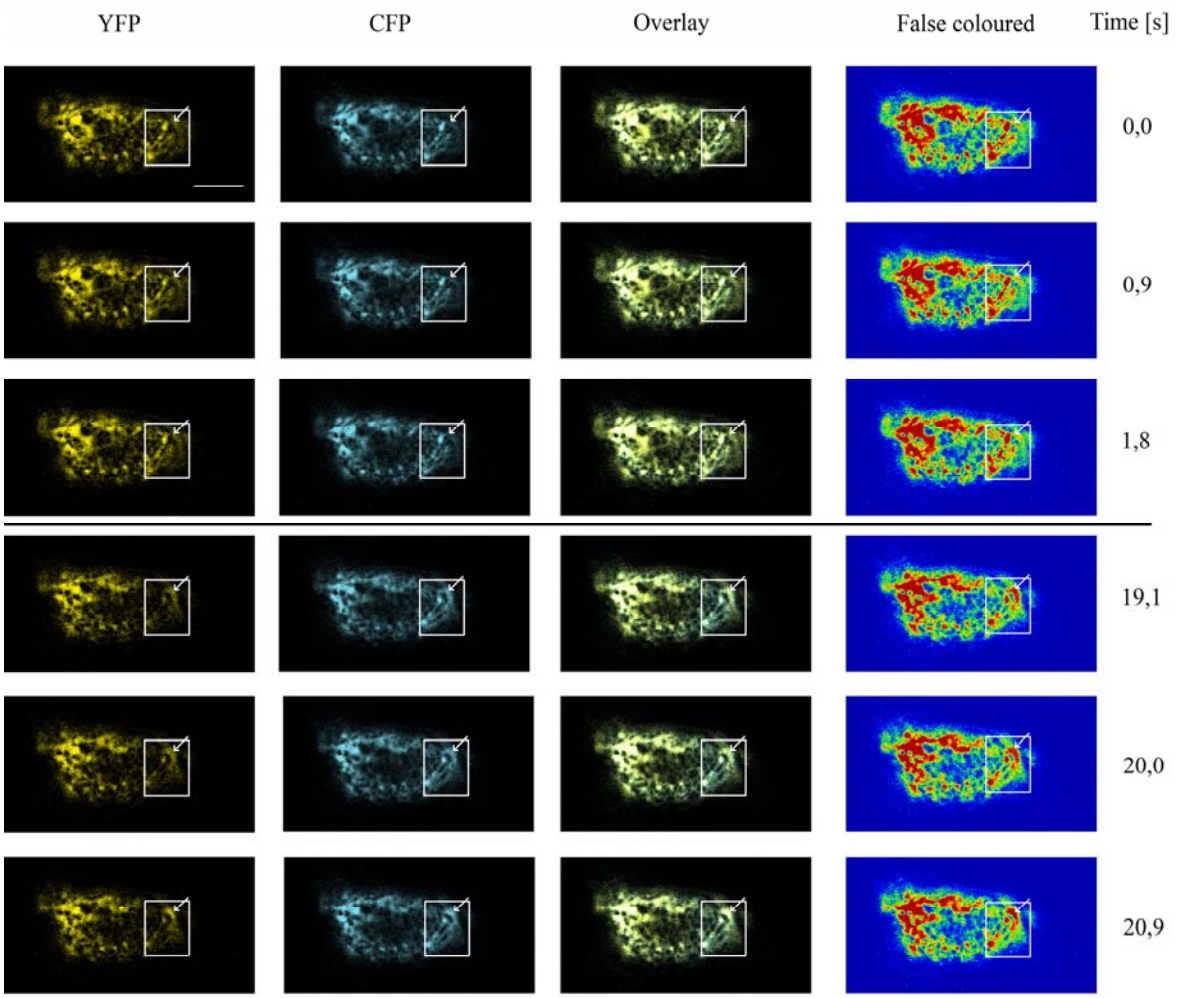

Figure 10. FRET-APB analysis in barley. Constructs encoding the fusion proteins EC4-YFP and *Hv*UBC-E2-CFP were transiently expressed in single barley epidermal cells. Fluorescence was examined by confocal laser microscopy. Three pictures were taken before and after bleaching (black line) in the indicated area of the cell (white rectangle), respectively. The time (s) when pictures were taken is given on the right side of the panels. Photobleaching of the YFP donor molecule resulted in FRET to the acceptor molecule CFP with an efficiency of 11%. However, it remains unclear if FRET had occurred, because of mass movement of fluorescent protein into the bleached area (white arrow) due to cytoplasmic streaming. False-colored images in the right panel show the intensity of the fluorescent material inside the cell. Size bar indicates 20 µm.

3.1.14 EC4 activates *Hv*UBC-E2; EC6 activates *Hv*TPMT

We hypothesized, that EC4 and EC6 may either inhibit or activate their respective interacting proteins *Hv*UBC-E2 and *Hv*TPMT. If EC4 and EC6 would activate their interacting host proteins, then increasing the levels of *Hv*UBC-E2 and *Hv*TPMT in barley should also enhance the *Bgh* haustorium index, if activity of these proteins is not controlled post-translationally. To test this hypothesis, we transiently expressed *Hv*TPMT and *Hv*UBC-E2 under the control of the constitutive maize ubiquitin promoter and subsequently inoculated the bombarded leaves with *Bgh* conidiospores.

In this set of experiments, the *Bgh* haustorium index was 70% after expression of the GUS reporter construct alone. Expression of *MLO* increased the haustorium index to 94%, while *HvUBC-E2* expression increased the haustorium index to 74% and *HvTPMT* expression increased it to 80% (**Figure 11**). Given that *EC4* expression increased the haustorium index to 79% and *EC6* expression increased it to 81%, we conclude that both *Hv*UBC-E2 and *Hv*TPMT are likely activated and not repressed by EC4 and EC6, respectively.

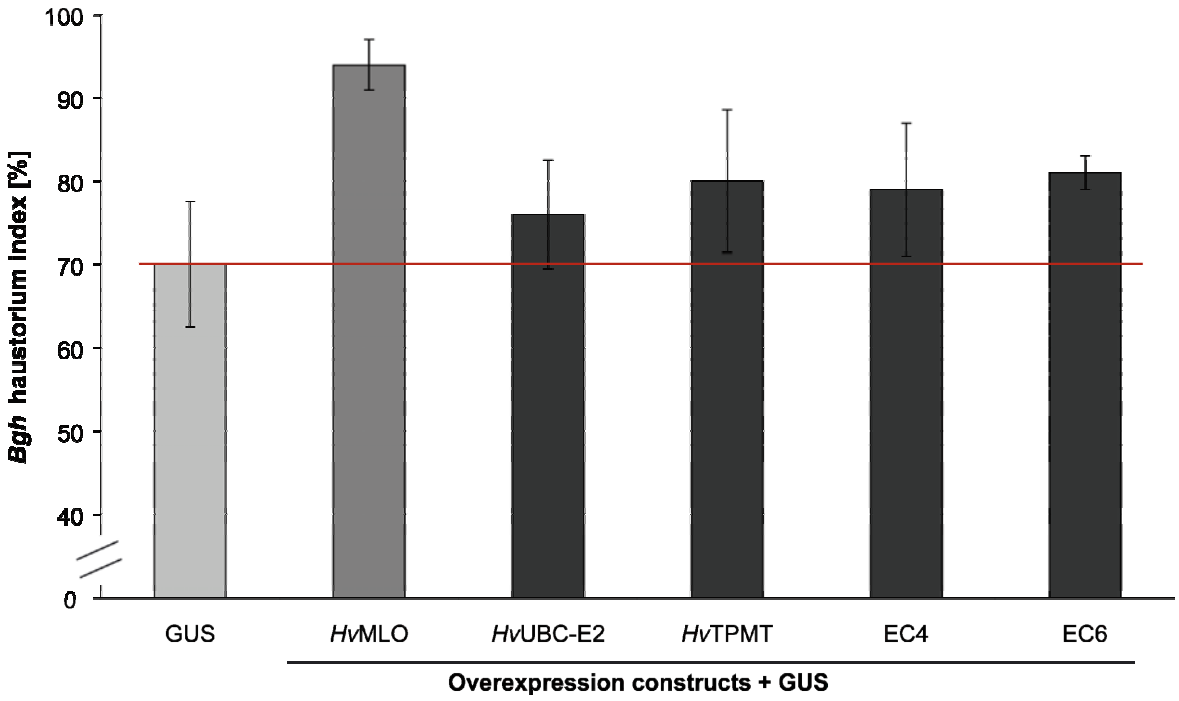

Figure 11. *Hv*UBC-E2 and *Hv*TPMT enhance *Bgh* haustorium formation. Single epidermal cells of seven days old barley leaves (cv. Golden Promise) were ballistically transformed with either a ß-Glucuronidase (GUS) reporter construct alone or together with an overexpression construct of *Hv*UBC-E2 or *Hv*TPMT. Subsequently leaves were inoculated with *Bgh* conidiospores and at 48 hpi stained for GUS activity, which renders transformed cells greenish-blue. Epiphytic fungal structures were stained with Coomassie Brilliant Blue. The ratio of transformed cells enabling haustorium formation divided by the total number of attacked transformed cells results in the haustorium index and is a measure for the impact to the tested gene on the infection success. Data shown represent means ± SD from three experiments. For each experiment and tested gene construct at least 100 transformed cells were evaluated. Barley MLO was used as a positive control. Values for EC4 and EC6 were included from Figure 1 for comparison. Asterisks indicate $p \leq 0{,}01$ (Student's t-test) compared to the negative control (GUS alone).

3.2 Identification and partial characterization of a *Bgh* gene family encoding putative RNase-like effectors

3.2.1 A *Bgh* multigene family encodes putative secreted RNase-like effectors

Screening the draft genome sequence of *Bgh* isolate DH14 for genes encoding secreted proteins, we discovered a multigene family of at least 80 members. Each protein family member contains a predicted N-terminal signal peptide for secretion and many family members possess a microbial RNase domain (RNase-like proteins). Some RNase-like proteins are encoded by genes without an intron, others contain one or two introns; the encoded RNase-like proteins vary in size from 155 to 379 amino acids. Besides variation in size, some RNase-like protein sequences cluster in specific clades of the phylogentic tree constructed with the deduced DH14 RNase-like protein sequences containing the RNase domain (**Figure 12**).

According to InterProScan analysis (Quevillon et al., 2005), the N-terminal part of the deduced AC protein sequences contains InterPro domain IPR016191. This domain represents a structural fold consisting of four-stranded antiparallel beta-sheets covering a single alpha-helix, found in the SCOP (Structural Classification of Proteins) superfamily of microbial ribonucleases (RNases). According to the SCOP hierarchy superfamilies bridge protein families with common functional and structural features inferred to originate from a common ancestor (Andreeva et al., 2008). The superfamily of microbial ribonucleases spans the greatest evolutionary divide of all known protein families (Steyaert, 1997). This superfamily consists of three protein families, each representing related sequences with distinct functions. Proteins of the three families - bacterial ribonucleases, fungal ribonucleases and ribotoxins are stabilized by disulfide bonds and share a conserved catalytic triad. Bacterial ribonucleases include barnase, binase and the cytotoxic RNase Sa3 (Makarov et al., 2008). Fungal ribonucleases include RNase T1 (*Aspergillus oryzae*), RNase U2 (*Ustilago sphaerogena)* and RNase Ms (*Aspergillus saitoi*) (Yoshida, 2001). Both fungal and bacterial ribonucleases adopt the so-called T1 fold and are small, secreted acidic proteins (Lacadena, 2007). The third family within the mircrobial ribonuclease superfamily is the ribotoxin family including mitogilin (*Aspergillus restrictus*), alpha-sarcin (*Aspergillus giganteus*) and hirsutellin A (*Hirsutella thompsonii*). Ribotoxins are basic proteins.

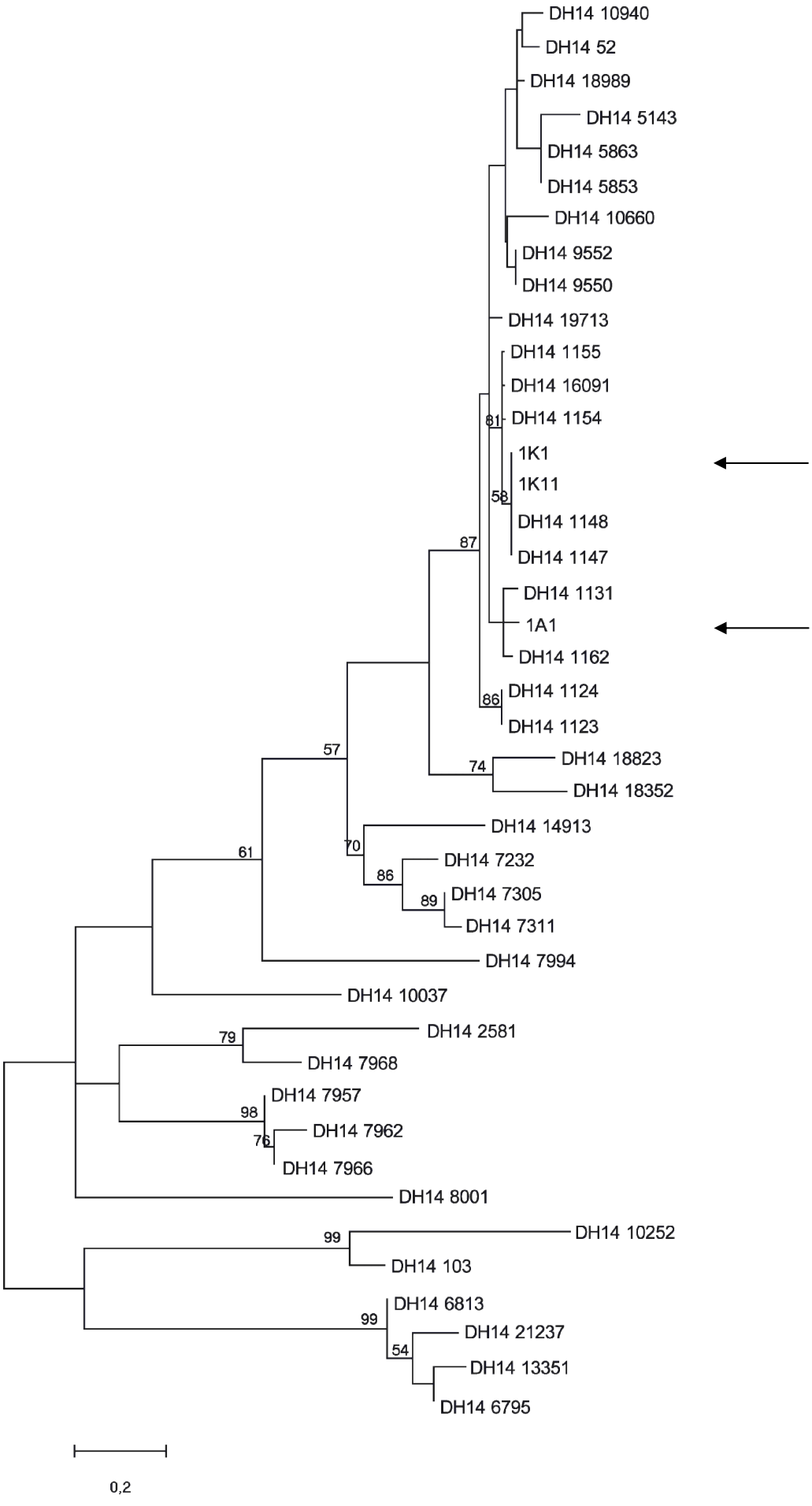
DH14 10940
DH14 52
DH14 18989
DH14 5143
DH14 5863
DH14 5853
DH14 10660
DH14 9552
DH14 9550
DH14 19713
DH14 1155
DH14 16091
DH14 1154
1K1
1K11
DH14 1148
DH14 1147
DH14 1131
1A1
DH14 1162
DH14 1124
DH14 1123
DH14 18823
DH14 18352
DH14 14913
DH14 7232
DH14 7305
DH14 7311
DH14 7994
DH14 10037
DH14 2581
DH14 7968
DH14 7957
DH14 7962
DH14 7966
DH14 8001
DH14 10252
DH14 103
DH14 6813
DH14 21237
DH14 13351
DH14 6795
81
58
87
86
57
74
61
70
86
89
79
98
76
99
99
54
0,2

Figure 12. Sequence relationship of *Bgh* RNase-like proteins. An unrooted tree was obtained by the Neighbor-Joining method using the full-length protein sequences of *Bgh* DH14 deduced RNase-like protein sequences containing InterPro domain IPR016191. The pairwise deletion and Poisson correction options were used. Boostrap values greater than 50% (for 1000 replications) are indicated on the interior branches. Arrows mark clades that include RNase-like proteins isolated from *Bgh* K1 and A6.

Ribotoxin cleavage inactivates the eukaryotic ribosome, additionally ribotoxins induce cell death (Lacadena, 2007). Compared to bacterial and fungal ribonucleases, they are larger proteins, due to insertions of long and charged loops in the common fold (Lacadena, 2007).

A phylogenetic analysis of the RNase domains of the putative *Bgh* RNase-like effectors, ribotoxins, fungal T1 RNases as well as fungal and plant T2 RNases revealed a distinct cluster of the putative *Bgh* RNase-like effectors. This cluster is closest related to a sister clade consisting of the fungal ribotoxins (**Figure 13**). Nevertheless, analysis of the predicted three-dimensional protein model using the protein prediction program Phyre (Kelley and Sternberg, 2009) suggests most structural homology with the fungal T1 RNases. These T1 RNases include RNaseMs (*A. saitoi*), RNase F1 *(Fusarium moniliforme*), RNase U2 (*U. sphaerogena*) and RNase T1 (*A. oryzae*) with an estimated precision of 60 to 85% for various analyzed putative *Bgh* RNase-like effectors even though the amino acid identity was very low (15-21%). However, in none of the analyzed *Bgh* RNase-like effectors the program could map the consensus functional sites onto the three dimensional protein models. The active sites of microbial ribonuclease superfamily members include two histidine residues and a glutamic acid residue that are directly involved in the catalytic mechanism (Martinez-Ruiz et al., 1999; Alvarez-Garcia et al., 2006). Though functional sites could not be mapped to the three-dimensional template, putative active histidine residues and a glutamic acid residue are present in the predicted RNase domain of the deduced *Bgh* RNase-like protein sequences (H48, E74 and H128) (**Figure 15**). In conlusion, *Bgh* RNase-like proteins appear to differ from ribotoxins and fungal T1 RNases in their size and in the position of putative catalytic residues.

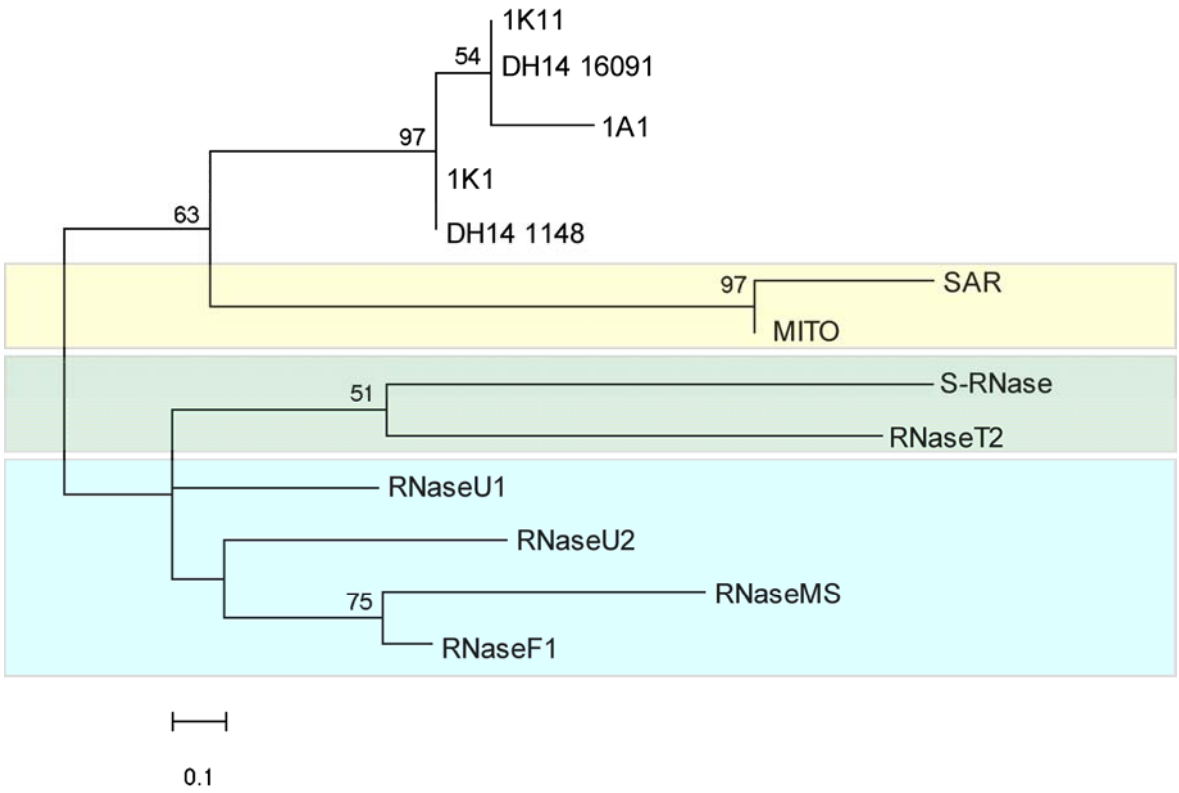

Figure 13. Phylogenetic relationship of *Bgh* RNAse-like proteins with plant and fungal secreted RNAses. An unrooted tree was obtained by the Neighbor-Joining method using protein sequences of the putative RNase domains. The pairwise deletion and Poisson correction options were used. The following proteins were included in the analysis: 1) putative RNase-like effectors from *Bgh* K1 (1K11 and 1K1), from *Bgh* A6 (1A1) (see below) and *Bgh* DH14 (DH14 1148 and DH14 16091; 2) fungal ribotoxins: α-Sarcin (SAR, *Aspergillus giganteus*, P00655) and mitogillin (MITO, *Aspergillus restrictus*, P67876); 3) T2 RNases: S-RNase (*Nicotiana altana*, P04007) and RNase T2 (*Aspergillus oryzae*, P10281); 4) fungal T1 RNases: RNaseU1 (*Ustilago maydis*, EAK82499), RNaseU2 (*Ustilago shaerogena*, P00654), RNaseMS (*Aspergillus phoenicis*, P00653) and RNaseF1 (*Giberella fujikuori*, P10282). Boostrap values greater than 50% (for 1000 replications) are indicated on the interior branches. The yellow box represents fungal ribotoxins, the green box fungal and plant T2 RNases and the blue box represents fungal T1 RNases.

BLAST searches using the draft genome sequences as well as ESTs of pea and Arabidopsis powdery mildew identified two *E. pisi* and a single *G.orontii* homologous contig for the putative *Bgh* RNase-like effectors, indicating that in these powdery mildew fungi the homologous RNase-like proteins are likely not part of a multigene family. The deduced *G. orontii* and *E. pisi* protein sequences differ in sequence and position of the RNase domain from the deduced protein sequences of putative RNase-like effectors DH14_16091 and DH14_1148 (**Figure 14**). However, the EST sequences from *G. orontii* and *E. pisi* are

more similar to the deduced protein sequences of DH14_10252 and DH14_103, which cluster in a different clade of the phylogenetic tree than DH14_16091 and DH14_1148 (**Figure 12**). In summary, the putative *Bgh* RNase-like AC effectors appear to belong to two different groups. A small group of the DH14 RNase-like effectors is also present in other powdery mildew species, while many additional RNase-like effectors appear to be absent in powdery mildew species infecting dicots.

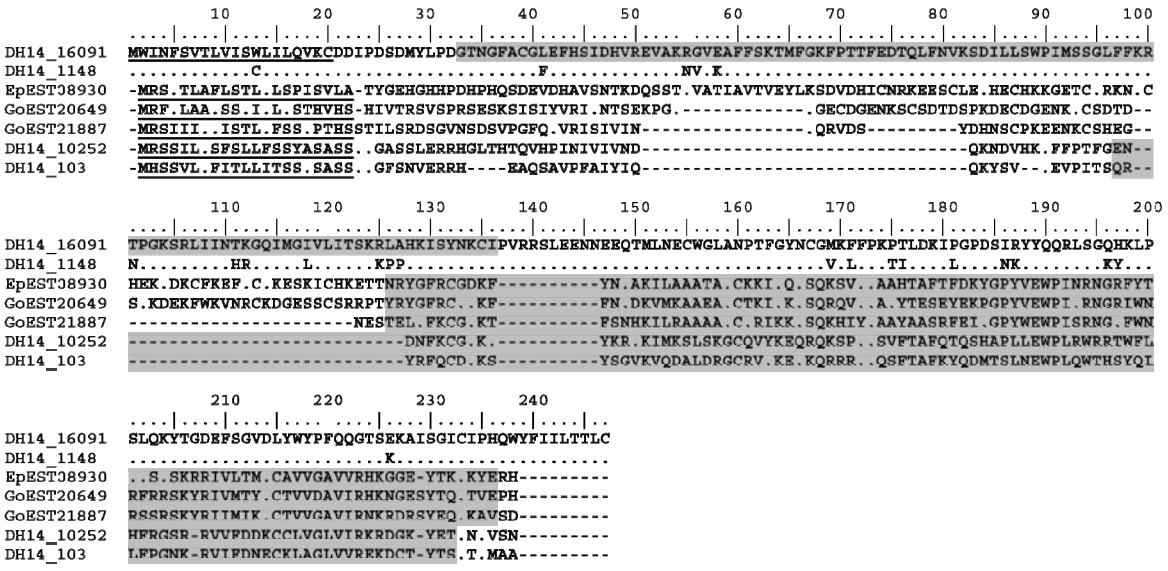

Figure 14. Sequence comparison of secreted RNase-like proteins from three powdery mildew species. Multiple sequence alignment of the deduced amino acid sequences of RNase-like proteins from barley powdery mildew (*Bgh*) isolate DH14 (DH14_16091, DH14_1148) and ESTs from the pea powdery mildew *Erysiphe pisi* (EpEST08930) and the Arabidopsis powdery mildew *Golovinomyces orontii* (GoEST20649, GoEST21887) containing InterPro domain IPR016191 (microbial ribonuclease). Sequences were aligned with ClustalW. The predicted signal peptides are underlined and the putative RNase domain is shaded grey. Identical amino acids are represented by dots.

3.2.2 Two genes encoding RNase-like effectors are sequence-conserved among six *Bgh* isolates

Next, we set out to determine sequence variation of the putative *Bgh* RNase-like effectors among six different *Bgh* isolates. To this end, we first attempted to sequence the genes with gene-specific primers for *Bgh* DH14 genomic contigs immediately following PCR-amplification from genomic DNA. By this method, we did not obtain enough DNA for sequencing. Instead, we isolated genes corresponding to DH14 contigs 1161 and 1162 with

a two step-PCR approach from genomic DNA of *Bgh* infected barley leaves (5 dpi). In the first round of PCR we used gene-specific primers, while in the second round of PCR we used “universal” primers (Uni1 and Uni2) matching the conserved regions surrounding the START and STOP codons of the genes (**Supplementary Table 1**). Subsequently the gene products were cloned in pTOPO4, amplified in *E. coli* and sequenced. The two genes were both present and strictly sequence-conserved among all six *Bgh* isolates (data not shown).

3.2.3 Multiple genes encoding RNase-like effectors are expressed in *Bgh* K1 and A6

We did not identify any *Bgh* ESTs matching the DH14 RNase-like protein sequences using BLAST, indicating that the genes are expressed at very low levels. To determine whether any and if so which gene family members are expressed during infection of barley, we amplified putative RNase-like effector cDNA by RT-PCR from RNA of barley leaves at one or two days post inoculation (1dpi or 2dpi) with either *Bgh* K1 or *Bgh* A6. We employed again two subsequent rounds of PCR using Gateway-compatible universal primers (GWYF and GWYR) matching the regions surrounding the START and STOP codons. PCR-products were cloned into pDONR using Gateway®-technology and the cDNAs were sequenced. Interestingly, at these early time points of infection different sets of the presumably secreted RNase-like genes appear to be expressed.

We isolated 13 putative RNase-like effector cDNAs from *Bgh* K1 RNA 1dpi (designated 1K1, 1K2, 1K3, 1K5, 1K9, 1K11, 1K14, 1K15, 1K17, 1K18, 1K21, 1K25, 1K28) and four from *Bgh* K1 RNA 2dpi (designated 2K7, 2K9, 2K13, 2K25). Additionally, we isolated 10 putative RNase effector cDNAs from *Bgh* A6 RNA 1dpi (designated 1A1, 1A3, 1A4, 1A5, 1A8, 1A9, 1A10, 1A11, 1A14, 1A25) and one from *Bgh* A6 RNA 2 dpi (designated 2A4). Some cDNAs isolated from the same time point and *Bgh* isolate were identical: a) 1K2, 1K3 and 1K17, b) 1K11 and 1K15, c) 1A4 and 1A9 and d) 2K7 and 2K9. Furthermore identical cDNAs were isolated from the same *Bgh* isolate, but from RNA of two different infection time points: 1A3, 1A8, 1A11 and 2A4. One cDNA was isolated both from *Bgh* A6 and *Bgh* K1: 1K21 and 1A14. In total, we isolated 23 different cDNAs from both isolates. The transcripts from *Bgh* K1 and A6 all encode RNase-like proteins of 247 amino acids with a N-terminal cleavable signal peptide of 20 amino acids and a predicted ribonuclease domain spanning amino acids 33-136. The strict length conservation of these transcripts might be due to the primer design employed to amplify the transcripts by RT-PCR from *Bgh*-infected barley leaves. Interestingly, all RNase-like amino acid sequences deduced from the isolated cDNAs from *Bgh* K1 and A6 cluster with the conceptual amino

acid sequences of DH14 AC contigs 16091, 1154, 1155, 1148, 1161 and 1160, for which homologs appear to be absent in other powdery mildew species (**Figure 12**).

Alignment of the deduced amino acid sequences of the early expressed putative RNase-like effectors revealed amino acid variation throughout the protein sequences. The C-terminal part (amino acids 138–247) of the RNase-like proteins did not exhibit signatures of any protein motif. Interestingly, the central part of the predicted RNase domain (residues 59-100) is devoid of polymorphic sites, except for one in 2K5, which might be a PCR-based error. One of the putative catalytic sites, H111, is polymorphic; a tyrosine can also be present at this residue position (**Figure 15**). Only three sequence variants were detected around another putative active site residue, H128. Sequence variant 1 (KKPP**H**KISYN) is present in 1K1, 1K2, 1K5, 1K18, 1K25, 2K5, 2K7, 2K13, 1A4, 1A9 and 1A25; sequence variant 2 (KRLA**H**KISYN) is present in 1K9, 1K14, 1K21 and 1A14; sequence variant 3 (KQP**H**EIILN) is present in1A1, 1A3, 1A5, 1A10, 1A11 and 2A4. Putative RNase-like effectors containing variants 1 or 2 fall into two distinct clades within the neighbor-joining tree, except for 1K14 (**Figure 13**). The majority of observed sequence polymorphisms were dimorphic; i.e. only two alternative amino acids were present at a residue position in the primary sequence. However, two residues have three alternative amino acids: residue 126 can be proline, glutamine or leucine and residue 171 can be leucine, serine or phenylalanine. Note, that the ladder polymorphic site residue 171 might also be dimorphic, because the serine is only present in the deduced amino acid sequence of two RNase-like cDNAs both isolated from *Bgh* K1 at the same infection time point. Therefore it might be a PCR-based error. Nevertheless, at least the polymorphic residue 126 might be either under less selective constraints or it might be more important for protein function than dimorphic sites, e.g. in substrate recognition.

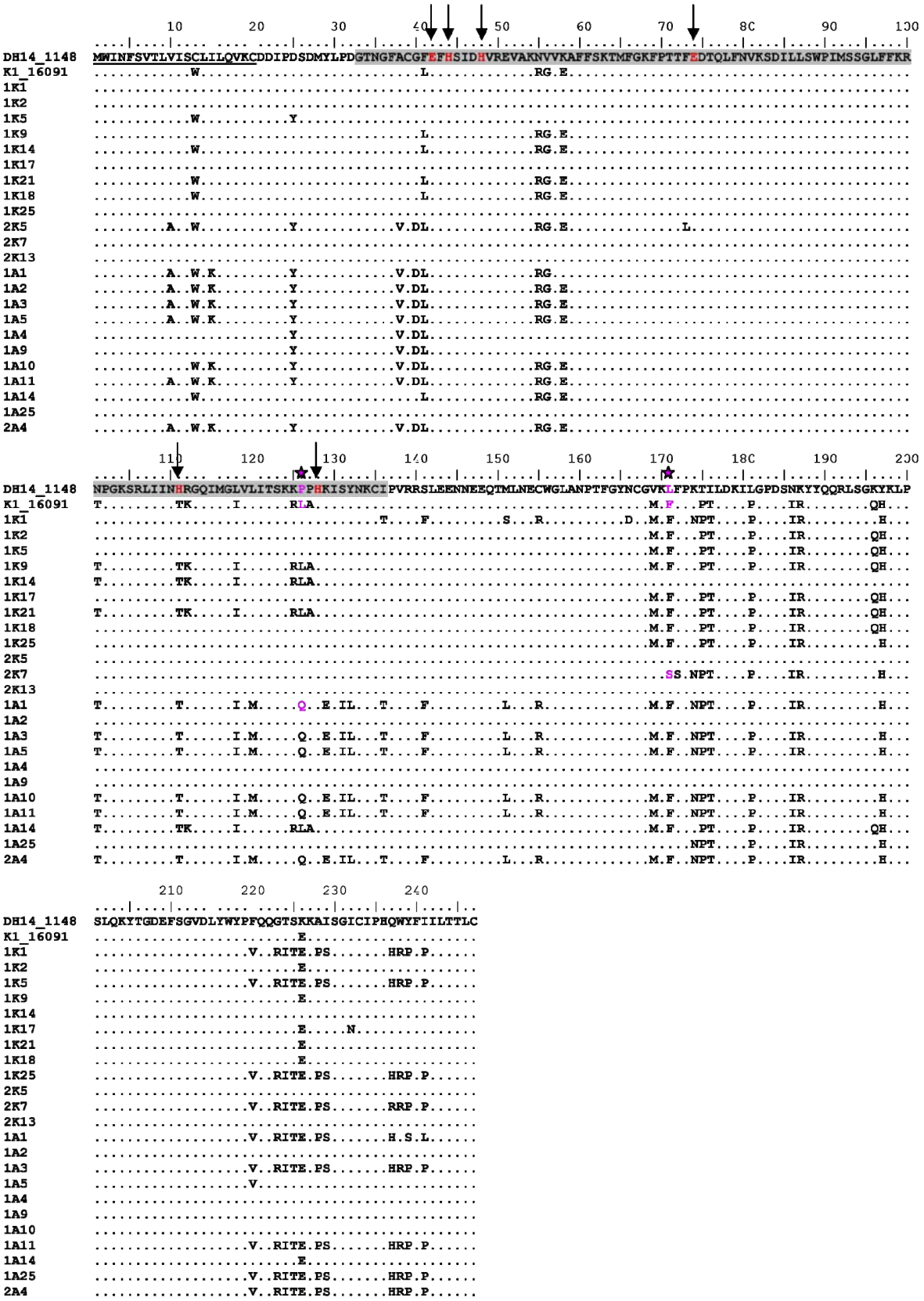

Figure 15. Sequence comparison of RNase-like proteins deduced from cDNAs of *Bgh* isolates K1 and A6. Multiple sequence alignment of the deduced protein sequences of RNase-like cDNAs isolated from *Bgh* K1 and A4 at one or two days post inoculation. RNase-like protein sequences were aligned with the deduced protein sequence of *Bgh* DH14 contig 1148

using ClustalW. The predicted signal peptide is underlined and the putative RNase domain is shaded grey. Putative catalytic residues are marked by an arrow and are printed in red. Polymorphic residues with three alternative amino acids (printed in pink) are marked by a pink star. Amino acids identical to those in the DH14_1148 sequence are represented by dots. Please note that the central part of the predicted RNase domain is devoid of polymorphic sites and that only three sequence variants are present around the putative catalytic site H128.

3.2.4 Are RNase-like proteins (ACs) recognized by MLA resistance proteins?

In a recent study on barley MLA resistance proteins, Seeholzer and colleagues not only identified 32 sites of positive selection in solvent-exposed parts of the LRR domain, but also inferred that MLA proteins directly bind polymorphic, but structurally related *Bgh* AVR_A effectors that are likely of similar or identical size (Seeholzer, 2009, submitted). The putative *Bgh* RNase-like effectors fulfill the criteria for AVR_A effectors; they are polymorphic, but structurally highly similar and of identical size. Therefore we designated them Avirulence Candidates (ACs).

MLA resistance proteins are encoded by alleles of the *MLA* locus, thus only one *MLA* gene is present in a given barley cultivar. However, a given *Bgh* isolate can be recognized by different MLA proteins, indicating that AVR_A effectors are encoded by members of a gene family, which is also the case for the *AC* family of putative RNase-like effectors. Moreover, genetic analysis revealed that multiple *AVR_A* genes cluster in genomic *Bgh* regions (Jensen et al., 1995). At least in the *Bgh* DH14 *AC* family this also applies for some family members (e.g. 1147, 1155, 1160, 1161 and 1161), which are localized on the same *Bgh* genomic supercontig. In the phylogenetic tree, these DH14 family members also cluster with the AC RNase-like effectors isolated from *Bgh* K1 and A6 at early infection time points (**Figure 13**) and they appear to be absent in other powdery mildew species.

To directly test a potential avirulence function of the AC RNase-like proteins, we transiently expressed the corresponding full-length cDNAs in single barley epidermal cells of near-isogenic barley lines encoding either the *MLA1* (P-01) or the *MLA6* (P-03) resistance gene. *Bgh* isolate K1 encodes the cognate avirulence gene for *MLA1*, while *Bgh* isolate A6 encodes the cognate avirulence gene for *MLA6* (Halterman et al., 2001). Together with each construct harboring the secreted RNase candidate, a second construct harboring *gfp* was co-expressed as a marker of cell vitality. Recognition of the cognate avirulence gene should result in cell death and thus in reduction of GFP fluorescence.

Putative AC RNase-like effectors isolated from *Bgh* isolate K1 (1K1, 1K2, 1K5, 1K9, 1K11, 1K13, 1K14, 1K18, 1K28, 2K7, 2K13, 2K25) were transiently expressed in single epidermal cells of barley P-01. At least five barley leaves per bombardment were microscopically evaluated for GFP fluorescence at two and four days after bombardment. No obvious reduction of GFP fluorescence was observed in P-01 barley epidermal cells expressing either of the *AC RNase-like* genes isolated from *Bgh* isolate K1 compared to expression of *gfp* alone.

Analogously, AC RNase-like effectors isolated from *Bgh* isolate A6 (1A1, 1A3, 1A4, 1A5, 1A10, 1A14, 1A25, 2A4) were transiently expressed in single epidermal cells of P-03. Again, no obvious reduction of GFP fluorescence was observed in P-03 epidermal cells expressing either of the *Bgh* A6 putative AC RNase-like effectors. In summary, none of the tested *Bgh* K1 or A6 AC RNase-like effectors appear to be recognized by the cognate barley resistance gene.

4 Discussion

4.1 Identification and functional characterization of *Bgh* effectors

4.1.1 Experimental Approach

In this study, we have successfully identified *Bgh* ESTs encoding small, secreted proteins without homology to known proteins as putative *Bgh* effectors using bioinformatic database mining. Bioinformatic mining of secreted proteins has been successfully employed to identify effectors from bacteria (Chang et al., 2004; Schechter et al., 2006), oomycetes (Torto et al., 2003; Tian et al., 2004) and rust fungi (Kemen et al., 2005; Catanzariti et al., 2006). Generally, bioinformatic identification of putative effectors is followed by functional assays, such as expression *in planta*. In contrast to the above mentioned studies we were not attempting to identify effectors with an avirulence function. Instead, we identified *Bgh* effectors, ECs, with a potential function in virulence by screening for effectors which positively contribute to pathogen entry and haustorium formation inside plant cells (**Figure 1**).

The most unambiguous way to unravel a virulence function of a particular effector protein is the analysis of a gene knock-out mutant. We could not use this technique due to the genetic intractability of obligate biotrophic fungi. However, knock-out mutants of fungal effectors were not always successful in identifying a role in virulence. For the *C. fulvum* effectors *Ecp1* and *Ecp2* as well as *F. oxysporum* effectors *Six1* knock-out mutants confirmed a virulence function (De Wit et al., 1997; Rep et al., 2005). Contrastingly, gene knock-out mutants of *C. fulvum* effectors *Avr9*, *U. maydis* effectors *Mig1* and *Mig2* and *M. grisea* effectors *BAS1, BAS2* and *BAS3* did not result in a noticeable virulence phenotype (Marmeisse et al., 1993; Basse et al., 2002; Farfsing et al., 2005; Mosquera et al., 2009). Also for bacterial type III effectors, elimination of a single effector protein often does not lead to a measurable phenotype. This might be due to redundancy of effector functions or the lack of sensitive assays capable of detecting the absence a single effector (Galán, 2009).

Instead of gene knock-out mutants we employed over-expression of the effectors inside plant cells. This assay is more sensitive and therefore more suitable to capture the subtle contributions of single effectors to virulence. Potential problems of over-expressing effectors are caused by the artificially high effector protein levels inside the host cell and

the biolistic delivery inside barley cells, which both do not occur in natural infections. However, to date no threshold levels required for virulence function of any effectors are reported and the route of fungal effector delivery inside the host remains to be established. Although the readout (haustorium index) is based on a complex process, transient expression of potential *Bgh* effectors inside cell barley epidermal cells exploits three main advantages of this unique pathosystem: (1) the sensitive single-cell assay amplifies subtle effector contributions; (2) effector expression is cell-autonomous and in epidermal cells, thus in the same tissue as in natural *Bgh* infection; and (3) subsequent inoculation with fungal spores might provide additional effectors required for acting in concert with the over-expressed effector protein. Consequently, we considered transient over-expression as the best method to identify *Bgh* effector candidates and we succeeded in identifying five *Bgh* EC proteins positively contributing to haustorium formation.

4.1.2 Bioinformatic Analysis- Effector structure

4.1.2.1 Structural homology/resemblance

One selection criterion for the *Bgh* EC proteins was the absence of homology to proteins present in public databases. Nevertheless, the identification of EC protein motifs provides some clues about the putative intrinsic function and the similarity to known effectors. EC2 and EC4 are cysteine-rich proteins (**Figure 4**). Many fungal effectors identified to date are small, secreted and cysteine-rich proteins (Rep, 2005; Stergiopoulos and de Wit, 2009). Based on the spacing and the number of cysteine residues, different motifs can be distinguished. At the beginning of this study, the cysteine residues of EC2 and EC4 were annotated as cysteine knot motifs. Cysteine knots are also present in the *C. fulvum* effector Avr9 and *M. lini* effector AvrP4 (van den Hooven et al., 2001; Catanzariti et al., 2006). Cysteine-knotted proteins resemble carboxypeptidase inhibitors and might accordingly inhibit peptidases (Vervoort et al., 1997). During the course of the study, the InterProScan annotation for the motif formed by the cysteine residues in EC2 and EC4 changed to annotation as a CFEM motif. CFEM motifs consist of eight cysteine residues and are common in - but not restricted to – fungal extracellular membrane proteins (Kulkarni et al., 2003). Interestingly, two *M. grisea* proteins, Pth11 and Aci1, contain CFEM motifs and both are required for appressorium development (Choi and Dean, 1997; DeZwaan et al., 1999). As *EC2* transcript levels increase at the time point of appressorium formation, it might also be involved in appressorium development.

EC5 is a glycine-rich protein (**Figure 4**). Another glycine-rich, hydrophilic effector protein is *M. grisea* PWL2, which confers avirulence on the alternative host weeping lovegrass, but not on any known rice cultivar (Sweigard et al., 1995). A virulence function for PWL2 is not known. Though no function was demonstrated so far for glycine-rich effectors, glycine-rich proteins are also present among RXLR effectors from *P. sojae* and *P. ramorum* (Bhattacharjee et al., 2006). Oomycete RXLR effectors are considered as haustorium-specific effectors and are translocated from haustoria into host cells (Whisson et al., 2007; Dou et al., 2008a). Likewise, *EC5* transcript levels increase at the time point of haustorium formation (**Figure 5**), suggesting that it is also a haustorium-specific effector.

EC6 contains a predicted C-terminal transmembrane domain. Yet the EC6-YFP fusion protein did not localize to membranes, but remained cytoplasmic after transient expression in barley cells (**Figure 6**). Furthermore, deletion of this domain did not alter the ability of EC6 to enhance the *Bgh* haustorial index in the transient expression assay (**Figure 1**). Therefore, the predicted transmembrane domain is probably a hydrophobic region of the protein, which is neither required for EC6 localization nor the EC6 ability to enhance haustorium formation.

4.1.2.2 Requirement of the signal peptide for virulence function

Transient expression of full-length *EC1, EC2, EC4* and *EC6* was more efficient in enhancing the haustorium index than expression of truncated versions lacking the N-terminal signal peptide (**Figure 1**). Similarly, the avirulence function of the *M. lini* effector AvrP4, the *P. infestans* effector Avr3a and the *P. sojae* effector Avr1b depend on the presence of their respective N-terminal signal peptides (Armstrong et al., 2005; Catanzariti et al., 2006; Dou et al., 2008b). For AvrP4 it has been suggested that the protein might require secretion into the extracellular space and subsequent re-entering of the cell (Catanzariti et al., 2006). Alternatively, some effectors might need a functional signal peptide for targeting to the ER to enable proper folding of the proteins, e.g. the formation of disulfide bonds. In this model, proteins lacking the signal peptide would not be directed to the ER, resulting in aberrant folding and reduced effector activity.

On the other hand, truncated EC5 was as efficient in enhancing *Bgh* haustorium index as the full-length EC5 protein. This is reminiscent of flax rust AvrM, *H. arabidopsidis* ATR13 and *P. sojae* Avr3c, which do not require their respective signal peptides for avirulence function (Allen et al., 2004; Catanzariti et al., 2006; Dong et al., 2009).

Furthermore, at least one flax rust effector, AvrL567, has stronger avirulence activity as a truncated version compared to the full-length protein (Dodds et al., 2004), suggesting that different effector proteins have variable requirements for the presence of a signal peptide.

4.1.3 The expression pattern of *EC2* and *EC5* suggests a role in appressorium and haustorium formation, respectively

EC1, *EC4* and *EC6* are constitutively expressed throughout the initial infection phase (**Figure 5**). Contrastingly, *EC2*, *EC4* and *EC5* display distinct expression profiles. *EC2* transcript levels increase at the time point of appressorium development (**Figure 5**). Likewise, transcript levels of a diverse set of genes encoding secreted proteins increase around the time of appressorium development in fungi and oomycetes. Among these genes are *Bgh catalase*, *M. grisea MPG1* and *ACE1* and *P. infestans Avr3a* (Soanes et al., 2002; Zhang et al., 2004; Collemare et al., 2008). *Bgh* catalase was detected by immunofluorscence at the appressorial germ tube tip and may act to scavenge H_2O_2 during the establishment of infection (Zhang et al., 2004). *MPG1* encodes a small, secreted hydrophobin involved in fungal attachment to the host surface (Talbot et al., 1996; Wosten, 2001). Targeted deletion of *MPG1* results in a mutant strain that is reduced in virulence as well as conidiation and appressorium formation (Talbot et al., 1996). *ACE1* behaves as a classical *Avr* gene. However, instead of a secreted protein, *ACE1* encodes a hybrid polyketide synthase-nonribosomal peptide synthetase (PKS-NRPS), which presumably synthesizes a secondary metabolite that is recognized by the rice Pi33 resistance protein (Bohnert et al., 2004). *Avr3a* transcript levels strongly increase not only during appressorium development, but also during the necrotrophic stage of infection, supporting a potential role in pathogenicity (Armstrong et al., 2005).

Both *EC4* and *EC5* transcripts accumulate at the time of haustorium formation. Yet the increase in *EC5* transcript levels is more drastic compared to *EC4* (**Figure 5**). Moreover, *EC4* expression data were variable (**Supplementary Figure 3**). As mentioned above, haustoria have been implicated in secretion of particular classes of fungal and oomycete effectors. Especially effectors with avirulence function were found to be secreted from haustoria and to be recognized within the host cell (Dodds et al., 2004; Catanzariti et al., 2006; Whisson et al., 2007). Additionally, the bean rust effector *Uf*-RTP1p - for which no avirulence function is reported - is exclusively expressed in haustoria as demonstrated by protein Western Blotting and it localizes to the host cell cytoplasm and the host nucleus (Kemen et al., 2005). Although we did not identify a potential translocation signal among

the EC proteins, it is tempting to speculate that EC5 and potentially also EC4 are likewise translocated into barley host cells to fulfill their effector activity.

4.1.4 The special case of EC3

False positives candidates represent a pitfall of every screening procedure. In our effector screen, EC3 was disclosed as a false positive candidate. EC3 was identified as a putative *Bgh* effector with a partial serine protease (subtilisin) domain. Though the SignalP score for the predicted N-terminal signal peptide was low (**Table 1**), we initially considered EC3 as an interesting candidate, reasoning that the predicted partial serine protease domain might point to a function for EC3 as a protease inhibitor. As outlined above, protease inhibition recently emerged as a common function for oomycete and fungal effectors. Transient expression of full-length *EC3* in barley cells increased the *Bgh* haustorium index to 81% (**Figure 1**), thus supporting our hypothesis that EC3 might positively contribute to *Bgh* virulence. However, the N-terminus of EC3 did not direct secretion of yeast invertase (**Figure 2**). Also, EC3 did neither suppress BAX-induced cell death nor trigger growth inhibition in yeast (**Figure 7**). During the course of the study, *Bgh* genome data became available and we discovered that EC3 is only the C-terminal part of a serine protease (**Supplementary Figure 1**). Mature serine proteases have an N-terminal catalytic domain containing the Asp-His-Ser catalytic triad (Siezen, 1996). Although the catalytic residues of DH14 contig 7906 reside in the N-terminal part of the protein, thus not overlapping with the EC3 sequence, Asp, His and Ser residues within the EC3 protein sequence reveal a similar spacing. It is possible that these residues might have mimicked the serine protease activity of DH14 contig 7906, thereby leading to an increase in *Bgh* haustorium formation. Moreover, subtilisin-like serine proteases have been implicated in virulence of *Mycobacterium tuberculosis* and the pathogenicity of certain fungi (Sreedhar et al., 1999; Brown et al., 2000). The fungal subtilisin-like serine proteases are believed to degrade the protein linkage in the host cell wall, thereby facilitating penetration. This would be consistent with the moderate transcriptional induction of *EC3* at the time point of appressorium formation (**Figure 5**). Serine proteases are too big to be considered as classical pathogen effectors; nevertheless they might contribute to virulence. In conclusion, *EC3* only encoded a partial serine protease, but the full-length serine protease encoded by the DH14 contig 7906 might itself fulfill a role in virulence, thus leading to the increase in haustorium formation in the transient gene expression assay.

4.1.5 EC sequence conservation might be due to a lack of selection pressure

EC1, EC2, EC4, EC5 and EC6 were found to be highly sequence conserved among six different *Bgh* isolates (**Figure 4)**. While EC1 and EC5 have one and two polymorphic sites, respectively, not a single polymorphic site was present in EC2, EC4 and EC6 at the protein level. Similarly, only a single polymorphic amino acid was identified in the *C. fulvum* effector Ecp6. Sequencing of *Ecp6* alleles in 50 *C. fulvum* strains revealed five single nucleotide polymorphisms (SNPs). Of these five SNPs, two were present in introns and only one SNP resulted in an amino acid exchange (non-synonymous SNP) (Bolton et al., 2008). As *Ecp6* has orthologs in 11 other fungi, the *Ecp6* genes are thought to have evolved from a recent common ancestor (Bolton et al., 2008).

Evolution from a common ancestor is difficult to assess for the *EC* genes, because we could only identify one homolog for one of the *EC* genes among other powdery mildew species. Nevertheless, it will be interesting to investigate whether the *EC2* homolog in the *G. orontii* genome (*Go*EC2) also positively contributes to haustorium formation (**Figure 3**). In view of the presumably early evolutionary divergence of powdery mildew fungi infecting monocotyledonous plants like *Bgh* and those infecting dicotyledonous plants like *G. orontii* (Glawe, 2008), a conservation of EC2 effector activity would point to a central role in virulence of powdery mildew fungi.

Studies on *C. fulvum* effectors have shown that genes encoding effectors that are recognized by resistance proteins deployed in commercial tomato cultivars accumulated many more polymorphisms than effector genes for which no resistance genes were deployed in commercial tomato cultivars (Stergiopoulos et al., 2007). Given that we are not aware of barley resistance proteins recognizing the EC proteins analyzed in this study, the sequence conversation of EC proteins might be due to the absence of selection pressure imposed on the fungus to escape recognition by resistance proteins.

4.1.6 EC localization in the host cytoplasm is consistent with the cytoplasmic localization of the EC4 and EC6 interacting barley proteins

Full-length EC-YFP fusion proteins co-localized with an ER-marker (**Figure 6**), indicating that the N-terminal signal peptide in each case is recognized by the host secretion machinery and that EC proteins are directed to the plant secretory pathway. Thus, the EC protein signal peptides are not only functional in yeast, but also in plants. We were not able to detect secreted EC proteins in the apoplast, likely due to quenching of the fluorophore in

the acidic extracellular environment. Therefore we could not address whether the EC proteins were secreted from the plant cell and re-entered the cell as has been suggested for some effector proteins from flax rust (Catanzariti et al., 2006; Ellis et al., 2007), or whether they ultimately localized to the apoplast. Effectors from *C. fulvum* and *F. oxysporum* were isolated from apoplastic fluid and they fulfill their function in the apoplast. However, apoplastic localization of fluorophore-tagged proteins has only been demonstrated for effectors from *M. grisea* and *U. maydis*. These effectors were expressed from transgenic fungal strains and they were detected in the membrane-sealed, protected compartment surrounding the infection hypha reminiscent of the bean rust effector *Uf*-RTP1p that was detected in the EHM as well as the host plant cell by immunolocalization (Kemen et al., 2005; Doehlemann et al., 2009; Mosquera et al., 2009).

Truncated EC proteins (lacking the N-terminal signal peptide) fused to YFP localized to the plant cytoplasm in the transient expression assay. Likely, this cytoplasmic localization reflects the authentic EC localization during *Bgh* infection, as it is currently believed that effectors first enter the secretion pathway of the pathogen and during ER entrance the signal peptide is co-translationally cleaved off. Not much is known about the intracellular host localization of effector proteins. Several bacterial type III effectors, like *P. syringae* AvrB, AvrRpm1, AvrPphB, AvrPto and HopF2, have a N-myristoylation motif and are targeted to the plasma membrane (Shan et al., 2000; Nimchuk et al., 2003; Robert-Seilaniantz et al., 2006). Additionally, some effectors localize to the host nucleus including bean rust *Uf*-RTP1p, *Ralstonia solanacearum* Pop2 and *Xanthomonas* XopD (Deslandes et al., 2003; Hotson et al., 2003; Kemen et al., 2005). So far, organelle localization has only been demonstrated for the *P. syringae* effector HopI1, which localizes to chloroplasts (Jelenska et al., 2007). Since the EC proteins do not possess predicted N-myristoylation motifs or nuclear localization signals, it is perhaps not surprising that they localize to the host cytoplasm. Moreover, localization in the cytoplasm is consistent with the cytoplasmic host interactors of EC4 and EC6 (see below).

4.1.7 One bioassay might be insufficient to capture a potential PCD suppressing activity of the EC proteins

A hallmark of successful host colonization by biotrophic pathogens is the suppression of programmed cell death (PCD) (Hahn and Mendgen, 2001). Many bacterial and oomycete effectors can suppress PCD. For example, 5 out of 19 tested *P. syringae* effectors suppressed the HopPsyA-triggered HR in tobacco. Out of these five effectors, four

effectors also suppressed BAX-induced PCD in yeast (Jamir et al., 2004). Likewise, *P. sojae* Avr1b suppressed BAX-induced cell death in yeast, soybean and *N. benthamiana* (Dou et al., 2008b). None of the tested EC proteins (EC1, EC2, EC5 and EC6) suppressed BAX-induced cell death in yeast. However, this does not exclude the possibility that EC proteins are capable of PCD suppression. For type III effectors it has been put forward that multiple bioassays will be required to identify all effectors with some ability to suppress PCD (Jamir et al., 2004). Presumably this also holds true for fungal and oomycete effectors.

There are numerous triggers for PCD, which likely activate different signaling cascades. The *P. infestans* effector Avr3a, for example, suppresses cell death induced by another *P. infestans* protein, INF1 (Bos et al., 2006). Furthermore, bacterial effectors display different PCD-suppressing characteristics, indicating that they function by different mechanisms. For example, the *P. syringae* effector AvrPtoB suppresses PCD in *N. benthamiana* induced by BAX and two different resistance proteins. Additionally it suppresses hydrogen peroxide-induced PCD in yeast (Abramovitch et al., 2003). On the other hand, four other *P. syringae* effectors capable of suppressing BAX-induced PCD did not suppress hydrogen peroxide-induced PCD in yeast (Jamir et al., 2004). Due to its broad anti-PCD activity, AvrPtoB was suggested to target a downstream component of PCD signaling (Abramovitch et al., 2003). This implies that effectors targeting upstream components of PCD signaling might not be unraveled by a single PCD suppression assay.

4.1.8 EC proteins do not cause prominent growth inhibition in yeast

Some bacterial effectors cause growth inhibition in yeast due to targeting conserved eukaryotic processes, e.g. interference with respiration or the host cytoskeleton (Aleman et al., 2005; Munkvold et al., 2008). Given that *Bgh* induces global changes in defense, metabolism and photosynthesis of the invaded host cell (Gjetting et al., 2007; Fabro et al., 2008) as well as cytoskeleton rearrangements (reviewed in Schmidt and Panstruga, 2007), we assayed the EC proteins for their ability to inhibit yeast growth. None of the tested EC proteins inhibited yeast growth (**Figure 7**). Considering that *EC* expression did not cause cytotoxity in barley cells, the finding that they also did not cause cytotoxity in yeast might not be surprising. However, the *P. syringae* effectors HopAO1 and HopN1 caused growth inhibition in yeast, but in plants they both suppress PCD, indicating that at least some effector targets in plants and yeast are different (Bretz et al., 2003; Espinosa and Alfano, 2004; Lopez-Solanilla et al., 2004; Munkvold et al., 2008). Thus, EC proteins might target

plant proteins that are either not present or not accessible in yeast and therefore we did not observe growth inhibition upon *EC* expression in yeast. Alternatively, EC proteins might induce subtle changes in yeast physiology that are not manifested as prominent growth inhibition.

4.1.9 EC4 might target the host vesicle trafficking pathway

To disclose the EC role in virulence, it was crucial to identify host interactors targeted by the EC proteins. The isolation of EC4- and EC6- interacting barley proteins suggests that these two *Bgh* effectors target distinct host signaling pathways.

EC4 interacts with *Hv*ARF-GAP (ADP-ribosylation factor (ARF)–GTPase-activating protein (GAP)) and *Hv*UBC-E2 in yeast (**Figure 8**). In plants, ARF proteins have been implicated in vacuolar-sorting to the lytic vacuole as well as in nonhost and *R*-gene mediated resistance in tobacco (Pimpl et al., 2003; Coemans et al., 2008). So far, ARF-GAPs have not been implicated directly in host immunity, but their counter-players, the ARF-GEFs (GTP-ase exchange factor) that activate ARFs, have been revealed as effector targets. The *P. syringae* effector HopM1 marks the Arabidopsis ARF-GEF MIN7 for proteasomal degradation, presumably to inhibit host vesicle trafficking (Nomura et al., 2006). Although the interaction of EC4 with *Hv*ARF-GAP was very strong in yeast (**Figure 8**) we could not confirm this interaction *in planta* by BiFC. This does not preclude an *in vivo* interaction between the proteins. One known constraint of the BiFC is the sterical orientation of the fluorophores in the fusion proteins, which might have resulted in insufficient flexibility, thereby preventing re-constitution of the YFP fragments. Due to this constraint of BiFC it has been suggested that the tested proteins should be fused at all possible orientations relative to the YFP fragment (Bracha-Drori et al., 2004). As we were unable to clone C-terminal fusions of YFP-segments to the C-terminal part of *Hv*ARF-GAP, so far we could not test all possible fusion protein combinations of *Hv*ARF-GAP and EC4 (**Supplementary Table 3**). If we would confirm interaction between EC4 and the *Hv*ARF-GAP, this would implicate EC4 in targeting the vesicle trafficking pathway of the invaded host cell.

In contrast to *Hv*ARF-GAP, the interaction of EC4 and *Hv*UBC-E2 in yeast was confirmed *in planta* by BiFC using various N- and C-terminally tagged fusion constructs (**Figure 9**). Targeting of the host ubiquitination pathway has emerged as a common theme in interactions of bacteria with their animal or plant hosts (Angot et al., 2007; Gohre and

Robatzek, 2008). Effectors like *P. syringae* AvrPtoB and *Agrobacterium tumefaciens* VirF exert ubiquitin ligase activity to exploit the host proteasomal machinery, and the *P. syringae* toxin syringolin A (SyrA) was found to inhibit the eukaryotic proteasome (Tzfira et al., 2004; Janjusevic et al., 2006; Groll et al., 2008). Interestingly, SyrA application on wheat abolishes powdery mildew infection, presumably by counteracting the suppression of host defense imposed by the fungus (Waspi et al., 2001). This might point to a role for *Bgh* in directing host proteins for proteasomal degradation.

Until now, effectors found to target the plant ubiquitin pathway are bacterial type III effectors mimicking components of the eukaryotic machinery (Gohre and Robatzek, 2008). UBC-E2s have not yet been implicated as effector targets of bacteria, fungi or oomycetes in plants. However, in plant-virus interactions and interactions of bacteria with animal hosts, UBC-E2s are established targets of pathogens. The ßC1 protein of the Cotton leaf curl Multan virus, for example, was found to interact *in vivo* and *in vitro* with a tomato UBC-E2, thereby potentially causing down-regulation of the host proteasome pathway (Eini et al., 2009). Better characterized is the effector activity of the *Shigella flexneri* effector OspG (Other Secreted Protein G). OspG binds to UBC-E2s, thus preventing proteasomal degradation of IκB proteins, which inhibit and retain NF-κB in the cytoplasm. Since in this situation NF-κB cannot be translocated to the nucleus to activate defense genes of the inflammatory pathway, OspG activity down-regulates the host innate immune response (Kim et al., 2005a).

Beyond directing proteins for degradation, ubiquitination can affect protein localization, activity, structure and interaction partners (Woelk et al., 2007). The diversity in ubiquitin-signaling is generated by the formation of different types of ubiquitin chains attached to one of the seven lysine residues within the 76 amino acids ubiquitin protein (Hochstrasser, 2009). Only polyubiquitin chains linked through K48 target proteins to the proteasome. Nevertheless, K48 fulfills additional functions, because K48-linked protein polyubiquitination, which is independent from the proteasome pathway, has been implicated in host defense of barley (Dong et al., 2006). Polyubiquitin chains linked through K63, similar to monoubiquitination, generate a non-proteolytic signal involved in DNA repair, transcriptional regulation, activation of protein kinases and endocytosis in animals (Galan and Haguenauer-Tsapis, 1997; Bach and Ostendorff, 2003; Huang and Schulman, 2006). Monoubiquitination involves the attachment of only one ubiquitin moiety to a single lysine residue. Recently, Hoeller *et al.* reported, that UBC-E2s can

monoubiquitinate target proteins in the absence of E3 ligases (Hoeller et al., 2007). In beans, monoubiquitination of actin was found to be induced in the interaction with symbiotic as well as pathogenic bacteria and oomycetes. It is thought to provide increased stability of the actin filaments to proteolytic degradation (Dantan-Gonzalez et al., 2001). In view of the massive cytoskeletal rearrangements in *Bgh*-infected cells (reviewed in Schmidt and Panstruga, 2007), actin targeting might be one function of EC4. However, considering that two forms of ubiquitination are connected to vesicle trafficking just like ARF-GAPs, we favor a model in which EC4 targets the vesicle trafficking pathway of the invaded host cell.

4.1.10 EC6 might induce volatile production

EC6 interacts with *Hv*TPMT (thiopurine-methyl-transferase) both in yeast and in the BiFC assay *in planta* (**Figure 9**). The *TPMT* gene is well characterized in humans. Its gene product inactivates the thiopurine-azathioprines 6-thioguanine (6-TG) and 6-mercaptopurine (6-MP), which are used as anti-inflammatory and immunosuppressive drugs, thereby reducing the effective thiopurine dose given to patients (Karran and Attard, 2008). Patients who inherited a low-activity variant allele of the *TPMT* gene suffer intense myelosuppression (decreased production of blood cells) if the administered thiopurine dose is not reduced. Although TPMT is conserved among species from bacteria to mammals, its wildtype function in mammals in unknown. A bacterial TPMT homolog converts selenium- and tellurium-containing compounds to less toxic, volatile methylated derivatives (Ranjard et al., 2004). Analogously, an Arabidopsis thiol methyltransferase (TMT) has been described that methylates hydrolysis products of glucosinolates to volatile sulfur compounds (Attieh et al., 2002). The authors speculated that these volatile compounds might have a role in defense against pathogens. Considering that *Hv*TPMT expression in barley enhances the *Bgh* haustorium index to a similar level as EC4 expression (**Figure 11**) - indicating that EC4 activates *Hv*TPMT – we do not think it is likely that *Hv*TPMT synthesizes a defense compound. Nevertheless, it might be involved in creating a volatile compound favoring fungal proliferation.

4.2 Putative RNase-like effectors encoded by a multigene family might have an important function for *Bgh*

4.2.1 *Bgh* RNase-like effectors are different from known secreted fungal RNases

The putative AC RNase-like effectors encoded by a gene family identified in the draft genome sequence of *Bgh* DH14 differs drastically from the EC proteins. While the latter apparently are encoded by single-copy genes, the *AC* genes constitute a large gene family with at least 80 members. Based on protein domains the AC RNase-like proteins resemble microbial ribonucleases. The superfamily of microbial ribonucleases includes fungal T1 RNases and ribotoxins. T1 RNases are guanine-specific ribonucleases that cleave single-stranded RNA after guanine residues, i.e., on their 3' end (Yoshida, 2001). Like ribotoxins, AC RNase-like proteins are larger than T1 RNases and both classes are basic proteins, whereas T1 RNases are acidic proteins (Alvarez-Garcia et al., 2006). However, AC proteins exceed ribotoxins in size and the catalytic residues conserved in T1 RNases and ribotoxins are not present in AC protein sequences (**Figure 12**). Furthermore, many of the RNase-like proteins encoded by the multigene family in the DH14 genome differ notably from RNase-like proteins of other powdery mildew species. At the same time, those RNase-like DH14 proteins are very similar to the RNase-like proteins isolated from *Bgh* K1 and A6 (**Figure 14**), suggesting that recent gene duplications gave rise to new members of the *Bgh* multigene family, which might fulfill *Bgh*-specific functions.

4.2.2 *Bgh* RNase-like effectors might have avirulence activity

Regardless of their intrinsic biochemical function, we tested whether AC RNase-like proteins isolated from *Bgh* K1 and A6 would be recognized by barley resistance proteins. So far, we did not identify AC RNase-like effectors with avirulence activity in barley cultivars encoding either the MLA1 or the MLA6 protein using transient co-expression with *gfp*. There are three possible explanations why we did not observe avirulence activity of the tested AC proteins: First, the GFP assay might not have been sensitive enough. Second, the presence of the N-terminal AC signal peptide might have interfered with recognition by barley resistance proteins. Third, the tested AC proteins are not recognized by MLA1 or MLA6 resistance proteins.

Co-expression with *gfp* has also been employed to demonstrate the avirulence function of *P. infestans Avr3a* (Armstrong et al., 2005). Instead of a qualitative analysis of the transformed leaves, the authors of the Avr3a-study performed quantitative analysis.

Variation in the number of *gfp*-expressing cells was substantial (Armstrong et al., 2005). Despite the technical variation in the co-expression assay with *gfp*, co-expression of *Avr3a* and the cognate *R* gene *R3a* in *N. benthamiana* induced a strong, macroscopically visible HR, indicating that the *gfp* co-expression assay is less sensitive (Armstrong et al., 2005). Huge variation in the number of transformed cells was also observed in a biolistic co-expression assay of *H. arabidopsidis ATR13* alleles and *gus*, although the absence of *gus*-expressing cells in resistant cultivars was obvious in this study (Allen et al., 2004). Collectively, these studies indicate that quantitative analysis of transformed cells is more appropriate, due to the high variation in transformed cell number.

In contrast to our AC expression assay, Armstrong *et al.* transiently expressed Avr3a candidates as truncated versions lacking the N-terminal signal peptide, and they never observed reduction in GFP fluorescence from any plants co-bombarded with full-length Avr3a constructs (Armstrong et al., 2005). Likewise, the signal peptides of *P. sojae* effector Avr3c, *H. arabidopsidis* ATR13 and *M. lini* AvrM abolished avirulence activity (Allen et al., 2004; Catanzariti et al., 2006; Dong et al., 2009). Collectively these data suggest that presence of a signal peptide might interfere with recognition by intracellular resistance proteins. Taking into account that barley MLA protein are predicted to be cytoplasmic, AC proteins lacking the signal peptide might be recognized by MLA1 or MLA6 in the *gfp*-co-expression assay.

Furthermore, AC proteins might be recognized by MLA proteins other than MLA1 and MLA6. Recently, successful expression of auto-active MLA variants in *N. benthamiana* has been reported (Qian-Hua Shen, personal communication). In the future, we will employ co-expression of AC proteins with MLA proteins in *N. benthamiana*, which allows macroscopic evaluation of cell death phenotypes, which has also been employed by Armstrong *et al.* (see above).

4.2.3 The polymorphic nature of the AC RNase-like proteins indicates that they are important for *Bgh*

We detected numerous polymorphic sites throughout the AC protein sequences. Interestingly, the central part of the predicted RNase domain, containing the putative catalytic site E74, is devoid of polymorphic sites, which might be due to selective constraints for maintaining the effector protein sequence (Stergiopoulos et al., 2007). Selective constraints have also been suggested for the *C. fulvum* effectors Ecp1 and Ecp2,

because disruption or modification of the protein sequences reduced virulence of the mutant *C. fulvum* strains (Wubben et al., 1994; Lauge et al., 1997).

Another putative catalytic site, H128, is surrounded by polymorphic sites, which constitute three possible sequence variants among the AC transcripts isolated from *Bgh* K1 and A6 (**Figure 15**). Assuming that H128 is a catalytic site, the close proximity of these polymorphic sites might indicate that these amino acids are involved in protein-substrate interaction. Similarly, amino acids that are under positive selection and are located close to the catalytic triad of *P. syringae* HopZ1 have been implicated in protein-substrate interaction (Ma et al., 2006). In some effectors the avirulence and the virulence function can be uncoupled. For examples, the avirulence and cell death suppression function of *P. infestans* Avr3a as well as *P. syringae* AvrPtoB can be uncoupled at the structural level (Abramovitch et al., 2003; Bos et al., 2006). AvrPtoB is recognized by the tomato protein Pto in the N-terminal module, while PCD suppression is mediated by the C-terminal module (Abramovitch et al., 2003). If this were the case for the AC RNase-like proteins, the C-terminus might be important for avoiding recognition by barley resistance proteins.

Alternatively, AC RNase-like proteins could be recognized by more than one resistance protein, as has been demonstrated for *H. arabidopsidis* ATR13. Like the AC RNase-like proteins, ATR13 has high levels of amino acid diversity across the entire protein as revealed by sequencing *ATR13* alleles from 16 *H. arabidopsidis* isolates (Allen et al., 2008). Phylogenetic analysis of the 47 alleles of the cognate *A. thaliana RPP13* gene combined with functional studies revealed that recognition of ATR13 is mediated by alleles in a single *RPP13* clade and that at least one gene unlinked to *RPP13* recognizes a different subgroup of *ATR13* alleles (Hall et al., 2009). Whether AC proteins are modular effectors like AvrPtoB or whether they are recognized by one or more resistance proteins will be determined by the current functional analysis.

4.2.4 AC RNase-like proteins might have multiple functions

We are currently testing whether AC proteins have RNase activity or merely display similar protein domains, but have a different biological activity. Some RNases have a biological activity besides the degradation of RNA. For example, plant T2-RNases encoded by the *S*-locus are responsible for pollen rejection in self-incompatible plants, by interacting with *S*-allele products to prevent self-fertilization (Sijacic et al., 2004). Another example is the extracellular T2 RNase ACTIBIND from *Aspergillus niger*, which was

demonstrated to bind to actin, thus altering orientation and inhibiting elongation of plant pollen tubes (Roiz et al., 2000). Intriguingly, the actin-binding activity of ACTIBIND does not require RNase activity (Roiz et al., 2006). If AC proteins are translocated inside plant cells, they could interfere with host translation like ribotoxins, which are also known as ribosome inactivating proteins (Kao and Davies, 1995). By cleaving a single phospodiester bond located in the highly conserved sarcin/ricin loop (SRL) in the larger rRNA molecule, ribotoxins inhibit protein biosynthesis (Endo et al., 1998). However, cell death induced by ribotoxins is independent of their ability to inhibit protein synthesis, indicating that they fulfill an additional function (Alford et al., 2009). If *Bgh* RNase-like proteins they are not translocated into barley cells, but remain in the apoplast, a possible function for extracellular AC RNases could be the uptake of phosphate by digesting extracellular polyribonucleotides. Acquisition of phosphate appears to play an important role during plant infection by fungi and bacteria. Secreted phosphatases and phytases of bacteria and the hemibiotrophic fungus *Colletotrichum graminicola* were found to be strongly induced during plant infection (Oh et al., 2004; Tang et al., 2006). Furthermore, a *Xanthomonas oryzae* phytase was identified as a virulence factor and a *Colletotrichum higgisianum* phosphate transporter was identified as a pathogenicity gene (Chatterjee et al., 2003; Huser et al., 2009). Consistent with this AC function, tomato RNaseLe was found to be secreted from phosphate-starved tomato cells, presumably to increase the availability of phosphate in the surrounding environment (Nurnberger et al., 1990). However, a simple function like uptake of phosphate is unlikely for a protein family with so many polymorphic sites, indicative of selection pressure imposed on the respective genes.

So far, we identified only two *AC* transcripts from *Bgh* K1 corresponding to DH14 contigs (contig 1148 and contig 16091, **Figure 15**), which might indicate difference in the *AC* genes inventory present and/or expressed among different *Bgh* isolates. Although we cannot distinguish between highly divergent alleles, paralogs and orthologs among the *AC* genes, a similar pattern of species-specific or only partially overlapping gene inventories was observed for the rodent eosinophil-associated RNase (EAR) family. Phylogenetic analysis of functional genes and pseudogenes unraveled an unusual pattern of rapid birth-and-death evolution followed by gene sorting (Zhang et al., 2000). Gene sorting describes a process characterized by rapid gene duplication and deactivation occurring differentially among lineages. Next to their RNase activity, EAR proteins exert bactericidal activity by destabilizing lipid membranes (Young et al., 1986; Rosenberg, 2008). Therefore, these proteins have been suggested as being specifically tailored to fight against distinct rodent

pathogens (Zhang et al., 2000). Given the high degree of co-evolution of grass powdery mildew fungi with their respective hosts, it is tempting to speculate that the *AC* gene family expansion resulted in “tailored” proteins to specifically infect the grass host, which would be consistent with the absence of huge RNase-like protein families in other powdery mildew species.

5 General Conclusion and Perspectives

The study of effector proteins from biotrophic plant pathogens has long been hampered by the fact, that these pathogens require the living host cells for growth and proliferation and are therefore not amenable to genetic manipulations. Recently, several flax rust effectors and two *Bgh* effectors were identified based on their avirulence function (Dodds et al., 2004; Catanzariti et al., 2006; Dodds et al., 2006; Ridout et al., 2006). However the biochemical function of these effectors and the host pathways they target remain elusive. In this study, we have identified a set of putative *Bgh* effector proteins that positively contribute to haustorium formation. Of these putative *Bgh* effectors, EC2 might be involved in appressorium formation and EC5 is likely secreted from haustoria. Interaction of EC4 with *Hv*ARF-GAP and *Hv*UBC-E2 points to EC4 targeting of the host vesicle trafficking pathway. Furthermore, EC6 interacts with *Hv*TPMT, which might be involved in the synthesis of a yet unknown volatile compatibility compound. Future studies will aim at the elucidation of the pathways targeted by the EC effectors. Of special interest is the ubiquitin machinery targeted by EC4. Identification of the E3 ligase interacting with *Hv*UBC-E2 and transducing the specific ubiquitin signal might allow us to test our hypothesis that EC4 targets the host vesicle trafficking pathway.

We also identified identified the AC multigene family of *Bgh* encoding putative secreted RNase-like proteins. Structurally, these proteins resemble microbial ribonucleases, which also comprise the family of ribotoxins – potent ribosome inhibitors. Currently, we do not know whether AC RNase-like proteins have RNase activity or exert another biochemical function. The striking number of polymorphic sites within the AC protein sequence points to strong selection pressure imposed on the respective genes and thus likely an important function of these proteins for *Bgh*. Next to improved assays for avirulence activity of the *Bgh* AC proteins, we are currently essaying AC proteins for their RNase activity *in vitro*. Once we established a biochemical activity for the AC RNase-like proteins mutational analysis will help to unravel their authentic function. Several potential sites for mutagenesis have already been identified within the AC protein sequences including the N-terminal part of the RNase-domain that is devoid of polymorphic sites.

6 References

Abramovitch, R.B., Kim, Y.J., Chen, S.R., Dickman, M.B., and Martin, G.B. (2003). Pseudomonas type III effector AvrPtoB induces plant disease susceptibility by inhibition of host programmed cell death. Embo Journal **22,** 60-69.

Akira, S., Uematsu, S., and Takeuchi, O. (2006). Pathogen recognition and innate immunity. Cell **124,** 783.

Aleman, A., Rodriguez-Escudero, I., Mallo, G.V., Cid, V.J., Molina, M., and Rotger, R. (2005). The amino-terminal non-catalytic region of Salmonella typhimurium SigD affects actin organization in yeast and mammalian cells. Cellular Microbiology **7,** 1432-1446.

Alford, S.C., Pearson, J.D., Carette, A., Ingham, R.J., and Howard, P.L. (2009). alpha-Sarcin catalytic activity is not required for cytotoxicity. Bmc Biochemistry **10**.

Allen, R.L., Bittner-Eddy, P.D., Grenville-Briggs, L.J., Meitz, J.C., and Rehmany, A.P. (2004). Host-parasite coevolutionary conflict between Arabidopsis and downy mildew. Science **306,** 1957.

Allen, R.L., Meitz, J.C., Baumber, R.E., Hall, S.A., Lee, S.C., Rose, L.E., and Beynon, J.L. (2008). Natural variation reveals key amino acids in a downy mildew effector that alters recognition specificity by an Arabidopsis resistance gene. Mol. Plant Pathol. **9,** 511-523.

Altschul, S., Gish, W., Miller, W., Myers, E., and Lipman, D. (1990). Basic local alignment search tool. Journal of Molecular Biology **215,** 403 - 410.

Altschul, S.F., Madden, T.L., Schaffer, A.A., Zhang, J.H., Zhang, Z., Miller, W., and Lipman, D.J. (1997). Gapped BLAST and PSI-BLAST: a new generation of protein database search programs. Nucleic Acids Research **25,** 3389-3402.

Alvarez-Garcia, E., Garcia-Ortega, L., Verdun, Y., Bruix, M., del Pozo, A.M., and Gavilanes, J.G. (2006). Tyr-48, a conserved residue in ribotoxins, is involved in the RNA-degrading activity of alpha-sarcin. Biol. Chem. **387,** 535-541.

Andreeva, A., Howorth, D., Chandonia, J.-M., Brenner, S.E., Hubbard, T.J.P., Chothia, C., and Murzin, A.G. (2008). Data growth and its impact on the SCOP database: new developments. Nucl. Acids Res. **36,** D419-425.

Angot, A., lie, Vergunst, A., Genin, S., phane, and Peeters, N. (2007). Exploitation of Eukaryotic Ubiquitin Signaling Pathways by Effectors Translocated by Bacterial Type III and Type IV Secretion Systems. PLoS Pathogens **3,** e3.

Angot, A., Peeters, N., Lechner, E., Vailleau, F., Baud, C., Gentzbittel, L., Sartorel, E., Genschik, P., Boucher, C., and Genin, S. (2006). Ralstonia solanacearum requires F-box-like domain-containing type III effectors to promote disease on several host plants. Proceedings of the National Academy of Sciences **103,** 14620-14625.

Armstrong, M.R., Whisson, S.C., Pritchard, L., Bos, J.I.B., Venter, E., Avrova, A.O., Rehmany, A.P., Bohme, U., Brooks, K., Cherevach, I., Hamlin, N., White, B., Frasers, A., Lord, A., Quail, M.A., Churcher, C., Hall, N., Berriman, M., Huang, S., Kamoun, S., Beynon, J.L., and Birch, P.R.J. (2005). An ancestral oomycete locus contains late blight avirulence gene Avr3a, encoding a protein that is recognized in the host cytoplasm. Proc. Natl. Acad. Sci. U. S. A. **102,** 7766-7771.

Attieh, J., Djiana, R., Koonjul, P., Etienne, C., Sparace, S.A., and Saini, H.S. (2002). Cloning and functional expression of two plant thiol methyltransferases: a new class of enzymes involved in the biosynthesis of sulfur volatiles. Plant Mol.Biol. **50,** 511-521.

Ausubel, F.M. (2005). Are innate immune signaling pathways in plants and animals conserved? Nat. Immunol. **6,** 973.

Axtell, M.J., and Staskawicz, B.J. (2003). Initiation of RPS2-specified disease resistance in Arabidopsis is coupled to the AvrRpt2-directed elimination of RIN4. Cell **112,** 369-377.

Axtell, M.J., McNellis, T.W., Mudgett, M.B., Hsu, C.S., and Staskawicz, B.J. (2001). Mutational analysis of the Arabidopsis RPS2 disease resistance gene and the corresponding Pseudomonas syringae avrRpt2 avirulence gene. Mol. Plant-Microbe Interact. **14,** 181-188.

Bach, I., and Ostendorff, H.P. (2003). Orchestrating nuclear functions: ubiquitin sets the rhythm. Trends in Biochemical Sciences **28,** 189-195.

Basse, C.W., Kolb, S., and Kahmann, R. (2002). A maize-specifically expressed gene cluster in Ustilago maydis. Mol. Microbiol. **43,** 75-93.

Belkhadir, Y., Nimchuk, Z., Hubert, D.A., Mackey, D., and Dangl, J.L. (2004). Arabidopsis RIN4 negatively regulates disease resistance mediated by RPS2 and RPM1 downstream or independent of the NDR1 signal modulator and is not required for the virulence functions of bacterial type III effectors AvrRpt2 or AvrRpm1. Plant Cell **16,** 2822-2835.

Bendtsen, J.D., Nielsen, H., von Heijne, G., and Brunak, S. (2004). Improved prediction of signal peptides: SignalP 3.0. Journal of Molecular Biology **340,** 783-795.

Berbee, M.L. (2001). The phylogeny of plant and animal pathogens in the Ascomycota. Physiol. Mol. Plant Pathol. **59,** 165-187.

Bhat, R., Lahaye, T., and Panstruga, R. (2006). The visible touch: in planta visualization of protein-protein interactions by fluorophore-based methods. Plant Methods **2,** 12.

Bhattacharjee, S., Hiller, N.L., Liolios, K., Win, J., Kanneganti, T.D., Young, C., Kamoun, S., and Haldar, K. (2006). The malarial host-targeting signal is conserved in the Irish potato famine pathogen. Plos Pathogens **2,** 453-465.

Birch, P.R., Boevink, P.C., Gilroy, E.M., Hein, I., Pritchard, L., and Whisson, S.C. (2008). Oomycete RXLR effectors: delivery, functional redundancy and durable disease resistance. Curr. Opin. Plant Biol. **11,** 373.

Birch, P.R.J., Armstrong, M., Bos, J., Boevink, P., Gilroy, E.M., Taylor, R.M., Wawra, S., Pritchard, L., Conti, L., Ewan, R., Whisson, S.C., van West, P., Sadanandom, A., and Kamoun, S. (2009). Towards understanding the virulence functions of RXLR effectors of the oomycete plant pathogen Phytophthora infestans. Journal of Experimental Botany **60,** 1133-1140.

Bittner-Eddy, P., Can, C., Gunn, N., Pinel, M., Tor, M., Crute, I., Holub, E.B., and Beynon, J. (1999). Genetic and physical mapping of the RPP13 locus, in arabidopsis, responsible for specific recognition of several Peronospora parasitica (downy mildew) isolates. Mol. Plant-Microbe Interact. **12,** 792-802.

Block, A., Li, G., Fu, Z.Q., and Alfano, J.R. (2008). Phytopathogen type III effector weaponry and their plant targets. Curr. Opin. Plant Biol. **11,** 396-403.

Bohnert, H.U., Fudal, I., Dioh, W., Tharreau, D., Notteghem, J.L., and Lebrun, M.H. (2004). A putative polyketide synthase peptide synthetase from Magnaporthe grisea signals pathogen attack to resistant rice. Plant Cell **16,** 2499-2513.

Boller, T., and He, S.Y. (2009). Innate Immunity in Plants: An Arms Race Between Pattern Recognition Receptors in Plants and Effectors in Microbial Pathogens. Science **324,** 742-744.

Boller, T., and Felix, G. (2009). A Renaissance of Elicitors: Perception of Microbe-Associated Molecular Patterns and Danger Signals by Pattern-Recognition Receptors. Annual Review of Plant Biology **60,** 379-406.

Bolton, M.D., van Esse, H.P., Vossen, J.H., De Jonge, R., and Stergiopoulos, I. (2008). The novel Cladosporium fulvum lysin motif effector Ecp6 is a virulence factor with orthologues in other fungal species. Mol. Microbiol. **69,** 119.

Bos, J.I., Kanneganti, T.-D., Young, C., Cakir, C., Huitema, E., Win, J., Armstrong, M.R., Birch, P.J., and Kamoun, S. (2006). The C-terminal half of Phytophthora infestansRXLR effector AVR3a is sufficient to trigger R3a-mediated hypersensitivity and suppress INF1-induced cell death in Nicotiana benthamiana. Plant J. **48,** 165-176.

Bracha-Drori, K., Shichrur, K., Katz, A., Oliva, M., Angelovici, R., Yalovsky, S., and Ohad, N. (2004). Detection of protein-protein interactions in plants using bimolecular fluorescence complementation. Plant J **40,** 419 - 427.

Bretz, J.R., Mock, N.M., Charity, J.C., Zeyad, S., Baker, C.J., and Hutcheson, S.W. (2003). A translocated protein tyrosine phosphatase of Pseudomonas syringae pv. tomato DC3000 modulates plant defence response to infection. Mol. Microbiol. **49,** 389-400.

Brown, G.D., Dave, J.A., Gey van Pittius, N., Stevens, L., Ehlers, M.R.W., and Beyers, A.D. (2000). The mycosins of Mycobacterium tuberculosis H37Rv: a family of subtilisin-like serine proteases. Gene **254,** 147-155.

Brown, J.K.M., and Jessop, A.C. (1995). Genetics of avirulences in Erysiphe graminis f. sp. hordei. Plant Pathol. **44,** 1039.

Carresi, L., Pantera, B., Zoppi, C., Cappugi, G., Oliveira, A.L., Pertinhez, T.A., Spisni, A., Scala, A., and Pazzagli, L. (2006). Cerato-platanin, a phytotoxic protein from Ceratocystis fimbriata: Expression in Pichia pastoris, purification and characterization. Protein Expression and Purification **49,** 159-167.

Casadevall, A., and Pirofski, L.A. (2003). The damage-response framework of microbial pathogenesis. Nature Reviews Microbiology **1,** 17-24.

Catanzariti, A.M., Dodds, P.N., Lawrence, G.J., Ayliffe, M.A., and Ellis, J.G. (2006). Haustorially expressed secreted proteins from flax rust are highly enriched for avirulence elicitors. Plant Cell **18,** 243.

Chang, J.H., Goel, A.K., Grant, S.R., and Dangl, J.L. (2004). Wake of the flood: ascribing functions to the wave of type III effector proteins of phytopathogenic bacteria. Current Opinion in Microbiology **7,** 11-18.

Chatterjee, S., Sankaranarayanan, R., and Sonti, R.V. (2003). PhyA, a secreted protein of Xanthomonas oryzae pv. oryzae, is required for optimum virulence and growth on phytic acid as a sole phosphate source. Mol. Plant-Microbe Interact. **16,** 973-982.

Chisholm, S.T., Dahlbeck, D., Krishnamurthy, N., Day, B., Sjolander, K., and Staskawicz, B.J. (2005). Molecular characterization of proteolytic cleavage sites of the Pseudomonas syringae effector AvrRpt2. Proc. Natl. Acad. Sci. U. S. A. **102,** 2087-2092.

Choi, W.B., and Dean, R.A. (1997). The adenylate cyclase gene MAC1 of Magnaporthe grisea controls Appressorium formation and other aspects of growth and development. Plant Cell **9,** 1973-1983.

Clough, J.S., and Bent, A. (1998). Floral dip: a simplified method for Agrobacterium-mediated transformation of Arabidopsis thaliana. Plant J. **16,** 735-743.

Coaker, G., Falick, A., and Staskawicz, B. (2005). Activation of a phytopathogenic bacterial effector protein by a eukaryotic cyclophilin. Science **308,** 548-550.

Coemans, B., Takahashi, Y., Berberich, T., Ito, A., Kanzaki, H., Matsumura, H., Saitoh, H., Tsuda, S., Kamoun, S., Sagi, L., Swennen, R., and Terauchi, R. (2008). High-throughput in planta expression screening identifies an ADP-

ribosylation factor (ARF1) involved in non-host resistance and R gene-mediated resistance. Mol. Plant Pathol. **9,** 25-36.

Collemare, J., Pianfetti, M., Houlle, A.E., Morin, D., and Camborde, L. (2008). Magnaporthe grisea avirulence gene ACE1 belongs to an infection-specific gene cluster involved in secondary metabolism. New Phytol. **179,** 196.

Collmer, A., Alfano, J.R., Buell, C.R., Cartinhour, S., Chatterjee, A.K., Martin, G.B., Schneider, D.J., and Tang, X. (2004). Pseudomonas syringae pathogenicity explored from the perspective of type III secretion systems and comparative genomics. Phytopathology **94,** S121-S121.

Damasceno, C.M.B., Bishop, J.G., Ripoll, D.R., Win, J., Kamoun, S., and Rose, J.K.C. (2008). Structure of the Glucanase Inhibitor Protein (GIP) Family from Phytophthora Species Suggests Coevolution with Plant Endo-Î²-1,3-Glucanases. Mol. Plant-Microbe Interact. **21,** 820-830.

Dangl, J., and Jones, J. (2001). Plant pathogens and integrated defence responses to infection. Nature **411,** 826.

Dantan-Gonzalez, E., Rosenstein, Y., Quinto, C., and Sanchez, F. (2001). Actin monoubiquitylation is induced in plants in response to pathogens and symbionts. Mol. Plant-Microbe Interact. **14,** 1267-1273.

Day, B., Dahlbeck, D., and Staskawicz, B.J. (2006). NDR1 interaction with RIN4 mediates the differential activation of multiple disease resistance pathways in Arabidopsis. Plant Cell **18,** 2782.

De Wit, P., Lauge, R., Honee, G., Joosten, M., and Vossen, P. (1997). Molecular and biochemical basis of the interaction between tomato and its fungal pathogen Cladosporium fulvum. Antonie van Leeuwenhoek **71,** 137.

DebRoy, S., Thilmony, R., Kwack, Y.-B., Nomura, K., and He, S.Y. (2004). A family of conserved bacterial effectors inhibits salicylic acid-mediated basal immunity and promotes disease necrosis in plants. Proc. Natl. Acad. Sci. U. S. A. **101,** 9927-9932.

Deslandes, L., Olivier, J., Peeters, N., Feng, D.X., Khounlotham, M., Boucher, C., Somssich, L., Genin, S., and Marco, Y. (2003). Physical interaction between RRS1-R, a protein conferring resistance to bacterial wilt, and PopP2, a type III effector targeted to the plant nucleus. Proc. Natl. Acad. Sci. U. S. A. **100,** 8024-8029.

DeYoung, B.J., and Innes, R.W. (2006). Plant NBS-LRR proteins in pathogen sensing and host defense. Nature Immunology **7,** 1243-1249.

DeZwaan, T.M., Carroll, A.M., Valent, B., and Sweigard, J.A. (1999). Magnaporthe grisea Pth11p is a novel plasma membrane protein that mediates appressorium differentiation in response to inductive substrate cues. Plant Cell **11,** 2013.

Ditta, G., Stanfield, S., Corbin, D., and Helinski, D.R. (1980). Broad Host Range DNA Cloning System for Gram-Negative Bacteria - Construction of a Gene Bank of Rhizobium-Meliloti. Proc. Natl. Acad. Sci. USA **77,** 7347-7351.

Dodds, P.N., Lawrence, G.J., Catanzariti, A.M., Ayliffe, M.A., and Ellis, J.G. (2004). The Melampsora lini AvrL567 avirulence genes are expressed in haustoria and their products are recognized inside plant cells. Plant Cell **16,** 755-768.

Dodds, P.N., Lawrence, G.J., Catanzariti, A.M., Teh, T., and Wang, C.I.A. (2006). Direct protein interaction underlies gene-for-gene specificity and coevolution of the flax resistance genes and flax rust avirulence genes. Proc. Natl. Acad. Sci. USA **103,** 8888.

Doehlemann, G., van der Linde, K., AÃŸmann, D., Schwammbach, D., Hof, A., Mohanty, A., Jackson, D., and Kahmann, R. (2009). Pep1, a Secreted Effector Protein of Ustilago maydis, Is Required for Successful Invasion of Plant Cells. PLoS Pathog **5,** e1000290.

Dong, S., Qutob, D., Tedman-Jones, J., Kuflu, K., Wang, Y., Tyler, B.M., and Gijzen, M. (2009). *The Phytophthora sojaeAvirulence Locus Avr3c* Encodes a Multi-Copy RXLR Effector with Sequence Polymorphisms among Pathogen Strains. PLoS ONE **4,** e5556.

Dong, W., Nowara, D., and Schweizer, P. (2006). Protein Polyubiquitination Plays a Role in Basal Host Resistance of Barley. Plant Cell **18,** 3321-3331.

Dou, D., Kale, S.D., Wang, X., Jiang, R.H.Y., Bruce, N.A., Arredondo, F.D., Zhang, X., and Tyler, B.M. (2008a). RXLR-Mediated Entry of Phytophthora sojae Effector Avr1b into Soybean Cells Does Not Require Pathogen-Encoded Machinery. Plant Cell **20,** 1930-1947.

Dou, D., Kale, S.D., Wang, X., Chen, Y., Wang, Q., Wang, X., Jiang, R.H.Y., Arredondo, F.D., Anderson, R.G., Thakur, P.B., McDowell, J.M., Wang, Y., and Tyler, B.M. (2008b). Conserved C-Terminal Motifs Required for Avirulence and Suppression of Cell Death by Phytophthora sojae effector Avr1b. Plant Cell **20,** 1118-1133.

Dyrløv Bendtsen, J., Nielsen, H., von Heijne, G., and Brunak, S. (2004). Improved Prediction of Signal Peptides: SignalP 3.0. Journal of Molecular Biology **340,** 783-795.

Egan, M.J., and Talbot, N.J. (2008). Genomes, free radicals and plant cell invasion: recent developments in plant pathogenic fungi. Curr. Opin. Plant Biol. **11,** 367-372.

Eichmann, R., and Huckelhoven, R. (2008). Accommodation of powdery mildew fungi in intact plant cells. Journal of Plant Physiology **165,** 5-18.

Eini, O., Dogra, S., Selth, L.A., Dry, I.B., Randles, J.W., and Rezaian, M.A. (2009). Interaction with a Host Ubiquitin-Conjugating Enzyme Is Required for the Pathogenicity of a Geminiviral DNA Î² Satellite. Mol. Plant-Microbe Interact. **22,** 737-746.

Elliott, C., Zhou, F.S., Spielmeyer, W., Panstruga, R., and Schulze-Lefert, P. (2002). Functional conservation of wheat and rice Mlo orthologs in defense modulation to the powdery mildew fungus. Mol. Plant-Microbe Interact. **15,** 1069-1077.

Ellis, J., Dodds, P., and Pryor, T. (2000). Structure, function and evolution of plant disease resistance genes. Curr. Opin. Plant Biol. **3,** 278-284.

Ellis, J.G., Dodds, P.N., and Lawrence, G.J. (2007). Flax Rust Resistance Gene Specificity is Based on Direct Resistance-Avirulence Protein Interactions. Annu. Rev. Phytopathol. **45**.

Endo, Y., Morishita, R., Imashevich, K.M., and Yoshinari, S. (1998). Mechanisms of action of ribotoxins. Journal of Toxicology-Toxin Reviews **17,** 427-439.

Espinosa, A., and Alfano, J.R. (2004). Disabling surveillance: bacterial type III secretion system effectors that suppress innate immunity. Cell Microbiol. **6,** 1027.

Fabro, G., Di Rienzo, J.A., Voigt, C.A., Savchenko, T., Dehesh, K., Somerville, S., and Alvarez, M.E. (2008). Genome-Wide Expression Profiling Arabidopsis at the Stage of Golovinomyces cichoracearum Haustorium Formation. Plant Physiol. **146,** 1421-1439.

Farfsing, J.W., Auffarth, K., and Basse, C.W. (2005). Identification of cis-active elements in Ustilago maydis mig2 promoters conferring high-level activity during pathogenic growth in maize. Mol. Plant-Microbe Interact **18,** 75.

Favre-Bonté, S., Ranjard, L., Champier, L., Cournoyer, B., and Nazaret, S. (2006). Distribution and genetic diversity of bacterial thiopurine methyltransferases in soils emitting dimethyl selenide. Biochimie **88,** 1573-1581.

Flor, H.H. (1955). Host-parasite interactions in flax rust"Its genetics and other implications. Phytopathology **45,** 680.

Freymark, G., Diehl, T., Miklis, M., Romeis, T., and Panstruga, R. (2007). Antagonistic Control of Powdery Mildew Host Cell Entry by Barley Calcium-Dependent Protein Kinases (CDPKs). Mol. Plant-Microbe Interact. **20,** 1213-1221.

Fu, Z.Q., Guo, M., Jeong, B.R., Tian, F., Elthon, T.E., Cerny, R.L., Staiger, D., and Alfano, J.R. (2007). A type III effector ADP-ribosylates RNA-binding proteins and quells plant immunity. Nature **447,** 284-U281.

Galan, J.E., and Wolf-Watz, H. (2006). Protein delivery into eukaryotic cells by type III secretion machines. Nature **444,** 567-573.

Galán, J.E. (2009). Common Themes in the Design and Function of Bacterial Effectors **5,** 571-579.

Galan, J.M., and HaguenauerTsapis, R. (1997). Ubiquitin Lys63 is involved in ubiquitination of a yeast plasma membrane protein. Embo Journal **16,** 5847-5854.

Gietz, R.D., and Woods, R.A. (2002). Transformation of yeast by lithium acetate/single-stranded carrier DNA/polyethylene glycol method. In Guide to Yeast Genetics and Molecular and Cell Biology, Pt B, pp. 87-96.

Gjetting, T., Hagedorn, P.H., Schweizer, P., Thordal-Christensen, H., Carver, T.L.W., and Lyngkjaer, M.F. (2007). Single-cell transcript profiling of barley attacked by the powdery mildew fungus. Mol. Plant-Microbe Interact. **20,** 235-246.

Glawe, D.A. (2008). The Powdery Mildews: A Review of the World's Most Familiar (Yet Poorly Known) Plant Pathogens. Annu. Rev. Phytopathol. **46,** 27-51.

Gohre, V., and Robatzek, S. (2008). Breaking the Barriers: Microbial Effector Molecules Subvert Plant Immunity. Annu. Rev. Phytopathol. **46,** 189-215.

Grant, S.R., Fisher, E.J., Chag, J.H., Mole, B.M., and Dangl, J.L. (2006). Subterfuge and manipulation: type III effector proteins of phytopathogenic bacteria. Annu. Rev. Microbiol. **60,** 425.

Grell, M.N., Holm, K.B., and Giese, H. (2005). Two novel Blumeria graminis f. sp hordei genes are induced in planta and up-regulated in mlo virulent isolates. Physiol. Mol. Plant Pathol. **66,** 79-89.

Groll, M., Schellenberg, B., Bachmann, A.S., Archer, C.R., and Huber, R. (2008). A plant pathogen virulence factor inhibits the eukaryotic proteasome by a novel mechanism. Nature **452,** 755.

Hahn, M., and Mendgen, K. (2001). Signal and nutrient exchange at biotrophic plant-fungus interfaces. Curr. Opin. Plant Biol. **4,** 322-327.

Hall, S.A., Allen, R.L., Baumber, R.E., Baxter, L.A., Fisher, K., Bittner-Eddy, P.D., Rose, L.E., Holub, E.B., and Beynon, J.L. (2009). Maintenance of genetic variation in plants and pathogens involves complex networks of gene-for-gene interactions. Mol. Plant Pathol. **10,** 449-457.

Halterman, D., Zhou, F., Wei, F., Wise, R.P., and Schulze-Lefert, P. (2001). The MLA6 coiled-coil, NBS-LRR protein confers AvrMla6-dependent resistance specificity to Blumeria graminis f. sp. hordei in barley and wheat. Plant J.l **25,** 335-348.

Halterman, D.A., and Wise, R.P. (2004). A single-amino acid substitution in the sixth leucine-rich repeat of barley MLA6 and MLA13 alleviates dependence on RAR1 for disease resistance signaling. Plant J. **38,** 215.

He, P., Shan, L., and Sheen, J. (2007). Elicitation and suppression of microbe-associated molecular pattern-triggered immunity in plant-microbe interactions. Cellular Microbiology **9,** 1385-1396.

Hein, I., Gilroy, E.M., Armstrong, M.R., and Birch, P.R.J. (2009). The zig-zag-zig in oomycete-plant interactions. Mol. Plant Pathol. **10,** 547-562.

Hochstrasser, M. (2009). Origin and function of ubiquitin-like proteins. Nature **458,** 422-429.

Hoeller, D., Hecker, C.-M., Wagner, S., Rogov, V., Dötsch, V., and Dikic, I. (2007). E3-Independent Monoubiquitination of Ubiquitin-Binding Proteins. Molecular Cell **26,** 891-898.

Hogenhout, S.A., Van der Hoorn, R.A.L., Terauchi, R., and Kamoun, S. (2009). Emerging Concepts in Effector Biology of Plant-Associated Organisms. Mol. Plant-Microbe Interact. **22,** 115-122.

Hotson, A., Chosed, R., Shu, H.J., Orth, K., and Mudgett, M.B. (2003). Xanthomonas type III effector XopD targets SUMO-conjugated proteins in planta. Mol. Microbiol. **50,** 377-389.

Houterman, P.M., Cornelissen, B.J.C., and Rep, M. (2008). Suppression of plant resistance gene-based immunity by a fungal effector. PLoS Pathog. **4**.

Huang, D.T., and Schulman, B.A. (2006). Breaking up with a kinky SUMO. Nature Structural & Molecular Biology **13,** 1045-1047.

Huser, A.l., Takahara, H., Schmalenbach, W., and O'Connell, R. (2009). Discovery of Pathogenicity Genes in the Crucifer Anthracnose Fungus Colletotrichum higginsianum, Using Random Insertional Mutagenesis. Mol. Plant-Microbe Interact. **22,** 143-156.

Inuma, T., Khodaparast, S.A., and Takamatsu, S. (2007). Multilocus phylogenetic analyses within Blumeria graminis, a powdery mildew fungus of cereals. Mol. Phylogenet. Evol. **44,** 741-751.

Ishii, K.J., Koyama, S., Nakagawa, A., Coban, C., and Akira, S. (2008). Host innate immune receptors and beyond: Making sense of microbial infections. Cell Host & Microbe **3,** 352-363.

Jacobs, K.A., CollinsRacie, L.A., Colbert, M., Duckett, M., GoldenFleet, M., Kelleher, K., Kriz, R., LaVallie, E.R., Merberg, D., Spaulding, V., Stover, J., Williamson, M.J., and McCoy, J.M. (1997). A genetic selection for isolating cDNAs encoding secreted proteins. Gene **198,** 289-296.

Jamir, Y., Guo, M., Oh, H.S., Petnicki-Ocwieja, T., Chen, S.R., Tang, X.Y., Dickman, M.B., Collmer, A., and Alfano, J.R. (2004). Identification of Pseudomonas syringae type III effectors that can suppress programmed cell death in plants and yeast. Plant J. **37,** 554-565.

Janjusevic, R., Abramovitch, R.B., Martin, G.B., and Stebbins, C.E. (2006). A bacterial inhibitor of host programmed cell death defenses is an E3 ubiquitin ligase. Science **311,** 222-226.

Javier Lacadena, E.Á.-G.N.C.-S.E.H.-G.J.A.-C.L.G.-O.M.O.J.G.G.Á.M.d.P. (2007). Fungal ribotoxins: molecular dissection of a family of natural killers. FEMS Microbiology Reviews **31,** 212-237.

Jelenska, J., Yao, N., Vinatzer, B.A., Wright, C.M., Brodsky, J.L., and Greenberg, J.T. (2007). A J domain virulence effector of Pseudomonas syringae remodels host chloroplasts and suppresses defenses. Current Biology **17,** 499-508.

Jensen, J., Jensen, H.P., and Jorgensen, J.H. (1995). Linkage Studies of Barley Powdery Mildew Virulence Loci. Hereditas **122,** 197-209.

Jia, Y., McAdams, S.A., Bryan, G.T., Hershey, H.P., and Valent, B. (2000). Direct interaction of resistance gene and avirulence gene products confers rice blast resistance. Embo Journal **19,** 4004-4014.

Jiang, R.H.Y., Tripathy, S., Govers, F., and Tyler, B.M. (2008). RXLR effector reservoir in two Phytophthora species is dominated by a single rapidly evolving superfamily with more than 700 members. Proc. Natl. Acad. Sci. USA **105,** 4874.

Jones, J.D., and Dangl, J.L. (2006). The plant immune system. Nature **444,** 323.

Jorgensen, J.H. (1992a). Multigene Families of Powdery Mildew Resistance Genes in Locus Mla on Barley Chromosome-5. Plant Breeding **108,** 53-59.

Jorgensen, J.H. (1992b). Discovery, Characterization and Exploitation of Mlo Powdery Mildew Resistance in Barley. Euphytica **63,** 141-152.

Jorgensen, J.H. (1994). Genetics of Powdery Mildew Resistance in Barley. Critical Reviews in Plant Sciences **13,** 97-119.

Kaku, H., Nishizawa, Y., Ishii-Minami, N., Akimoto-Tomiyama, C., and Dohmae, N. (2006). Plant cells recognize chitin fragments for defense signaling through a plasma membrane receptor. Proc. Natl. Acad. Sci. USA **103,** 11086.

Kamoun, S. (2006). A catalogue of the effector secretome of plant pathogenic oomycetes. Annu. Rev. Phytopathol. **44,** 41.

Kamoun, S. (2007). Groovy times: filamentous pathogen effectors revealed. Curr. Opin. Plant Biol. **10,** 358-365.

Kao, R., and Davies, J. (1995). Fungal ribotoxins: A family of naturally engineered targeted toxins? Biochemistry and Cell Biology-Biochimie Et Biologie Cellulaire **73,** 1151-1159.

Karpova, T.S., Baumann, C.T., He, L., Wu, X., Grammer, A., Lipsky, P., Hager, G.L., and McNally, J.G. (2003). Fluorescence resonance energy transfer from cyan to yellow fluorescent protein detected by acceptor photobleaching using confocal microscopy and a single laser. Journal of Microscopy **209,** 56-70.

Karran, P., and Attard, N. (2008). Thiopurines in current medical practice: molecular mechanisms and contributions to therapy-related cancer. Nat Rev Cancer **8,** 24-36.

Kelley, L.A., and Sternberg, M.J.E. (2009). Protein structure prediction on the Web: a case study using the Phyre server. Nature Protocols **4,** 363-371.

Kemen, E., Kemen, A.C., Rafiqi, M., Hempel, U., Mendgen, K., Hahn, M., and Voegele, R.T. (2005). Identification of a protein from rust fungi transferred from haustoria into infected plant cells. Mol. Plant-Microbe Interact. **18,** 1130-1139.

Kim, D.W., Lenzen, G., Page, A.L., Legrain, P., Sansonetti, P.J., and Parsot, C. (2005a). The Shigella flexneri effector OspG interferes with innate immune responses by targeting ubiquitin-conjugating enzymes. Proc. Natl. Acad. Sci. U. S. A. **102,** 14046-14051.

Kim, H.S., Desveaux, D., Singer, A.U., Patel, P., Sondek, J., and Dangl, J.L. (2005b). The Pseudomonas syringae effector AvrRpt2 cleaves its C-terminally acylated target, RIN4, from Arabidopsis membranes to block RPM1 activation. Proc. Natl. Acad. Sci. U. S. A. **102,** 6496-6501.

Klein, R.D., Gu, Q.M., Goddard, A., and Rosenthal, A. (1996). Selection for genes encoding secreted proteins and receptors. Proc. Natl. Acad. Sci. U. S. A. **93,** 7108-7113.

Kolonin, M.G., Zhong, J.H., and Finley, R.L. (2000). Interaction mating methods in two-hybrid systems. In Applications of Chimeric Genes and Hybrid Proteins, Pt C (San Diego: Academic Press Inc), pp. 26-46.

Krijger, J.-J., Horbach, R., Behr, M., Schweizer, P., Deising, H.B., and Wirsel, S.G.R. (2008). The Yeast Signal Sequence Trap Identifies Secreted Proteins of the Hemibiotrophic Corn Pathogen Colletotrichum graminicola. Mol. Plant-Microbe Interact. **21,** 1325-1336.

Kulkarni, R.D., Kelkar, H.S., and Dean, R.A. (2003). An eight-cysteine-containing CFEM domain unique to a group of fungal membrane proteins. Trends in Biochemical Sciences **28,** 118-121.

Kumar, S., Nei, M., Dudley, J., and Tamura, K. (2008). MEGA: A biologist-centric software for evolutionary analysis of DNA and protein sequences. Brief Bioinform **9,** 299-306.

Kunoh, H., Komura, T., Kobayashi, I., and Yamaoka, N. (1990). Induced Accessibility and Enhanced Inaccessibility at the Cellular-Level in Barley Coleoptiles .7.

Enhancement of Inaccessibility at the Prepenetration Stage of a Nonpathogen. Physiol. Mol. Plant Pathol. **37,** 399-407.

Larkin, M.A., Blackshields, G., Brown, N.P., Chenna, R., McGettigan, P.A., McWilliam, H., Valentin, F., Wallace, I.M., Wilm, A., Lopez, R., Thompson, J.D., Gibson, T.J., and Higgins, D.G. (2007). Clustal W and Clustal X version 2.0. Bioinformatics **23,** 2947-2948.

Lauge, R., Joosten, M., VandenAckerveken, G., VandenBroek, H.W.J., and DeWit, P. (1997). The in planta-produced extracellular proteins ECP1 and ECP2 of Cladosporium fulvum are virulence factors. Mol. Plant-Microbe Interact. **10,** 725-734.

Lawrence, G.J., Shepherd, K.W., and Mayo, G.M.E. (1981a). Fine-Structure of Genes-Controlling Pathogenicity in Flax Rust, Melampsora-Lini. Heredity **46,** 297-313.

Lawrence, G.J., Mayo, G.M.E., and Shepherd, K.W. (1981b). Interactions between Genes-Controlling Pathogenicity in the Flax Rust Fungus. Phytopathology **71,** 12-19.

Lindeberg, M., Cartinhour, S., Myers, C.R., Schechter, L.M., Schneider, D.J., and Collmer, A. (2006). Closing the circle on the discovery of genes encoding Hrp regulon members and type III secretion system effectors in the genomes of three model Pseudomonas syringae strains. Mol. Plant-Microbe Interact. **19,** 1151-1158.

Liston, P., Fong, W.G., and Korneluk, R.G. (2003). The inhibitors of apoptosis: there is more to life than Bcl2. Oncogene **22,** 8568-8580.

Link, T., Voegle, R.T. (2008). Secreted proteins of Uromyces fabae: similarities and stage specificity. Mol. Plant Pathol. **9,** 59-66.

Liu, J., Elmore, J.M., Fuglsang, A.T., Palmgren, M.G., Staskawicz, B.J., and Coaker, G. (2009). RIN4 Functions with Plasma Membrane H+-ATPases to Regulate Stomatal Apertures during Pathogen Attack. Plos Biology **7**.

Lopez-Solanilla, E., Bronstein, P.A., Schneider, A.R., and Collmer, A. (2004). HopPtoN is a Pseudomonas syringae Hrp (type III secretion system) cysteine protease effector that suppresses pathogen-induced necrosis associated with both compatible and incompatible plant interactions. Mol. Microbiol. **54,** 353-365.

Lotze, M.T., Zeh, H.J., Rubartelli, A., Sparvero, L.J., and Amoscato, A.A. (2007). The grateful dead: damage-associated molecular pattern molecules and reduction/oxidation regulate immunity. Immunol. Rev. **220,** 60.

Lyngkjaer, M.F., Carver, T.L.W., and Zeyen, R.J. (2001). Virulent Blumeria graminis infection induces penetration susceptibility and suppresses race-specific hypersensitive resistance against avirulent attack in Mla1-barley. Physiol. Mol. Plant Pathol. **59,** 243-256.

Ma, W.B., Dong, F.F.T., Stavrinides, J., and Guttman, D.S. (2006). Type III effector diversification via both pathoadaptation and horizontal transfer in response to a coevolutionary arms race. Plos Genetics **2,** 2131-2142.

Mackey, D., and McFall, A.J. (2006). MAMPs and MIMPs: proposed classifications for inducers of innate immunity. Mol. Microbiol. **61,** 1365-1371.

Mackey, D., Holt, B.F., Wiig, A., and Dangl, J.L. (2002). RIN4 interacts with Pseudomonas syringae type III effector molecules and is required for RPM1-mediated resistance in Arabidopsis. Cell **108,** 743-754.

Mackey, D., Belkhadir, Y., Alonso, J.M., Ecker, J.R., and Dangl, J.L. (2003). Arabidopsis RIN4 is a target of the type III virulence effector AvrRpt2 and modulates RPS2-mediated resistance. Cell **112,** 379-389.

Makarov, A.A., Kolchinsky, A., and Ilinskaya, O.N. (2008). Binase and other microbial RNases as potential anticancer agents. Bioessays **30,** 781-790.

Manning, V.A., Hamilton, S.M., Karplus, P.A., and Ciuffetti, L.M. (2008). The Arg-Gly-Asp-containing, solvent-exposed loop of Ptr ToxA is required for internalization. Mol. Plant-Microbe Interact. **21,** 315-325.

Marmeisse, R., Van Den Ackerveken, G., Goosen, T., De Wit, P., and Van Den Broek, H.W.J. (1993). Disruption of the avirulence gene avr9 in two races of the tomato pathogen Cladosporium fulvum causes virulence on tomato genotypes with the complementary resistance gene Cf9. Mol. Plant-Microbe Interact. **6,** 412.

Martinez-Ruiz, A., Kao, R., Davies, J., and del Pozo, A.M. (1999). Ribotoxins are a more widespread group of proteins within the filamentous fungi than previously believed. Toxicon **37,** 1549-1563.

Mendgen, K., and Hahn, M. (2002). Plant infection and the establishment of fungal biotrophy. Trends in Plant Science **7,** 352-356.

Meyers, B.C., Kozik, A., Griego, A., Kuang, H.H., and Michelmore, R.W. (2003). Genome-wide analysis of NBS-LRR-encoding genes in Arabidopsis. Plant Cell **15,** 809.

Miya, A., Albert, P., Shinya, T., Desaki, Y., and Ichimura, K. (2007). CERK1, a LysM receptor kinase, is essential for chitin elicitor signaling in Arabidopsis. Proc. Natl. Acad. Sci. USA **104,** 19613.

Mosquera, G., Giraldo, M.C., Khang, C.H., Coughlan, S., and Valent, B. (2009). Interaction Transcriptome Analysis Identifies Magnaporthe oryzae BAS1-4 as Biotrophy-Associated Secreted Proteins in Rice Blast Disease. Plant Cell**,** tpc.107.055228.

Mouratou, B., Biou, V., Joubert, A., Cohen, J., Shields, D., Geldner, N., Jurgens, G., Melancon, P., and Cherfils, J. (2005). The domain architecture of large guanine nucleotide exchange factors for the small GTP-binding protein Arf. BMC Genomics **6,** 20.

Munkvold, K.R., Martin, M.E., Bronstein, P.A., and Collmer, A. (2008). A Survey of the Pseudomonas syringae pv. tomato DC3000 Type III Secretion System Effector Repertoire Reveals Several Effectors That Are Deleterious When Expressed in Saccharomyces cerevisiae. Mol. Plant-Microbe Interact. **21,** 490-502.

Nelson, B.K., Cai, X., and Nebenführ, A. (2007). A multicolored set of *in vivo* organelle markers for co-localization studies in Arabidopsis and other plants. The Plant Journal **51,** 1126-1136.

Nie, Z., and Randazzo, P.A. (2006). Arf GAPs and membrane traffic. J Cell Sci **119,** 1203-1211.

Nielsen, H., Engelbrecht, J., Brunak, S., and von Heijne, G. (1997). Identification of prokaryotic and eukaryotic signal peptides and prediction of their cleavage sites. Protein Eng. **10,** 1-6.

Nimchuk, Z., Eulgem, T., Holt, B.E., and Dangl, J.L. (2003). Recognition and response in the plant immune system. Annu. Rev. Genet. **37,** 579.

Nomura, K., DebRoy, S., Lee, Y.H., Pumplin, N., Jones, J., and He, S.Y. (2006). A bacterial virulence protein suppresses host innate immunity to cause plant disease. Science **313,** 220-223.

Nurnberger, T., Abel, S., Jost, W., and Glund, K. (1990). Induction of an Extracellular Ribonuclease in Cultured Tomato Cells upon Phosphate Starvation. Plant Physiol **92,** 970 - 976.

O'Connell, R.J., and Panstruga, R. (2006). Tete a tete inside a plant cell: establishing compatibility between plants and biotrophic fungi and oomycetes. New Phytol. **171,** 699-718.

Ogawa, T., Pan, L., Kawai-Yamada, M., Yu, L.H., Yamamura, S., Koyama, T., Kitajima, S., Ohme-Takagi, M., Sato, F., and Uchimiya, H. (2005). Functional

analysis of Arabidopsis ethylene-responsive element binding protein conferring resistance to Bax and abiotic stress-induced plant cell death. Plant Physiol. **138,** 1436-1445.

Oh, B.C., Choi, W.C., Park, S., Kim, Y.O., and Oh, T.K. (2004). Biochemical properties and substrate specificities of alkaline and histidine acid phytases. Appl. Microbiol. Biotechnol. **63,** 362-372.

Panstruga, R. (2003). Establishing compatibility between plants and obligate biotrophic pathogens. Curr. Opin. Plant Biol. **6,** 320-326.

Parlange, F., Daverdin, G., Fudal, I., Kuhn, M.L., and Balesdent, M.H. (2009). Leptosphaeria maculans avirulence gene AvrLm4-7 confers a dual recognition specificity by the Rlm4 and Rlm7 resistance genes of oilseed rape, and circumvents Rlm4-mediated recognition through a single amino acid change. Mol. Microbiol. **71,** 851.

Pazzagli, L., Pantera, B., Carresi, L., Zoppi, C., Pertinhez, T.A., Spisni, A., Tegli, S., Scala, A., and Cappugi, G. (2006). Cerato-platanin, the first member of a new fungal protein family - Cloning, expression, and characterization. Cell Biochemistry and Biophysics **44,** 512-521.

Pemberton, J.M., and Penfold, R.J. (1992). High-Frequency Electroporation and Maintenance of Puc-Based and Pbr-Based Cloning Vectors in Pseudomonas-Stutzeri. Current Microbiology **25,** 25-29.

Perfect, S.E., and Green, J.R. (2001). Infection structures of biotrophic and hemibiotrophic fungal plant pathogens. Mol. Plant Pathol. **2,** 101-108.

Pimpl, P., Hanton, S.L., Taylor, J.P., Pinto-daSilva, L.L., and Denecke, J. (2003). The GTPase ARF1p controls the sequence-specific vacuolar sorting route to the lytic vacuole. Plant Cell **15,** 1242-1256.

Quevillon, E., Silventoinen, V., Pillai, S., Harte, N., Mulder, N., Apweiler, R., and Lopez, R. (2005). InterProScan: protein domains identifier. Nucl. Acids Res. **33,** W116-120.

Rairdan, G., and Moffett, P. (2007). Brothers in arms? Common and contrasting themes in pathogen perception by plant NB-LRR and animal NACHT-LRR proteins. Microbes Infect. **9,** 677.

Ranjard, L., Prigent-Combaret, C., Favre-Bonté, S., Monnez, C., Nazaret, S., and Cournoyer, B. (2004). Characterization of a novel selenium methyltransferase from freshwater bacteria showing strong similarities with the calicheamicin methyltransferase. Biochimica et Biophysica Acta (BBA) - Gene Structure and Expression **1679,** 80-85.

Rehmany, A.P., Gordon, A., Rose, L.E., Allen, R.L., and Armstrong, M.R. (2005). Differential recognition of highly divergent downy mildew avirulence gene alleles by RPP1 resistance genes from two Arabidopsis lines. Plant Cell **17,** 1839.

Rep, M. (2005). Small proteins of plant-pathogenic fungi secreted during host colonization. Fems Microbiology Letters **253,** 19-27.

Rep, M., Meijer, M., Houterman, P.M., Van Der Does, H.C., and Cornelissen, B.J.C. (2005). Fusarium oxysporum evades I-3-mediated resistance without altering the matching avirulence gene. Mol. Plant-Microbe Interact. **18,** 15.

Ridout, C.J., Skamnioti, P., Porritt, O., Sacristan, S., Jones, J.D.G., and Brown, J.K.M. (2006). Multiple avirulence paralogues in cereal powdery mildew fungi may contribute to parasite fitness and defeat of plant resistance. Plant Cell **18,** 2402-2414.

Robert-Seilaniantz, A., Shan, L.B., Zhou, J.M., and Tang, X.Y. (2006). The Pseudomonas syringae pv. tomato DC3000 type III effector HopF2 has a putative

myristoylation site required for its avirulence and virulence functions. Mol. Plant-Microbe Interact. **19,** 130-138.

Roiz, L., Ozeri, U., Goren, R., and Shoseyov, O. (2000). Characterization Aspergillus niger B-l RNase and its inhibitory effect on pollen germination and pollen tube growth in selected tree fruit. Journal of the American Society for Horticultural Science **125,** 9-14.

Roiz, L., Smirnoff, P., Bar-Eli, M., Schwartz, B., and Shoseyov, O. (2006). ACTIBIND, an actin-binding fungal T2-RNase with antiangiogenic and anticarcinogenic characteristics. Cancer **106,** 2295-2308.

Rooney, H.C.E. (2005). Cladosporium Avr2 inhibits tomato Rcr3 protease required for Cf-2-dependent disease resistance (vol 308, pg 1783, 2005). Science **310,** 54-54.

Rose, J.K.C., Ham, K.S., Darvill, A.G., and Albersheim, P. (2002). Molecular cloning and characterization of glucanase inhibitor proteins: Coevolution of a counterdefense mechanism by plant pathogens. Plant Cell **14,** 1329-1345.

Rosenberg, H.F. (2008). RNase A ribonucleases and host defense: an evolving story. J Leukoc Biol **83,** 1079-1087.

Saitou, N., and Nei, M. (1987). The Neighbor-Joining Method - a New Method for Reconstructing Phylogenetic Trees. Molecular Biology and Evolution **4,** 406-425.

Sanger, F., Nicklen, S., and Coulson, A.R. (1977). DNA sequencing with chain-terminating inhibitors. Proc. Natl. Acad. Sci. U. S. A. **74,** 5463-5467.

Sarma, G.N., Manning, V.A., Ciuffetti, L.M., and Karplus, P.A. (2005). Structure of Ptr ToxA: An RGD-Containing Host-Selective Toxin from Pyrenophora tritici-repentis. Plant Cell **17,** 3190-3202.

Sato, S., St-Pierre, C., Bhaumik, P., and Nieminen, J. (2009). Galectins in innate immunity: dual functions of host soluble beta-galactoside-binding lectins as damage-associated molecular patterns (DAMPs) and as receptors for pathogen-associated molecular patterns (PAMPs). Immunological Reviews **230,** 172-187.

Schechter, L.M., Vencato, M., Jordan, K.L., Schneider, S.E., Schneider, D.J., and Collmer, A. (2006). Multiple approaches to a complete inventory of Pseudomonas syringae pv. tomato DC3000 type III secretion system effector proteins. Mol. Plant-Microbe Interact. **19,** 1180-1192.

Scheuermann, T.H., Lolis, E., and Hodsdon, M.E. (2003). Tertiary Structure of Thiopurine Methyltransferase from Pseudomonas syringae, a Bacterial Orthologue of a Polymorphic, Drug-metabolizing Enzyme. Journal of Molecular Biology **333,** 573-585.

Schmidt, S.M., and Panstruga, R. (2007). Cytoskeleton functions in plant-microbe interactions. Physiol. Mol. Plant Pathol. **71,** 135-148.

Schweizer, P., Christoffel, A., and Dudler, R. (1999). Transient expression of members of the germin-like gene family in epidermal cells of wheat confers disease resistance. The Plant Journal **20,** 541-552.

Sekar, R.B., and Periasamy, A. (2003). Fluorescence resonance energy transfer (FRET) microscopy imaging of live cell protein localizations. J Cell Biol **160,** 629 - 633.

Shabab, M., Shindo, T., Gu, C., Kaschani, F., and Pansuriya, T. (2008). Fungal effector protein AVR2 targets diversifying defense-related cys proteases of tomato. Plant Cell **20,** 1169.

Shan, L.B., Thara, V.K., Martin, G.B., Zhou, J.M., and Tang, X.Y. (2000). The pseudomonas AvrPto protein is differentially recognized by tomato and tobacco and is localized to the plant plasma membrane. Plant Cell **12,** 2323-2337.

Shen, Q.H., Saijo, Y., Mauch, S., Biskup, C., and Bieri, S. (2007). Nuclear activity of MLA immune receptors links isolate-specific and basal disease-resistance responses. Science **315,** 1098.

Shen, Q.H., Zhou, F.S., Bieri, S., Haizel, T., Shirasu, K., and Schulze-Lefert, P. (2003). Recognition specificity and RAR1/SGT1 dependence in barley Mla disease resistance genes to the powdery mildew fungus. Plant Cell **15,** 732-744.

Shirasu, K., Nielsen, K., Piffanelli, P., Oliver, R., and Schulze-Lefert, P. (1999). Cell-autonomous complementation of mlo resistance using a biolistic transient expression system. Plant J. **17,** 293-299.

Siezen, R.J. (1996). Subtilases: Subtilisin-like serine proteases. Subtilisin Enzymes - Practical Protein Engineering **379,** 75-93.

Sijacic, P., Wang, X., Skirpan, A.L., Wang, Y., Dowd, P.E., McCubbin, A.G., Huang, S., and Kao, T.H. (2004). Identification of the pollen determinant of S-RNase-mediated self-incompatibility. Nature **429,** 302-305.

Soanes, D.M., and Talbot, N.J. (2006). Comparative genomic analysis of phytopathogenic fungi using expressed sequence tag (EST) collections. In Molecular Plant Pathology, pp. 61-70.

Soanes, D.M., Kershaw, M.J., Cooley, R.N., and Talbot, N.J. (2002). Regulation of the MPG1 hydrophobin gene in the rice blast fungus Magnaporthe grisea. Mol. Plant-Microbe Interact. **15,** 1253-1267.

Sohn, K.H., Lei, R., Nemri, A., and Jones, J.D.G. (2007). The Downy Mildew Effector Proteins ATR1 and ATR13 Promote Disease Susceptibility in Arabidopsis thaliana. Plant Cell**,** tpc.107.054262.

Song, W.Y., Pi, L.Y., Wang, G.L., Gardner, J., Holsten, T., and Ronald, P.C. (1997). Evolution of the rice Xa21 disease resistance gene family. Plant Cell **9,** 1279-1287.

Sreedhar, L., Kobayashi, D.Y., Bunting, T.E., Hillman, B.I., and Belanger, F.C. (1999). Fungal proteinase expression in the interaction of the plant pathogen Magnaporthe poae with its host. Gene **235,** 121-129.

Stergiopoulos, I., and de Wit, P.J.G.M. (2009). Fungal Effector Proteins. Annu. Rev. Phytopathol. **47,** 233-263.

Stergiopoulos, I., De Kock, M.J.D., Lindhout, P., and De Wit, P. (2007). Allelic variation in the effector genes of the tomato pathogen Cladosporium fulvum reveals different modes of adaptive evolution. Mol. Plant-Microbe Interact. **20,** 1271.

Steyaert, J. (1997). A Decade of Protein Engineering on Ribonuclease T1 - Atomic Dissection of the Enzyme-Substrate Interactions. European Journal of Biochemistry **247,** 1-11.

Sweigard, J.A., Carroll, A.M., Kang, S., Farrall, L., Chumley, F.G., and Valent, B. (1995). Identification, cloning, and characterization of PWL2, a gene for host species specificity in the rice blast fungus. Plant Cell **7,** 1221.

Takken, F.L.W., and Tameling, W.I.L. (2009). To Nibble at Plant Resistance Proteins. Science **324,** 744-746.

Talbot, N.J., Kershaw, M.J., Wakley, G.E., deVries, O.M.H., Wessels, J.G.H., and Hamer, J.E. (1996). MPG1 encodes a fungal hydrophobin involved in surface interactions during infection-related development of Magnaporthe grisea. Plant Cell **8,** 985-999.

Talcott, B., and Moore, M.S. (1999). Getting across the nuclear pore complex. Trends in Cell Biology **9,** 312-318.

Tang, W., Coughlan, S., Crane, E., Beatty, M., and Duvick, J. (2006). The Application of Laser Microdissection to In Planta Gene Expression Profiling of the Maize Anthracnose Stalk Rot Fungus Colletotrichum graminicola. Mol. Plant-Microbe Interact. **19,** 1240-1250.

Tian, M., Huitema, E., da Cunha, L., Torto-Alalibo, T., and Kamoun, S. (2004). A Kazal-like extracellular serine protease inhibitor from Phytophthora infestans targets the tomato pathogenesis-related protease P69B. J. Biol. Chem. **279,** 26370.

Tian, M.Y., Win, J., Song, J., van der Hoorn, R., van der Knaap, E., and Kamoun, S. (2007). A Phytophthora infestans cystatin-like protein targets a novel tomato papain-like apoplastic protease. Plant Physiol. **143,** 364-377.

Torto, T.A., Li, S.A., Styer, A., Huitema, E., Testa, A., Gow, N.A.R., van West, P., and Kamoun, S. (2003). EST mining and functional expression assays identify extracellular effector proteins from the plant pathogen Phytophthora. Genome Research **13,** 1675-1685.

Tosa, Y. (1989). Evidence on Wheat for Gene-for-Gene Relationship between Formae-Speciales of Erysiphe-Graminis and Genera of Gramineous Plants. Genome **32,** 918-924.

Tzfira, T., Vaidya, M., and Citovsky, V. (2004). Involvement of targeted proteolysis in plant genetic transformation by Agrobacterium. Nature **431,** 87 - 92.

van de Veerdonk, F.L., Kullberg, B.J., van der Meer, J.W.M., Gow, N.A.R., and Netea, M.G. (2008). Host-microbe interactions: innate pattern recognition of fungal pathogens. Current Opinion in Microbiology **11,** 305-312.

Van Den Burg, H.A., Westerink, N., Francoijs, K.J., Roth, R., and Woestenenk, E. (2003). Natural disulfide bond-disrupted mutants of AVR4 of the tomato pathogen Cladosporium fulvum are sensitive to proteolysis, circumvent Cf-4-mediated resistance, but retain their chitin binding ability. J. Biol. Chem. **278,** 27340.

Van Den Burg, H.A., Harrison, S.J., Joosten, M., Vervoort, J., and De Wit, P. (2006). Cladosporium fulvum Avr4 protects fungal cell walls against hydrolysis by plant chitinases accumulating during infection. Mol. Plant-Microbe Interact. **19,** 1420.

van den Hooven, H.W., van den Burg, H.A., Vossen, P., Boeren, S., de Wit, P., and Vervoort, J. (2001). Disulfide bond structure of the AVR9 elicitor of the fungal tomato pathogen Cladosporium fulvum: Evidence for a cystine knot. Biochemistry **40,** 3458-3466.

van der Hoorn, R.A.L., and Kamoun, S. (2008). From Guard to Decoy: A New Model for Perception of Plant Pathogen Effectors. Plant Cell **20,** 2009-2017.

van der Hoorn, R.A.L., Leeuwenburgh, M.A., Bogyo, M., Joosten, M.H.A.J., and Peck, S.C. (2004). Activity Profiling of Papain-Like Cysteine Proteases in Plants. Plant Physiol. **135,** 1170-1178.

van Loon, L.C., Rep, M., and Pieterse, C.M.J. (2006). Significance of inducible defense-related proteins in infected plants. Annu. Rev. Phytopathol. **44,** 135.

Van Poppel, P., Jiang, R.H.Y., Sliwka, J., and Govers, F. (2009). Recognition of Phytophthora infestans Avr4 by potato R4 is triggered by C-terminal domains comprising W motifs. Mol. Plant Pathol. **10,** 611-620.

Verveer, P.J., Rocks, O., Harpur, A.G., and Bastiaens, P.I.H. (2006). Imaging Protein Interactions by FRET Microscopy: FLIM Measurements. Cold Spring Harbor Protocols **2006,** pdb.prot4599-.

Vervoort, J., Van Den Hooven, H.W., Berg, A., Vossen, P., and Vogelsang, R. (1997). The race-specific elicitor AVR9 of the tomato pathogen Cladosporium fulvum: a cystine knot protein. Sequence-specific 1H NMR assignments, secondary structure and global fold of the protein. FEBS Lett. **404,** 153.

Vleeshouwers, V.G.A.A., Rietman, H., Krenek, P., Champouret, N., Young, C., Oh, S.-K., Wang, M., Bouwmeester, K., Vosman, B., Visser, R.G.F., Jacobsen, E., Govers, F., Kamoun, S., and Van der Vossen, E.A.G. (2008). Effector Genomics Accelerates Discovery and Functional Profiling of Potato Disease Resistance and Phytophthora Infestans Avirulence Genes. PLoS ONE **3,** e2875.

Waadt, R., and Kudla, J. (2008). In Planta Visualization of Protein Interactions Using Bimolecular Fluorescence Complementation (BiFC). Cold Spring Harbor Protocols **2008,** pdb.prot4995-.

Walter, M., Chaban, C., Schütze, K., Batistic, O., Weckermann, K., Näke, C., Blazevic, D., Grefen, C., Schumacher, K., Oecking, C., Harter, K., and Kudla, J. (2004). Visualization of protein interactions in living plant cells using bimolecular fluorescence complementation. Plant J. **40,** 428-438.

Wan, J.R., Zhang, X.C., Neece, D., Ramonell, K.M., and Clough, S. (2008). A LysM receptor-like kinase plays a critical role in chitin signaling and fungal resistance in Arabidopsis. Plant Cell **20,** 471.

Wang, C.-I.A., Guncar, G., Forwood, J.K., Teh, T., Catanzariti, A.-M., Lawrence, G.J., Loughlin, F.E., Mackay, J.P., Schirra, H.J., Anderson, P.A., Ellis, J.G., Dodds, P.N., and Kobe, B. (2007). Crystal Structures of Flax Rust Avirulence Proteins AvrL567-A and -D Reveal Details of the Structural Basis for Flax Disease Resistance Specificity. Plant Cell **19,** 2898-2912.

Wang, C.H., Leffler, S., Thompson, D.H., and Hrycyna, C.A. (2005). A general fluorescence-based coupled assay for S-adenosylmethionine-dependent methyltransferases. Biochem. Biophys. Res. Commun. **331,** 351-356.

Waspi, U., Schweizer, P., and Dudler, R. (2001). Syringolin Reprograms Wheat to Undergo Hypersensitive Cell Death in a Compatible Interaction with Powdery Mildew. Plant Cell **13,** 153-161.

Whisson, S.C., Boevink, P.C., Moleleki, L., Avrova, A.O., and Morales, J.G. (2007). A translocation signal for delivery of oomycete effector proteins into host plant cells. Nature **450,** 115.

Win, J., Morgan, W., Bos, J., Krasileva, K.V., Cano, L.M., Chaparro-Garcia, A., Ammar, R., Staskawicz, B.J., and Kamoun, S. (2007). Adaptive evolution has targeted the C-terminal domain of the RXLR effectors of plant pathogenic oomycetes. Plant Cell **19,** 2349-2369.

Woelk, T., Sigismund, S., Penengo, L., and Polo, S. (2007). The ubiquitination code: a signalling problem. Cell Division **2,** 11.

Wosten, H.A.B. (2001). Hydrophobins: Multipurpose proteins. Annual Review of Microbiology **55,** 625-646.

Wubben, J.P., Joosten, M., and Dewit, P. (1994). Expression and Localization of 2 in Planta Induced Extracellular Proteins of the Fungal Tomato Pathogen Cladosporium-Fulvum. Mol. Plant-Microbe Interact. **7,** 516-524.

Yoshida, H. (2001). The ribonuclease T1 family. In Ribonucleases, Pt A, pp. 28-41.

Young, J.D., Peterson, C.G.B., Venge, P., and Cohn, Z.A. (1986). Mechanism of Membrane Damage Mediated by Human Eosinophil Cationic Protein. Nature **321,** 613-616.

Zha, H.B., Fisk, H.A., Yaffe, M.P., Mahajan, N., Herman, B., and Reed, J.C. (1996). Structure-function comparisons of the proapoptotic protein Bax in yeast and mammalian cells. Molecular and Cellular Biology **16,** 6494-6508.

Zhang, J., Dyer, K.D., and Rosenberg, H.F. (2000). Evolution of the rodent eosinophil-associated RNase gene family by rapid gene sorting and positive selection. Proc. Natl. Acad. Sci. U. S. A. **97,** 4701-4706.

Zhang, Z., Henderson, C., and Gurr, S.J. (2004). Blumeria graminis secretes an extracellular catalase during infection of barley: potential role in suppression of host defence. Mol. Plant Pathol. **5,** 537-547.

Zhou, F., Kurth, J., Wei, F., Elliott, C., Vale, G., Yahiaoui, N., Keller, B., Somerville, S., Wise, R., and Schulze-Lefert, P. (2001). Cell-Autonomous Expression of Barley Mla1 Confers Race-Specific Resistance to the Powdery Mildew Fungus via a Rar1-Independent Signaling Pathway. Plant Cell **13,** 337-350.

Zierold, U., Scholz, U., and Schweizer, P. (2005). Transcriptome analysis of mlo-mediated resistance in the epidermis of barley. Mol. Plant Pathol. **6,** 139-151.

7 Supplementary Material

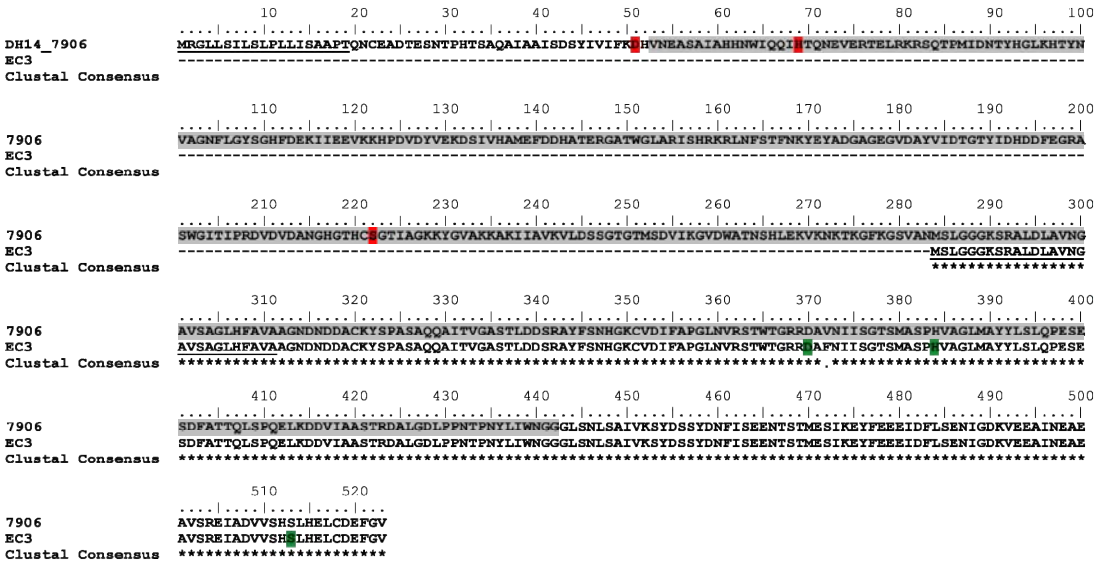

Supplementary Figure 1. EC3 is a partial subtilisin-like protease. Pairwise alignment of the deduced protein sequences of EC3 and contig 7906 (DH14 genome). The *EC3* homologous DNA contig was identified by BLAST searches against the draft genome sequence of *Bgh* DH14. The predicted signal peptides are underlined and the putative full-length protease domain of contig 7906 is shaded grey. Conserved catalytic residues are printed in red, potential mimics of these residues in the EC3 protein are printed in green.

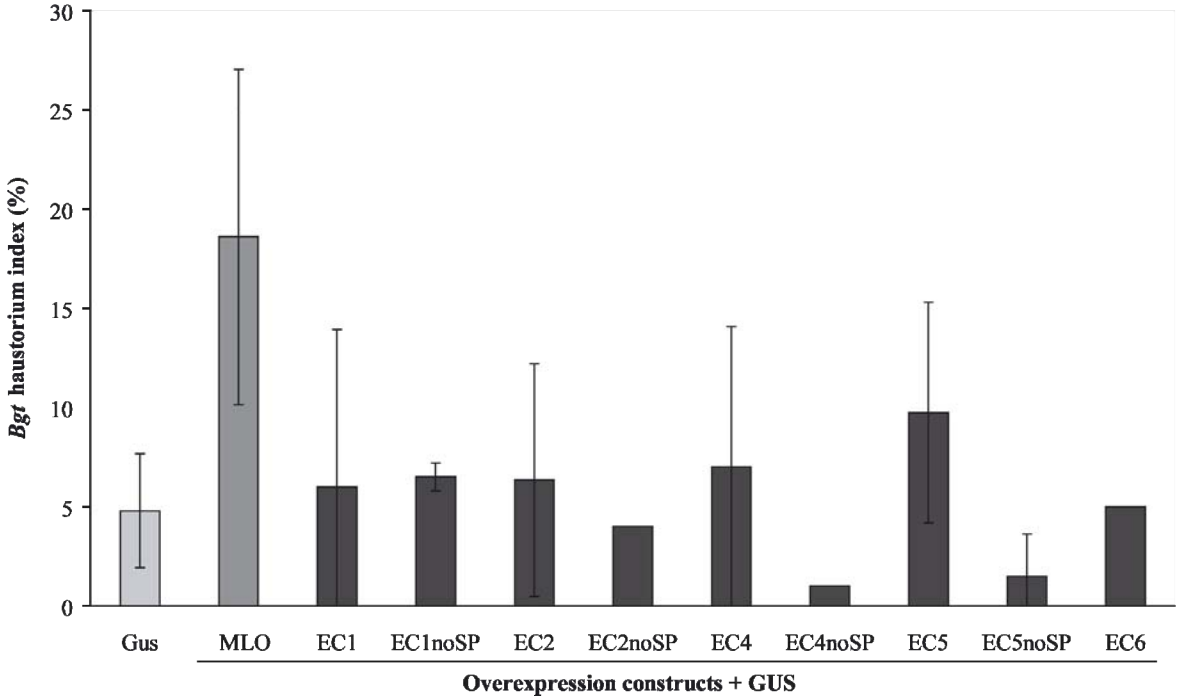

Supplementary Figure 2. EC proteins do not alter resistance of barley to attack by the nonhost fungus *Blumeria graminis* f. sp. *tritici* (*Bgt*). Single epidermal cells of seven days old barley leaves (cv. Golden Promise) were ballistically transformed with either a ß-Glucuronidase (GUS) reporter construct alone or together with an overexpression construct of the ECs. Subsequently leaves were inoculated with conidiospores of the nonhost fungus *Bgt* and at 48 hpi stained for GUS activity. Epiphytic fungal structures were stained with Coomassie Brilliant Blue. The ratio of transformed cells enabling haustorium formation divided by the total number of attacked transformed cells results in the haustorium index and is a measure for the impact of the tested gene on the infection success. Data shown represent means ± SD from at least three experiments, except for EC2noSP and EC4noSP (only one experiment each). For each experiment and tested gene construct at least 20 transformed cells were evaluated. Barley MLO was used as a positive control and GUS alone as a negative control. Abbreviation: noSP: constructs lacking the N-terminal secretion peptide.

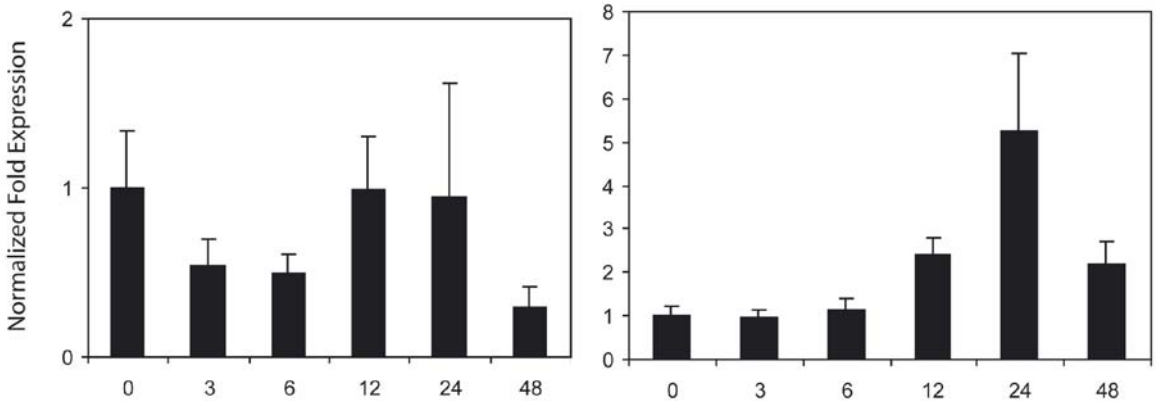

Supplementary Figure 3. *EC4* expression varies during *Bgh* infection. The expression levels of *EC4* were monitored during the compatible interaction of *Bgh* with *H. vulgare* (cv. Golden Promise) at 0, 3, 6, 12, 24 and 48 hours post inoculation (hpi). Total RNA was isolated from barley leaves at the indicated time points. Subsequently, quantitative RT-PCR was performed for *EC4*. *Bgh ß-tubulin* expression was used to normalize the expression value in each sample, and expression values were determined against the average expression value at time point 0 hpi. Please note that the results obtained in two independent experiments with independent biological material differ. While *EC4* transcript levels do not change in one experiment (left graph), *EC4* transcripts appear to increase at 24 hpi in another experiment (right graph). The standard deviation was calculated from three to four technical replicates each.

Supplementary Table 1. Primers used in this study

target	sequence 5' → 3'	purpose
Con0232	CAAAGGACGATAGGTGAATTTG	sequencing
Con0232	GCAACAATGCGGCGTTTCTTCC	sequencing
Con0314	(GWR)GTCATTGTTTTAATGGCGC	sequencing
Con0314	CCGGTATATACTAATTCAACGCTCC	sequencing
Con0314	ACCTCAAGTCACTCGTTATACAACC	sequencing
Con0329	CGTTAAGTCTTCTTAAAGCCAATGAAGC	sequencing
Con0329	GTCCCGCGAGTCGGACTTCGTT	sequencing
Con0895	CTATCTTTCGTCAACATGCAAG	sequencing
Con1691	CCACAATACTGAAAATCATTTATTAGAGCC	sequencing
Con1691	CAACAGAGGGTGATGGAGAC	sequencing
EC1	CATACATGTTATGACTCATGAG	sequencing
EC1	TCCACATTCGCCTCGTCCTTG	sequencing
EC2	CAAAGTCGCGAATCTATGTAGGC	sequencing
EC2	CACTCTCATTCGAAATCCATTC	sequencing
EC3	AGGTCTTTACGCCCGCTTAC	sequencing
EC3	ACCAAGTTGGCGCTGGAA	sequencing
EC3	GAGCAATTGTATAAGTGTAGACC	sequencing
EC3	ATGTCATAAAGGGCGTTGACTGGGCTA	sequencing
EC4	CTATAGCTCGAGCGTGAACGCTG	sequencing

EC4	CCATCTAATTCGCAACTCCTGCCTA	sequencing
EC5	CTCGGCAAGGATTACAGCATG	sequencing
EC5	TCTCAACCTAATTCTCCTCCAA	sequencing
EC7	GGTAGCATGGCGGCTTGCT	sequencing
EC7	ATCCACTCAGCTCTCGTCAG	sequencing
*Go*EC2	ACCGATCGTTACTCCTCTCC	sequencing
*Go*EC2	GATTGTTGTTTCCAGGTCTAATG	sequencing
*Hv*ARF-GAP	TGGAGGCCCCTCTCTCATCC	sequencing
*Hv*ARF-GAP	CGAATCCCTGCGATCTCCCCT	sequencing
*Hv*TPMT	CAGAGGGCAGGTCTGATAGTG	sequencing
*Hv*TPMT	GGCTCTGTCTGTACGCCTGT	sequencing
*Hv*UBC-E2	TGGCCACGCAATTTACACTTC	sequencing
*Hv*UBC-E2	ACCACCGGCCGCTTAGCGA	sequencing
S. typhimurium SigD	CAAGCTTTCAAGATGTGATTAATGAAG	sequencing
S. typhimurium SigD	GGGATCCATGCAAATACAGAGCTTC	sequencing
DH14_1161	GCAGTTTCTGCCTATTAG	sequencing
DH14_1161	ATCATAGCTAGGAAGTCT	sequencing
DH14_1162	AATTTATTGGCAGTTTCTGA	sequencing
DH14_1162	GTTGGATCCAGTCGTTCGT	sequencing
Con0866 *Bgh* ß-tubulin	CTCGACTTCCATCCAAGAGC	qRT-PCR
Con0866 *Bgh* ß-tubulin	TCCATTTCGTCCATTCCTTC	qRT-PCR
EC1	TGGAGTATCAGGCTGCTCGT	qRT-PCR
EC1	GGTCAAGTTGCCATGGTCTT	qRT-PCR
EC2	TGCAAAGCACACTTGGGTAG	qRT-PCR
EC2	GCAGCATCTCCCTACTCGAC	qRT-PCR
EC3	ACATGGACGGGAAGGAGAG	qRT-PCR
EC3	AGACCAGCAACGTGTGGAG	qRT-PCR
EC4	ATCGTTTACCGCATTCAGGA	qRT-PCR
EC4	GCTCTAGCTGCTCTCGTCGT	qRT-PCR
EC5	ATTGATCATTCCCACGGTGT	qRT-PCR
EC5	CTTGCATTCTGGCTGGTGTA	qRT-PCR
EC6	CATGCCACCAATAACTGCAA	qRT-PCR
EC6	CTCCGGCTCTGGATCTACTG	qRT-PCR
AVR_{A10}	(GWYF)[1]ACATAATGGACTCCAGCCATTCA	cloning
AVR_{A10} full-length	(GWR)[2]GTGCTGTTGTTGATGCTGC	cloning
Bg13901727	(GWF)ACATAATGAAGATAAAAAAT	cloning
Bg13901728 full-length	(GWR)GTCATGGACGGGTTGTCAC	cloning
Bg13901727 without STOP codon	(GWR)GTTTGTGCGATACAGTGACAGT	cloning
Con0314	(GWF)ACATAATGCATTACACTCAGGAA	cloning
Con0314 full-length	(GWR)GTCATTGTTTTAATGGCGC	cloning
Con0329	(GWF)ACATAATGGCTACTCCCAGA	cloning
Con0329 full-length	(GWR)GTTAGTGACCCACGTT	cloning
Con0895	(GWF)ACATAATGCTCAATATATTTCAA	cloning
Con0895 full-length	(GWR)GCTACTTCATCTGACTTGT	cloning
Con1691 full-length	(GWR)GTTATTCTAAGGCTTG	cloning
Con1691	(GWF)ACATAATGGAGACAGCAACT	cloning
EC1	(GWF)ACATAATGCAGATTCTATCT	cloning
EC1 full-length	(GWR)GTTATATTCTCAATGA	cloning
EC1 without SP	(GWF)ACATAATGCCAGCGGTCAAGTTG	cloning
EC1 without STOP codon	(GWR)GTATTCTCAATGAACG	cloning
EC2	(GWF)ACATAATGCAATTAATTCGCCTC	cloning
EC2 without SP	(GWF)ACATAATGCACACTGAAGGCGGCAAA	cloning
EC2 without STOP codon	(GWR)GATTGTAGGAGTCAGTGTC	cloning
EC2 full-length	(GWR)GTTAATTGTAGGAGTCAGT	cloning
EC3	(GWF)ACATAATGTCTCTCGGTGGA	cloning

EC3 full-length	(GWR)GCTAGACTCCAAATTC	cloning
EC7 full-length	(GWR)GCTAGATTCCACATGCGCT	cloning
EC3 without STOP codon	(GWR)GGACTCCAAATTCATC	cloning
EC4	(GWF)ACATAATGAAGACTATGCAAACC	cloning
EC4 full-length	(GWR)GTCACAAAAACAGAGCTGC	cloning
EC4 without SP	(GWF)ACATAATGCAGACTGGTGATAATCTT	cloning
EC4 without STOP codon	(GWR)GCAAAAACAGAGCTGCTAG	cloning
EC5	(GWF)ACATAATGCGGTCAGCAAAGAGC	cloning
EC5 full-length	(GWR)GTTACCGATAGTATGGATC	cloning
EC5 without SP	(GWF)ACATAATGCAGGTTAGAACTTATCAA	cloning
EC5 without STOP codon	(GWR)GCCGATAGTATGGATCGCA	cloning
EC6	(GWF)ACATAATGCAGTTCAACTTCTTC	cloning
EC6 full-length	(GWR)GTTAAATCAATAGTGCCATGCCACC	cloning
EC6 without STOP codon	(GWR)GAATCAATAGTGCCATGCCACC	cloning
EC6 without TM	(GWR)GTTATCCAGTGTATGGCATTGGGGG	cloning
EC7	(GWF)ACATAATGAAGATCTTCTCGAGC	cloning
EC7	(GWR)GCTAGATTCCACATGCGCT	cloning
GoEC2	(GWF)ACATAATGCAATTCACCAAACTC	cloning
GoEC2 without SP	(GWF)ACATAACTCCATCAGGTTTGAAC	cloning
GoEC2 full-length	(GWR)GTCAAACGTCCGAGTTCTG	cloning
GoEC2 without STOP codon	(GWR)GAACGTCCGAGTTCTGCAT	cloning
EC1 N-terminus	(GWR)GTCCGTCGTCTGGAGA	cloning
EC2 N-terminus	(GWR)GGGTGCAAGCGAAGTCTGC	cloning
EC3 N-terminus	(GWR)GGGCGTCTCTCCTTCC	cloning
EC4 N-terminus	(GWR)GACCTCCAGCGCCGGCCGA	cloning
EC5 N-terminus	(GWR)GTGCGACGTGTTGGAATTG	cloning
EC7 N-terminus	(GWR)GGCTCCATCCGTTGATGAA	cloning
AVRa10 N-terminus	(GWR)GGGGTATGTCGGCCTCTTT	cloning
*Hv*ARF-GAP C-terminus	(GWF)ACATAGAACCAGAGTCATCTTCCCAC	cloning
*Hv*ARF-GAP	(GWF)ACATAATGAACGAGAAGGCCTCCGTC	cloning
*Hv*ARF-GAP full-length	(GWR)GTCATCGCTTCGAGAACATTCC	cloning
*Hv*ARF-GAP without STOP codon	(GWR)GTCGCTTCGAGAACATTCCTTG	cloning
*Hv*TPMT C-terminus	(GWF)ACATAGACGTCTGCGACGCCGTC	cloning
*Hv*TPMT full-length	(GWR)GTCATATCGGTGTTTCTGT	cloning
*Hv*TPMT	(GWF)ACATAATGGCGTCGACGGCCGTG	cloning
*Hv*TPMT without STOP codon	(GWR)GTATCGGTGTTTCTGTTCC	cloning
*Hv*UBC-E2 C-terminus	(GWF)ACATACCAGGTGGCTATCCCTTTGAG	cloning
*Hv*UBC-E2 full-length	(GWR)GTCAGCCAGAGCAGAGCTTCTCGAG	cloning
*Hv*UBC-E2	(GWF)ACATAATGGTGGACGTGTCGCGCGTG	cloning
*Hv*UBC-E2 without STOP codon	(GWR)GGCCAGAGCAGAGCTTCTCGAGAGC	cloning
1K15, 1K1, 1K2,1K25 without SP	(GWF)ACATAGATGACATCCCAGACTCG	cloning
1K5, 1A1, 1A3,1A4, 1A9, 1A10, 1A11, 2A4 without SP	(GWF)ACATAGATGACATCCCATACTCG	cloning
1A14,1K14, 1K18, 1K21, 1K28 without SP	(GWF)ACATAGATGACATACCAGACTCA	cloning
A12 without SP	(GWF)ACATAGATGACATACCAGACTCA	cloning
DH14_1148 without SP	(GWF)ACATAGATGACATCCCAGACTCG	cloning
AC universal GWYR	(GWR)GCTAGCAAAGAGTCGTTAG	cloning
AC universal GWYF	(GWF)ACATAATGTGGATTAATTTCAGC	cloning
AC Uni1	ACAGGTCTTCAGACGAAGATG	cloning
AC Uni2	GATATTTACCAGGCGGACCTA	cloning

S39	GAAAGCAACCTGACCTACAGGAAAGAG	sequencing
S40	GCATGACGCCGAAAACCATTCTT	pB42AD

[1] GWYF: forward attB1 primer Gateway® compatible
[2] GWYR: reverse attB2 primer Gateway® compatible

Supplementary Table 2. Vectors used in this study

Vector	Purpose
pDONR201	INVITROGEN, entry vector for cloning
pUbi-Gate	Transient oever-expression in barley
pUbi-GUS	Transient over-expression in barley
pUbi-MLO	Transient over-expression in barley
pSST-GWY	Signal sequence trap, expression in yeast
pAM-PAT-GWY	Stable expression in Arabidopsis
pAM-PAT-GWY-3xHA	Stable expression in Arabidopsis
pUbi-GFP-nos	Transient over-expression in barley, cell death assay
p35S-GWY-YFP	Localization studies, transient over-expression in barley, N-terminal fusion to YFP
p35S-YPF-GWY	Localization studies, transient over-expression in barley, C-terminal fusion to YFP
pYES2	INVITROGEN, expression in yeast under the control of a galactose-inducible promotor
pB42AD	contains the *Hv/Bgh* cDNA library
pB42AD-GWY	Yeast-two-hybrid screen, expression of prey constructs
pLexA-GWY	Yeast two-hybrid screen, expression of bait constructs
pE-Spyne/Spyce-GWY	BiFC assay, C-terminal fusions to YFP-segments
pUC-GWY-Spyne/Spyce	BiFC assay, N-terminal fusions to YFP segments
pDEST17	INVITROGEN, heterologous expression in *E. coli*

Supplementary Table 3. Plasmid combinations used for the Bimolecular Fluorescence Complementation (BiFC) assay

	pE-Spyne-EC4	pE-Spyce-EC4	pUC-Spyne-EC4	pUC-Spyce-EC4	pE-Spyne-EC6	pE-Spyce-EC6	pUC-Spyne-EC6	pUC-Spyce-EC6
pE-Spyne-*Hv*UBC-E2								
pE-Spyce-*Hv*UBC-E2	Figure 9 D							
pUC-Spyne-*Hv*UBC-E2								
pUC-Spyce-*Hv*UBC-E2	Figure 9 C							
pE-Spyne-*Hv*UBC-E2 C-term								
pE-Spyce-*Hv*UBC-E2 C-term								
pUC-Spyne-*Hv*UBC-E2 C-term								
pUC-Spyce-*Hv*UBC-E2 C-term								
pE-Spyne-*Hv*ARF-GAP								
pE-Spyce-*Hv*ARF-GAP								
pUC-Spyne-*Hv*ARF-GAP								
pUC-Spyce-*Hv*ARF-GAP								
pE-Spyne-*Hv*ARF-GAP C-term								
pE-Spyce-*Hv*ARF-GAP C-term								
pUC-Spyne-*Hv*ARF-GAP C-term								
pUC-Spyce-*Hv*ARF-GAP C-term								
pE-Spyne-*Hv*TPMT								Figure 9 B
pE-Spyce-*Hv*TPMT								
pUC-Spyne-*Hv*TPMT								Figure 9 A
pUC-Spyce-*Hv*TPMT								
pE-Spyne-*Hv*TPMT C-term								
pE-Spyce-*Hv*TPMT C-term								
pUC-Spyne-*Hv*TPMT C-term								
pUC-Spyce-*Hv*TPMT C-term								

Grey: not tested, because the respective constructs contain the same YFP-segment
Black: no BiFC *in planta*; Yellow: BiFC *in planta;* White: not tested

8 Additional Material

8.1 Methods

8.1.1 EC2 protein expression in *E. coli*

To create 6xHis-EC2, *EC2* was recombined into pDEST17 by a Gateway LR reaction. 6xHis-EC2 protein was overexpressed in *E.coli* ROSETTA and purified using Ni-NTA agarose under native conditions according to the manufacturer's instructions (Quiagen). Proteins were separated by SDS-PAGE and detected after immunoblot analysis using Penta-His HRP conjugate (Quiagen).

8.1.2 Barley infection with *P. syringae*

P. syringae pv. *aptata* and *P. syringae* pv. *japonica* were transformed either by electroporation or by triparental mating. Electroporation was carried out as described (Pemberton and Penfold, 1992) using a BioRad Gene Pulser. For triparental mating plasmids were mobilized from *E. coli* DH5α to the respective *P. syringae* strain using *E.coli* HB101 (pRK2013) as a helper strain (Ditta et al., 1980). To monitor *P. syringae* growth in planta, *Hordeum vulgare* (cv. Golden Promise) leaves were hand-inoculated with 10^7 cfu (colony forming unit) per ml suspension of bacteria in 10 mM MgCl2 using a needleless syringe. For each *P. syringae* strain analyzed, two leaf discs (Ø 0,4 mm) per time point were collected from one leaf, pooled, ground in 10 mM $MgCl_2$ and then spotted on nutrient yeast glycerol agar (NYGA) plates to determine the bacterial load in each inoculated leaf. Three biological replicates (i.e. three plants) were used and the experiment was repeated twice.

8.1.3 Activity-based protease profiling

Protein extracts were isolated from barley leaves with dH2O. Four leaf discs (0,5 cm2) per barley leaves were pooled and ground in 600 µl water and cell debris pelleted by centrifugation. Protease activity profiling of the supernatant was essentially performed as described (van der Hoorn et al., 2004). Briefly, protein extracts were labeled with 2 µM DCG-04 for 5 h at room temperature. Competition with E-64 was done by adding 200 µM E-64 (Sigma-Aldrich) 30 minutes before adding DCG-04. Proteins were precipitated with

acetone. Protein gel blot analysis and detection of biotinylated proteins was performed as described using streptavidin-HRP polymer (Sigma-Aldrich) (van der Hoorn et al., 2004).

8.2 Results

8.2.1 An attempt to elucidate translocation of the EC proteins into the plant cell

Bacterial pathogens use the type III secretion system to directly deliver effector proteins into the host cell cytoplasm (Grant et al., 2006). Indication that fungal proteins are translocated into host cells is indirect and mainly inferred from the recognition of effectors by intracellular plant resistance proteins (Egan and Talbot, 2008). However, the mechanism of fungal effector translocation into the host cell remains a mystery (Birch et al., 2008). So far, only the rust protein *Uf*-RTP1p and its homolog *Us*-RTP1p were immunologically detected in the extrahaustorial matrix and the host cytoplasm, respectively (Kemen et al., 2005). To demonstrate translocation of effectors inside the host cells during *Bgh* infection we planned to obtain polyclonal antibodies and to use them in an analogous manner for immunoelectron microscopy of powdery mildew-infected barley leaves. We generated constructs for the heterologous expression of His-tagged fusion proteins of EC2, EC3, EC4, EC5 and EC6. The fusion proteins were detected with anti-His-tag-antibody after over-expression and induction with IPTG in *E. coli*. EC3, EC3 and EC5 were detected in the soluble fraction, whereas EC4 appeared to be insoluble (data not shown). EC6 could not be detected and is probably not expressed in bacteria. We pursued purification of the soluble proteins EC2 and EC5 using immobilized metal-ion affinity chromatography under native conditions. An EC5 protein band was not detectable in Western Blots after purification. The band corresponding to the EC2 protein on a Coomassie-stained protein gel was analyzed by mass spectrometry. Unfortunately, the protein corresponded strongly to a protein from *E. coli* (Mascot score: 232) (data not shown), indicating that EC2 is also not expressed in *E. coli*.

8.2.2 A functional screen for *Bgh* effector candidates

In addition to screening for effectors with unknown function we aimed at developing a function-related screen for *Bgh* effector proteins. One known function of effectors is the inhibition of plant hydrolytic pathogenesis-related (PR) proteins, e.g. proteases in the apoplast, which has presumably evolved as an active counter-defense mechanism to cope with plant defense responses. To identify potential secreted protease inhibitors of *Bgh* we employed protease activity profiling. Protease activity profiling is based on the use of the

broad-range protease inhibitor E-64 that interacts with the active group of a cysteine protease substrate (van der Hoorn et al., 2004). Upon reaction with the active protein the reversible complex is converted into an irreversible protein-ligand complex that can be subsequently isolated. This method has been employed to identify secreted protease inhibitors from oomycetes and fungi in Arabidopsis and tomato plants (Tian et al., 2004; Rooney, 2005; Tian et al., 2007).

As a first step we wanted to know whether it is possible to apply protease activity profiling in barley and whether barley proteases are activated upon *Bgh* infection. For this purpose, protein extracts of seven days old barley leaves, which were inoculated with *Bgh* conidiospores for additional four days, were *in vitro* labeled with DCG-04, a biotinylated form of E-64. E-64 is an irreversible inhibitor of active papain-like cysteine proteases and was used as a competitive inhibitor to verify specific labeling of cysteine proteases. Biotinylated proteases were detected on a protein gel blot using a streptavidin-specific antiserum. DCG-04 labeling revealed three major bands of approximately 30 kD, 35 kD and 40 kD. Pretreatment of the samples with E-64 eliminated DCG-04 labeling suggesting that the cysteine proteases were specifically labeled. These three signals were stronger in protein extracts from *Bgh*-infected plants compared with protein extracts from non-infected plants, indicating that cysteine protease activity is induced in barley during *Bgh* infection (**Additional Figure 1**).

However the temporal and spatial resolution of the protease activity profiling was not sufficient to identify *Bgh* effector proteins inhibiting the active proteases for two reasons. Regarding the temporal resolution, one would assume that apoplastic defense and fungal counter-defense mechanisms are activated early during the infection process prior to the fungal penetration of the cell wall around 12 hpi. A time-course labeling experiment using barley leaves that were inoculated with *Bgh* for one, two, three or four days (dpi) revealed that the increase of active cysteine proteases in infected leaves was only detectable at 3 dpi (data not shown) and not at early time points during fungal pathogenesis. Regarding the spatial resolution, secretion of *Bgh* protease inhibitors might locally inhibit active host proteases, but the fungus infects and remains within single barley epidermal cells. With the *in vitro* labeling assay we were looking at both locally and systemically induced active barley proteases, because we used whole-leaf protein extracts. To specifically resolve the potential local inhibition of plant proteases, one would need a fluorescently-labeled probe suitable for *in vivo* labeling.

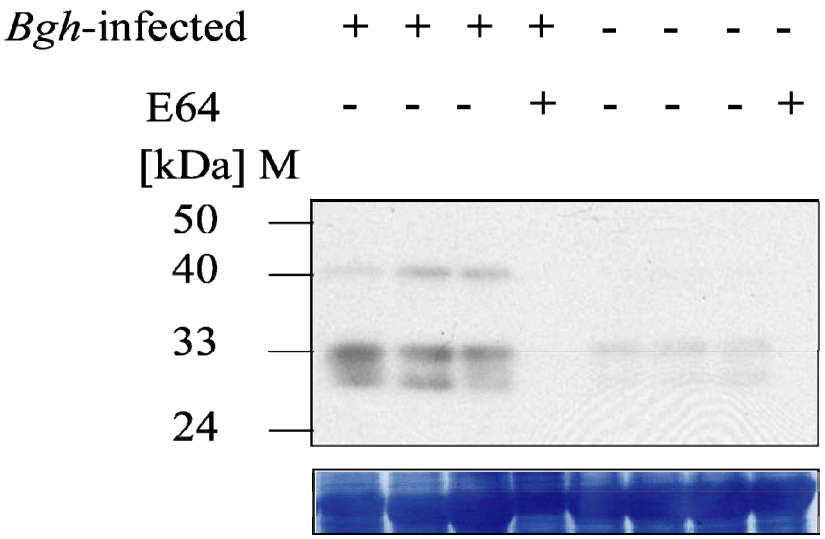

Additional Figure 1. *Bgh* induces cysteine protease activity in barely. Protein extracts from *Bgh*-infected (4 dpi) or non-infected barley leaves were labeled with the biotinylated cysteine protease inhibitor DCG-04. Proteins were acetone-precipitated and separated on a 12% polyacrylamide gel. Biotinylated proteins were detected on a protein blot with streptavidin-HRP (upper panel). Pretreatment with an excess of the competitive inhibitor E-64 specifically abolished DCG-04 labeling of active cysteine protease. Three replicates are shown for both infected and non-infected leaf samples. The composition of the reaction mixes is indicated by the + and - signs at the top. Molecular marker masses are indicated on the left. The Coomassie Brilliant Blue-stained gel demonstrates equal loading (lower panel).

8.2.3 A potential, alternative way to deliver the effector candidates into barley

Transient gene expression by bombardment with DNA-coated gold particles is a rather artificial approach of delivering effector proteins into host cells. For this reason we attempted to develop a more natural delivery route into barley cells by heterologous expression of effector candidates in another plant pathogen. Recently, the *P. syringae* type III secretion system has been successfully employed to deliver effector proteins of the oomycete *H. arabidopsis* (Sohn et al., 2007). We created constructs harboring the effector candidates fused to the N-terminus of the *P. syringae* effector protein AvrRPS4. This so-called “effector-detector-vector” enables secretion through the bacterial type III system. To adapt the system developed by Sohn and co-workers we required a *P. syringae* pathovar that was virulent on barley and could be used for delivery of the “effector-detector-vector” encoded fusion proteins. Two pathovars, *P.s.* pv. *japonica* and *P.s.* pv. *aptata*, were inoculated with a syringe into ten days old barley leaves. At 0, 2 and 4 days after inoculation leaf bacterial titers were measured. No increase in colony forming units (CFU) cm-2 was observed for *P.s.* pv. *aptata* and *P.s.* pv. *tomato* DC3000 (negative control),

respectively. In contrast, the *P.s.* pv. *japonica* titer increased 100-fold within four days, indicating virulence of this strain on barley (**Additional Figure 2**). Unfortunately, *P.s.* pv. *japonica*, unlike *P.s.* pv *aptata* and *P.s.* DC3000, was neither transformable by triparental mating nor by *Agrobacterium tumefaciens* – mediated transformation in our conditions (data not shown).

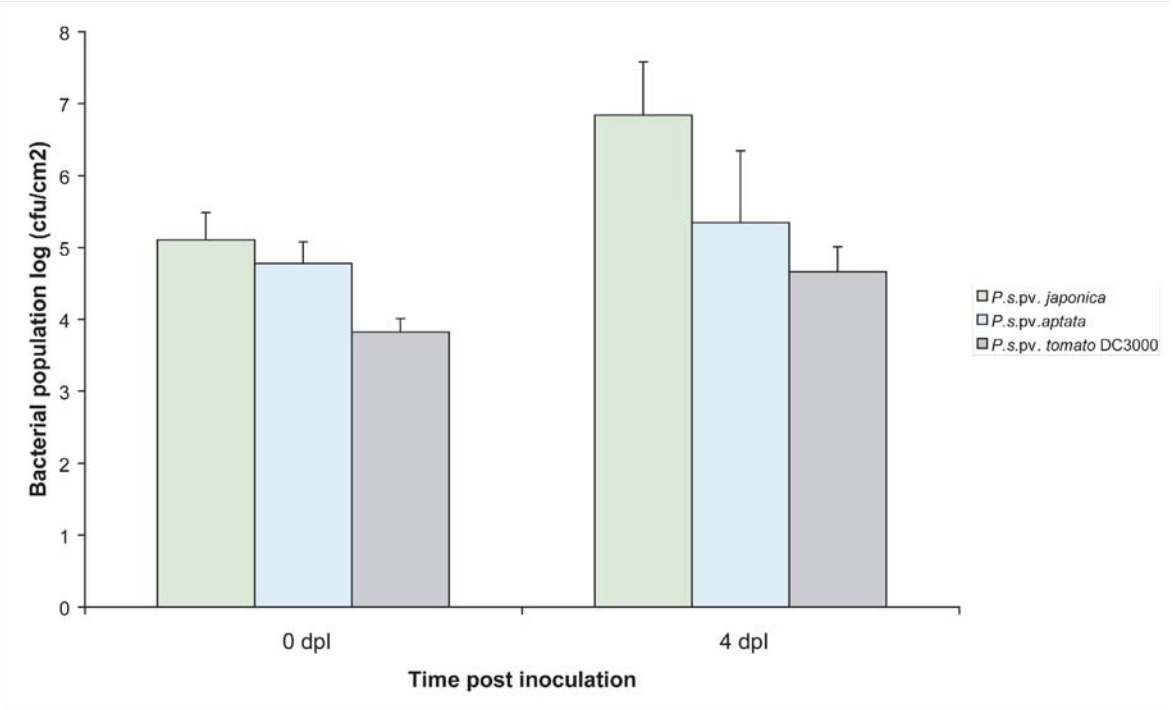

Additional Figure 2. *Pseudomonas syringae* pv. *japonica* is virulent on barley. Three *P. syringae* pathovars (pv. *japonica*, pv. *aptata*, pv. *tomato* DC3000) were syringe-inoculated in barley (*Hordeum vulgare* cv. Golden Promise) leaves with a 10^7 cfu/ml (colony forming units per ml) suspension of the respective bacterial strain. Leaf bacterial populations were determined at 0 and 4 d post infiltration (0 dpi, 4 dpi). Data points represent mean log cfu per cm^2 ± SD of three technical replicates. The experiments were repeated twice yielding similar results.

Acknowledgements

Ich möchte mich bei allen herzlich bedanken, die zum Gelingen dieser Doktorarbeit beigetragen haben, insbesondere danke ich:

Dr. Ralph Panstruga, für die Möglichkeit meine Doktorarbeit in Deiner Gruppe durchzuführen, für die vielen gemeinsamen Stunden vor dem Mikroskop und dem Computer, die Anregungen und Deine mitreißende Begeisterung für Wissenschaft.

Prof. Paul Schulze-Lefert danke ich für die Möglichkeit am MPIZ zu promovieren. Die Diskussioen mit Dir und Deine wissenschaftliche Meinung waren sehr hilfreich.

Prof. M. Hülskamp danke ich für die freundliche Übernahme des Korreferats.

Many thanks to Dr. Frank Takken for being the external examiner of my thesis commitee.

Prof. U.-I. Flügge danke ich für die Übernahme des Prüfungsvorsitzes.

I am deeply grateful to Cristina Micali, who started the *Bgh* effector project, introduced me to the effector world and always had a solution for every situation in life and in the lab. Thank you so much!

I thank all the present and past members for their kind help inside and outside the lab, for a great working atmosphere and culinary precious festivities. These are Anja Reinstädler, Chiara Consonni, Sandra Noir, Nana Keinath, Justine Lorek, Takaki Maekawa, Matt Humphry, Johana Acevedo and Przemyslaw Bidzinski.

Mark Kwaaitaal deserves a special THANK YOU for all his help, the introduction to the CLSM and for letting me use his computer when mine broke down under the load of my thesis.

Mein besonderer Dank gilt Corinna Liller, die mir bei dem Yeast-Two-Hybrid Screen und zahlreichen „niederen Laborarbeiten“ sehr geholfen hat.

Steffen Rietz und Tom Colby danke ich für ihre Hilfe bei der Proteinexpression *E. coli*.

Farnusch Kaschani danke ich für seine Einweisung in das ABPP.

I thank Ainel Aleman, the COGEME consortium, Pietro Piffanelli, Quian-Hua Shen, Armin Töller and Lennart Wirthmüller for kindly sharing cDNA libraries, constructs, genome data and antibodies.

Vielen Dank an Martin Grieger, der mir eine wunderbare Atmosphäre zum Schreiben geschaffen hat und mich gut bekocht hat.

Shermineh Shahi mag zwar diese Danksagungen nicht, aber ich danke Dir trotzdem dafür, dass Du es immer im richtigen Moment schaffst mich anzutreiben.

Erklärung

Ich versichere, dass ich die von mir vorgelegte Dissertation selbständig angefertigt, die benutzten Quellen und Hilfsmittel vollständig angegeben und die Stellen der Arbeit - einschließlich Tabellen, Karten und Abbildungen -, die anderen Werken im Wortlaut oder dem Sinn nach entnommen sind, in jedem Einzelfall als Entlehnung kenntlich gemacht habe; dass diese Dissertation noch keiner anderen Fakultät oder Universität zur Prüfung vorgelegen hat; dass sie - abgesehen von den auf Seite III angegebenen Teilpublikationen - noch nicht veröffentlicht worden ist sowie, dass ich eine solche Veröffentlichung vor Abschluss des Promotionsverfahrens nicht vornehmen werde. Die Bestimmungen dieser Promotionsordnung sind mir bekannt. Die von mir vorgelegte Dissertation ist von Prof. Dr. Paul Schulze-Lefert betreut worden.

Köln, 29. September 2009 _____

Sarah Schmidt

Lebenslauf

Angaben zur Person

Name:	Sarah Maria Schmidt
Geburtsdatum/-ort:	22. Mai 1982 in Marburg/Lahn
Nationalität:	deutsch
Familienstand:	ledig

Ausbildung

seit 10/2006	**Promotions-Studium** an der Universität zu Köln, Köln, Deutschland Max-Plank-Institut für Züchtungsforschung, unter der Leitung von Prof. Dr. P. Schulze-Lefert Stipendium der *International Max-Planck-Research School*
10/2004 – 03/2005	**Austauschsemester** Phytopathologie an der Université Paul Sabatier, Toulouse, Frankreich
10/2003 – 09/2006	**Hauptstudium** Biologie an der Rheinischen Friedrich-Wilhelms-Universität, Bonn, Deutschland Hauptfach: Botanik, Nebenfächer: Organische Chemie, Zellbiologie Abschluss: Diplom-Biologin Stipendium der *Studienstiftung des Deutschen Volkes*
10/2001 – 09/2003	**Grundstudium** Biologie an der Goethe Universität, Frankfurt am Main, Deutschland
07/2001	**Abitur**, St. Ursula Gymnasium, Dorsten, Deutschland

Köln, 29. September 2009 _____

Sarah Schmidt